

Response to reviewers

Manuscript: ACP-2017-1030

Manuscript title: Chemical characteristics of size resolved atmospheric aerosols in Iasi, north-eastern Romania. Nitrogen-containing inorganic compounds controlling aerosols chemistry in the area

The discussion below includes the complete text from the reviewer (italic), along with our responses to the specific comments and the corresponding changes made to the revised manuscript. All line numbers refer to the original manuscript.

Response to **Reviewer #2 Comments**

General

This is a comprehensive field and analytical study of aerosol particles sampled under size-resolution in north-eastern Romania. It contains a wealth of data on the aerosol chemical composition in this area where not many data are available for comparison which is generally true for Eastern Europe. The whole manuscript is a bit lengthy and it might be good if the authors could explore potential for shortening some sections of the paper.

Overall, I think the manuscript requires only minor modification and can then be published in ACP.

We are grateful for the reviewer's constructive comments and suggestions and the manuscript has been revised accordingly. Reviewer's concerns and suggestions are addressed here below and we would like also to point out the following:

- 1) A Supplement Material is accompanying now the manuscript (attached to the present response).
- 2) The manuscript is now presented in a more concise manner (reduction from 53 pages to 46 pages) (the revised manuscript is attached to the present response).
- 3) In the revised manuscript amendments related to reviewer #2 concern are highlighted in green colour.
- 4) The revised manuscript contains 4 additional references.
- 5) Considering language-related suggestion from one of the reviewers, we have requested a well known English speaking scientist, Prof. Davide Vione from University of Torino, to offer us support in polishing the composition. Language polishing has resulted in a considerably improvement of the manuscript quality.
- 6) In the revised manuscript all language-related changes are highlighted in blue colour. Blue colour reflects: *i)* corrected grammar errors, *ii)* the place where cuts occurred within former sentences, *iii)* extra-words used in the revised manuscript, *iv)* full sentences addressing more succinctly ideas from the original manuscript.
- 7) We kindly ask the editorial office to accept our proposal colour-related since working in the track-changes mode significantly affects the readability of the manuscript.

In the revised manuscript the title is proposed in the form

Chemical characteristics of size resolved atmospheric aerosols in Iasi, north-eastern Romania: Nitrogen-containing inorganic compounds **control** aerosols chemistry in the area

Details

Page 3. line 3: '... great concern of interest....' - Maybe better '...great concern and of interest....' Please check the English throughout the manuscript again, possibly but a native speaker or an English language editing service.

As raised under point 5 of the present answer, in the revised form of the manuscript, language problems have been checked. Reviewers suggestion have been also taken into account. In the revised manuscript text composition is significantly improved, mainly as a result of sentences shortening with “sharper” meaning.

Section 2.2: Can anything be said how reliable the sampling of the very small size fractions by the DLPI is? Has this been characterised?

In the manuscript under Section 2.2 after revision we have

“The DLPI unit performs aerosol size classification in 13 specific fractions (with size cuts at 0.0276, 0.0556, 0.0945, 0.155, 0.260, 0.381, 0.612, 0.946, 1.60, 2.39, 3.99, 6.58 and 9.94 μm at 50 % calibrated aerodynamic cut-point diameters and at 21.7 $^{\circ}\text{C}$, inlet pressure 1013.3 mbar, outlet pressure 100 mbar and 29.85 L min^{-1} flow rate).”

However, these aspects should be corroborated with details presented now in Section S1 of the supplement material (SM) where we give:

Section S 1

“Possible explanations for the differences/similarities between afore mentioned studies might be seen as a result of the contributions brought from various factors. As shown below the differences in the PM mass concentrations reported in Galon et al. and those reported in Arsene et al. (2011) might be only slightly controlled by changes in the particle size cut-off and/or by the difference in sampling site altitude (25 m in Galon et al. vs. 35 m in Arsene et al. (2011)) which is too small to account for the difference in PM concentrations.

In Arsene et al. (2011) study, aerosol sampling has been undertaken by using a stacked filter unit (SFUs) consisting of a 8.0 μm pore size 47-mm diameter Isopore polycarbonate filter mounted in front of a 0.4 μm pore size 47-mm diameter Isopore filter. According to details in Arsene et al. (2011) and references included therein, the 50% cut-point diameter (D50) of the 8.0 μm pore size filter was estimated to be of the order on 1.5 ± 0.2 μm aerodynamic equivalent diameter (AED). Consequently, particles collected on the 8 μm pore size filters, with a diameter larger than 1.5 μm AED, were referring to the aerosol coarse fraction, while the particles collected on the 0.4 μm pore size filters were attributed to particles with a diameter below 1.5 μm AED. In Galon et al. work aerosols samples were collected on 25 mm in diameter ungreaed aluminum filters using a cascade Dekati Low-Pressure Impactor (DLPI), operating at a flow rate of 29.85 L min^{-1} . Enhanced sampling efficiency of the DLPI unit used in Galon et al. work, with regard to fine and ultrafine particles, has been observed in comparison with the SFU unit reported by Arsene et al. (2011). Parallel DLPI and SFU sampling runs (performed within January–July 2016) showed that the DLPI unit could collect in average with ~ 6 $\mu\text{g m}^{-3}$ more particles than the SFU system and this observation allowed us suggesting that most probably the operational limits of the SFU system with regard to fine and ultrafine particles could suppress to some extend the values reported by Arsene et al. (2011).

The difference observed between the PM_{10} mass concentration, i.e. 18.9 ± 9.3 $\mu\text{g m}^{-3}$, reported by Galon et al. and the PM_{total} mass concentration, i.e. 38.3 ± 25.4 $\mu\text{g m}^{-3}$, reported by Arsene et al. (2011) might actually be the result of sampling in different years with emission sources of various prevalence. Implementation of environmental quality management systems in various sectors with anthropogenic activity may account for that (e.g. attempts given by the local administrative sector in settling down soil- or road-resuspended dust especially over the warm seasons by wetting the roads, protecting areas with intense building activities, etc.).

Regarding other literature available values, in a study from 2016, Alastuey et al. (2016) report for PM_{10} concentrations in Moldova (the closest point to our sampling site), values as high as ~ 25

$\mu\text{g m}^{-3}$ over summer and of $\sim 25\text{--}30 \mu\text{g m}^{-3}$ over winter period, yielding an annual averaged value of $\sim 27.5 \mu\text{g m}^{-3}$ which is much higher than the $18.9 \mu\text{g m}^{-3}$ value reported in the present work, for Iasi, north-eastern Romania. However, the elevated concentrations observed at the eastern sites were attributed to regional or local sources (Alastuey et al., 2016). In Alastuey et al. (2016) the author reports only the altitude above sea level (i.e. 156 m for Moldova's location) and the sampling a.g.l. is not mentioned. It might be that in Alastuey et al. (2016) study if the Moldavian sampling location was assigned as an EMEP site than the sampling a.g.l. was settled in agreement with an EC Directive recommending an a.g.l. of ~ 4 or 8 m. It is believed that the difference observed between Galon et al. site (i.e. $18.9 \pm 9.3 \mu\text{g m}^{-3}$) in comparison with other European sites might actually reflect that sampling altitude would be an important controlling factor to the atmospheric aerosol burden at a site.

In Iasi, north-eastern Romania, mass concentrations in the 5 to $10 \mu\text{g m}^{-3}$ range, for the PM_{10} and $\text{PM}_{2.5}$ fractions were especially observed in samples collected after raining events (i.e., May, June, August, and October). Such behaviour would be expected since particles from the atmosphere might be efficiently removed by precipitation (Arsene et al., 2011). However, during events with strong natural or anthropogenic contributions the PM_{10} and $\text{PM}_{2.5}$ mass concentrations exceeded the averages observed at AMOS. For example, an event collected in April 2016, from 9th to 11th, with $34.3 \mu\text{g m}^{-3}$ in $\text{PM}_{2.5}$ and $43.9 \mu\text{g m}^{-3}$ in PM_{10} , was actually highly influenced by the long range transport phenomena of African dust and marine aerosols from the Black and Aegean/Mediterranean seas (i.e., event described in detail later in the text). For other events, the exceeding fine fraction mass concentrations are believed to be a result of more variable sources (combustion, biogenic, local mineral dust, meteorological factors, etc.).”

Table 2: Maybe the names of the sampling locations from the EMEP measurements can be given.

The names of the sampling locations from the EMEP measurements (Alastuey et al., 2016) are given as a Note under Table 2.

SE12 – Aspvreten (Sweden)
 IE321 – Mace Head (Ireland)
 FR09 – Revin (France)
 DE44 – Melpitz (Germany)
 SK06 – Starina (Slovak Republic)
 HU02 – K-Pusztta (Hungary)
 MD13 – Leova II (Moldavian Republic)
 ES22 – Montsec (Spain)
 IT01 – Montelibretti (Italy)
 GR02 – Finokalia (Greece)

P9, l13: ...Figure... This should be capitalized all over the manuscript.

“Figure...” or “Fig.” has been replaced with “**FIGURE**” or “**FIG.**” in the entire manuscript but the final decision is to be taken by the editorial office.

P15, l21: Is the comparison to the Kanpur measurement helpful here? I cannot fully understand what CaCO₃ has to do with nitrate.

In order to answer referee's question we have included in the revised manuscript:

“Higher abundances of particulate NO_3^- , SO_4^{2-} , NH_4^+ and K^+ in winter compared to summer are reported for other European (Schwarz et al., 2012; Voutsas et al., 2014) and non-European sites as

well (Sharma et al., 2007). Sharma et al. (2007) also suggest a potential role of CaCO_3 in controlling particulate NO_3^- abundance in Kanpur, India.”

This aspect is actually completed by the information given in the manuscript in regard with the potential effect played by dust in the distribution of particulate NO_3^- with a clear shift from the fine- to the coarse-mode. For Iasi, north-eastern Romania we have actually identified that MgCO_3 and not CaCO_3 will be involved in the formation of the coarse mode NO_3^- .

P27, l23: But shouldn't biomass burning have a seasonal pattern?

In order to answer referee's question we have reformulated this aspect in the revised manuscript: “The size distributions of particulate K^+ reflect the occurrence of one dominant fine mode (with maxima at 381 nm) during both the cold and the warm seasons, and of a second less important mode during the warm seasons (with maxima in the 0.946–1.6 μm range). Such behaviour most likely reflects contributions from biomass burning all over the year (Schmidl et al., 2008; Pachon et al., 2013).”

However, potential implications of the biomass burning process towards K^+ seasonal pattern (i.e. K^+ as a tracer of the biomass burning process) has been addressed in more details within the discussion on FIG. 6e.

P28, l30: Please check sentence: '... such as to.....

Language editing problems are entirely addressed within the revised manuscript.

References

- Alastuey, A., Querol, X., Aas, W., Lucarelli, F., Perez, N., Moreno, T., Cavalli, F., Areskoug, H., Balan, V., Catrambone, M., Ceburnis, D., Cerro, J. C., Conil, S., Gevorgyan, L., Hueglin, C., Imre, K., Jaffrezo, J. L., Leeson, S. R., Mihalopoulos, N., Mitosinkova, M., O'Dowd, C. D., Pey, J., Putaud, J. P., Riffault, V., Ripoll, A., Sciare, J., Sellegri, K., Spindler, G., and Yttri, K. E.: Geochemistry of PM_{10} over Europe during the EMEP intensive measurement periods in summer 2012 and winter 2013, *Atmos. Chem. Phys.*, 16, 6107–6129, doi:10.5194/acp-16-6107-2016, 2016.
- Pachon, J. E., Weber, R. J., Zhang, X., Mulholland, J. A., and Russell, A. G.: Revising the use of potassium (K) in the source apportionment of $\text{PM}_{2.5}$, *Atmos. Pollut. Res.*, 4, 14–21, doi: 10.5094/APR.2013.002, 2013.
- Schwarz, J., Stefancova, L., Maenhaut, W., Smolik, J., and Zdimal, V.: Mass and chemically speciated size distribution of Prague aerosol using an aerosol dryer - The influence of air mass origin, *Sci Total. Environ.*, 437, 348–362, doi:10.1016/j.scitotenv.2012.07.050, 2012.
- Schmidl, C., Marr, I. L., Caseiro, A., Kotianova, P., Berner, A., Bauer, H., Kasper-Giebla A., and Puxbaum, H.: Chemical characterisation of fine particle emissions from wood stove combustion of common woods growing in mid-European Alpine regions, *Atmos. Environ.*, 42, 126–141, doi:10.1016/j.atmosenv.2007.09.028, 2008.
- Sharma, M., Kishore, S., Tripathi, S. N., and Behera, S. N.: Role of atmospheric ammonia in the secondary particulate matter: a study at Kanpur, India, *J. Atmos. Chem.*, 58, 1–17, doi:10.1007/s10874-007-9074-x, 2007.
- Voutsas, D., Samara, C., Manoli, E., Lazarou, D., and Tzoumaka, P.: Ionic composition of $\text{PM}_{2.5}$ at urban sites of northern Greece: secondary inorganic aerosol formation, *Environ. Sci. Pollut. Res.*, 21, 4995–5006, doi:10.1007/s11356-013-2445-8, 2014.

Chemical characteristics of size resolved atmospheric aerosols in Iasi, north-eastern Romania: Nitrogen-containing inorganic compounds **control** aerosols chemistry in the area

5 Alina Giorgiana Galon-Negru¹, Romeo Iulian Olariu^{1,2}, Cecilia Arsene^{1,2}

¹"Alexandru Ioan Cuza" University of Iasi, Faculty of Chemistry, Department of Chemistry, 11 Carol I, 700506 Iasi, Romania

²"Alexandru Ioan Cuza" University of Iasi, Integrated Centre of Environmental Science Studies in the North Eastern Region, 11 Carol I, Iasi 700506, Romania

10 *Correspondence to:* Cecilia Arsene (carsene@uaic.ro); Phone number: +40-232-201354; Fax: +40-232-201313; Postal address: Cecilia Arsene, "Alexandru Ioan Cuza" University of Iasi, Faculty of Chemistry, Department of Chemistry, 11 Carol I, 700506 Iasi, Romania

Abstract. This study assesses the effects of particle size and season on the content of the major inorganic and organic aerosol ionic components in the Iasi urban area, north-eastern Romania. Continuous measurements were carried out over 15 2016 by means of a cascade Dekati Low-Pressure Impactor (DLPI) performing aerosol size classification in 13 specific fractions over the 0.0276-9.94 μm size range. Fine particulate Cl^- , NO_3^- , NH_4^+ and K^+ exhibited clear minima during the warm seasons and clear maxima over the cold seasons, mainly due to trends in emission sources, changes in the mixing layer depth and specific meteorological conditions. Fine particulate SO_4^{2-} did not show much variation with respect to seasons. Particulate NH_4^+ and NO_3^- ions were identified as critical parameters controlling aerosols chemistry in the area, and their 20 measured concentrations in fine mode ($\text{PM}_{2.5}$) aerosols were found to be in reasonable good agreement with modelled values for winter but not for summer. The likely reason is that NH_4NO_3 aerosols are lost due to volatility over the warm seasons. We found that NH_4^+ in $\text{PM}_{2.5}$ is primarily associated with SO_4^{2-} and NO_3^- but not with Cl^- . Actually, indirect ISORROPIA-II estimations showed that the atmosphere in the Iasi area might be ammonia-rich during both the cold and warm seasons, enabling enough NH_3 to be present to neutralize H_2SO_4 , HNO_3 and HCl acidic components and to generate fine particulate 25 ammonium salts, in the form of $(\text{NH}_4)_2\text{SO}_4$, NH_4NO_3 and NH_4Cl . ISORROPIA-II runs allowed us to estimate that over the warm seasons $\sim 35\%$ of the total analysed samples had very strong acidic pH (0–3), a fraction that rose to $\sim 43\%$ over the cold seasons. Moreover, while in the cold seasons the acidity is mainly accounted for by inorganic acids, in the warm ones there is an important contribution by other compounds, possibly organic. Indeed, changes in aerosols acidity would most likely impact the gas–particle partitioning of semi-volatile organic acids. Overall, we estimate that within the aerosol mass 30 concentration the ionic mass brings contribution as high as 40.6 %, with the rest still being unaccounted for.

Keywords: urban aerosols, ionic chemical composition, ammonium, nitrate, pH, long range transport, Iasi, Romania.

1 Introduction

Despite dramatic progress made to improve air quality, global air pollution continues harming people's health and the environment. The problem of aerosols or particulate matter (PM) is still a great concern (Olariu et al., 2015) in Europe and many other areas in the world (e.g., China, India, USA). Atmospheric aerosols, described as complex mixtures of liquid and/or solid particles suspended in a gas (Olariu et al., 2015), are mainly originating from anthropogenic and natural sources (Querol et al., 2004). Fine PM_{2.5} particles (airborne particles with an equivalent aerodynamic diameter < 2.5 µm) are air pollutants with significant effects on human health (Pope et al., 2004; Dominici et al., 2006; WHO, 2006a; Directive 2008/50/EC, 2008; Sicard et al., 2011; Ostro et al., 2014) as well as air quality (Directive 2008/50/EC, 2008; Freney et al., 2014), visibility (Tsai and Cheng, 1999; Directive 2008/50/EC, 2008), ecosystems, weather and climate (Ramanathan and Collins, 2001; Directive 2008/50/EC, 2008; IPCC, 2013). Aerosols are also known to play a significant role within the chemistry of the atmosphere (Prinn, 2003), acting as surfaces for heterogeneous chemical reactions (Ravishankara, 1997). Safety threshold values for both PM_{2.5} (10 or 17 µg m⁻³ air, as annual mean) and PM₁₀ (airborne particles with an equivalent aerodynamic diameter < 10 µm; 20 or 28 µg m⁻³ air, as annual mean) are addressed by the WHO (2006b) or by the 2008/50/EC Directive (2008) on ambient air quality and cleaner Europe. With regard to the PM_{2.5} fraction, the EEA Report 5 (2015) indicates that in 2013 the EU daily limit values for PM₁₀ and PM_{2.5} were exceeded in, respectively, 22 and 7 out of the 28 EU member states. However, a decreasing trend was observed when compared with the WHO Report data (2006b). Moreover, on a global scale the PM_{2.5} exposure leads to about 3.3 million premature deaths per year (predominantly in Asia), a figure that could double by 2050 (Lelieveld et al., 2015). Indeed, PM air pollution imparts a tremendous burden to the global public health, because it ranks as the 13th leading cause of mortality (Brook, 2008).

Up to now the chemical composition of atmospheric aerosols is reported for various urban European sites (Bardouki et al., 2003; Hitzenberger et al., 2006; Tursic et al., 2006; Gerasopoulos et al., 2007; Schwarz et al., 2012; Laongsri and Harrison, 2013; Wonaschutz et al., 2015; Sandrini et al., 2016), but such information is very scarce in Eastern Europe (Arsene et al., 2011). Sulfate (SO₄²⁻), nitrate (NO₃⁻) and ammonium (NH₄⁺) ions, which are major inorganic particle constituents (Wang et al., 2005; Bressi et al., 2013; Hasheminassab et al., 2014; Voutsas et al., 2014) are mainly secondary species formed in the atmosphere by chemical reactions of their precursor gases and by physical processes (nucleation, condensation, etc.) (Aksoyoglu et al., 2017). Ammonium aerosols, with an atmospheric lifetime of 1–15 days, have a clear tendency to deposit at large distances from their emission sources (Aneja et al., 2000) and seem to play a very important role in atmospheric chemistry. In urban air, the abundance of NO₃⁻ on fine particles seems to mainly depend on the reaction between HNO₃ and NH₃ (Stockwell et al., 2000). On a global scale, HNO₃ heterogeneous reactions on mineral dust and sea salt particles might be the predominant source of particulate NO₃⁻ (Athanasopoulou et al., 2008; Karydis et al., 2011). The human health effects of atmospheric ammonia, primarily exerted through particulate NH₄NO₃, are gradually acquiring importance compared to NO_x emissions (Sutton et al., 2011).

Relative humidity (RH; Jang et al., 2002) and gas–particle partitioning processes of semi-volatile species (NH_3 , HNO_3 , HCl and some organic acids) affect the hydronium ion (H_3O^+) concentrations (Keene et al., 2004; Guo et al., 2016) as well as aerosol formation and chemical composition. Aerosol acidity is often estimated with ion balance methods (Trebs et al., 2005; Metzger et al., 2006; Arsene et al., 2011), phase partitioning (Meskhidze et al., 2003; Keene et al., 2004) and thermodynamic equilibrium models (e.g., E-AIM, (Clegg et al., 1998; Wexler and Clegg, 2002) or ISORROPIA-II (Nenes et al., 1999; Fountoukis and Nenes, 2007; Hennigan et al., 2015; Guo et al., 2015, 2016; Fang et al., 2017). Acidity might influence transition metals solubility and enhance aerosols toxicity and the delivery of nutrients by atmospheric deposition in marine areas (Meskhidze et al., 2003; Fang et al., 2017).

Unfortunately, the aerosols role in the global atmospheric system is not yet sufficiently understood. The main related challenges are the occurrence of multiple sources (e.g., soil erosion, sea spray, biogenic emissions, volcano eruptions, soot from combustion, condensation of precursor gases) and the complexity of interactions with other atmospheric constituents (Zhang et al., 2015). Nowadays, sources, distribution and behaviour of natural and anthropogenic aerosols are still a matter of debate, exacerbate by the scarcity of aerosols-related work for eastern EU countries (EEA Report 5, 2015) but also by the existent discrepancies between models and field measurements. The main uncertainties are related to secondary inorganic aerosols that control the availability of atmospheric sulfuric acid (H_2SO_4), nitric acid (HNO_3) and ammonia (NH_3) (Ianniello et al., 2011). The existing knowledge gaps bring high uncertainty in the estimated radiative forcing, although they do not impair the conclusion that warming of the climate system is unequivocal (IPCC, 2013).

Despite a growing international recognition of the importance of air pollution and air quality problems, there is a definite need to assess air pollution patterns in Romania. The existing data for north-eastern Romania concern the chemical characteristics of ambient air pollutants such as the water-soluble ionic constituents of aerosols (Arsene et al., 2011) and rainwater (Arsene et al., 2007). Recent work performed by Arsene's group in the field of atmospheric chemistry has clearly shown that, in the Iasi urban environment (north-eastern Romania), ~ 59 % of the total aerosol mass concentration is still unaccounted for. The present work reports for the first time detailed information on the chemical composition and seasonal variation of size-segregated, water-soluble ions in aerosol samples collected throughout 2016 in the Iasi urban area, also taking into account the potential ongoing chemistry and the contributions of critical driving forces such as meteorological factors (relative humidity, temperature), mixing layer depth and emission sources intensity. As a first attempt to assess particles acidity in the area, the present work highlights the existence of significant aerosol fractions characterized by pH values in the very strong acidity range (0-3 pH units), with potentially important implications on acid rain. Moreover, the potential importance of gaseous precursors (e.g., NH_3 , HNO_3 , HCl) on secondary inorganic PM is also discussed.

2 Experimental

2.1 Measurement site

Measurements were performed in Iasi, north-eastern Romania, at the Air Quality Monitoring Station (AMOS, 47°9' N latitude and 27°35' E longitude) of the Integrated Centre of Environmental Science Studies in the North Eastern Region, "Alexandru Ioan Cuza" University of Iasi, CERNESIM-UAIC, Romania. AMOS is located north-east from the city centre, on the rooftop of the highest University building (~ 35 m above the ground level), in a totally open area that characterises the site as a urban receptor point most probably influenced by well-mixed air masses. A comprehensive demo-geographical characterization of Iasi is described in detail by Arsene et al. (2007, 2011). However, according to a more recent estimate of the Romanian National Institute of Statistics, in 2016 the population in Iasi reached about 362,142 inhabitants (Ichim et al., 2016).

2.2 Field measurements

Size resolved atmospheric aerosols were collected on ungreased aluminium filters (25 mm diameter) using a cascade Dekati Low-Pressure Impactor (DLPI) operating at a flow rate of 29.85 L min⁻¹. Similar devices have been successfully used in other studies (Kocak et al., 2007; Wonaschutz et al., 2015). The DLPI unit performs aerosol size classification in 13 specific fractions (with size cuts at 0.0276, 0.0556, 0.0945, 0.155, 0.260, 0.381, 0.612, 0.946, 1.60, 2.39, 3.99, 6.58 and 9.94 µm at 50 % calibrated aerodynamic cut-point diameters and at 21.7 °C, inlet pressure 1013.3 mbar, outlet pressure 100 mbar and 29.85 L min⁻¹ flow rate). Sampling performance of the DLPI unit was verified through comparison with simultaneous measurements performed with a stacked filter unit (SFU) system previously used by Arsene et al. (2011). Before each reuse the sampler's components were cleaned with ultra pure water and methanol. Disposable polyethylene gloves were always used to avoid hand contact with sampler's components, which were assembled and disassembled in a Labguard Class II Safety Biological Cabinet, NuAire. The DLPI sampler was transported to and from the field in tightened polyethylene bags. Sampling was performed in 2016 twice a week, on weekend and working days, for a total of 84 sampling events (41 during the cold seasons from October to March, and 43 during the warm seasons from April to September), generating 1092 size resolved aerosol samples. Sampling took place on a 36 h basis, with each sampling event starting at 18:00 local time. It was collected an average volume of 64.33 ± 0.85 m³ per sampling. At least two field blanks (consisting of loaded sampler taken to and from the field but never removed from its tightened bag) were generated and simultaneously analysed together with the laboratory blanks, in order to assess possible contamination during sampler loading, transport, or analysis. Meteorological parameters including atmospheric temperature (AT), relative humidity (RH), wind speed (WS), wind direction and global radiation were provided by a Hawk GSM-240 weather station, running at the AMOS site. Information about the mixing layer depth (atmospheric boundary layer) and its ability to dilute atmospheric pollutants at the investigated site was obtained from the NOAA Air Resources Laboratory (ARL) website (Stein et al., 2015; Rolph et al., 2017).

2.3 Sample analyses

Aerosols masses for both the PM_{2.5} and PM₁₀ fractions were gravimetrically determined with a Sartorius microbalance (MSU2.7S-000-DF, $\pm 0.2 \mu\text{g}$ sensitivity) by weighing aluminium filters before and after sampling. Before weighing, filters stored in Petri dishes were kept for at least 3 days in a conditioned room at $40 \pm 2\%$ RH and at $20 \pm 2^\circ\text{C}$. In between different procedure, they were appropriately stored in zipped plastic bags.

Chemical analyses for water-soluble anions (i.e., acetate, ($\text{C}_2\text{H}_3\text{O}_2^-$), formate, (HCO_2^-), fluoride, (F^-), chloride, (Cl^-), nitrite, (NO_2^-), nitrate, (NO_3^-), phosphate, (PO_4^{3-}), sulfate, (SO_4^{2-}) and oxalate, ($\text{C}_2\text{O}_4^{2-}$)) and water-soluble cations (i.e., sodium, (Na^+), potassium, (K^+), ammonium, (NH_4^+), magnesium, (Mg^{2+}) and calcium (Ca^{2+})) were performed by ion chromatography (IC) on a ICS-5000⁺ DP DIONEX system (Thermo Scientific, USA). Analyses were performed within a week from sampling, in aqueous extracts of the collected samples. For chemical analysis, steps in the analytical procedures were strictly quality-controlled to avoid contamination.

After sampling and all other required preparative steps, one half of each collected filter was ultrasonically extracted for 45 minutes in 5 mL deionized water (resistivity of $18.2 \text{ M}\Omega\cdot\text{cm}$) produced by a Milli-Q Advantage A10 system (Millipore). Filtered extracts ($0.2 \mu\text{m}$ pore size cellulose acetate filters, ADVANTEC) were analysed on an IonPac CS12A ($4\times 250 \text{ mm}$) analytical column for cations and an IonPac AS22 ($4\times 250 \text{ mm}$) column for anions, running simultaneously on the IC system. The chromatographic instrumental set-up was completed by CSRS $300\times 4 \text{ mm}$ and AERS $500\times 4 \text{ mm}$ electrochemical suppressors and conductivity detectors. Ions analyses were performed under isocratic elution mode, using $\text{CO}_3^{2-}/\text{HCO}_3^-$ ($4.5/1.4 \text{ mM}$, 1.2 mL min^{-1}) as mobile phase for anions and methanesulfonic acid (20 mM , 1.0 mL min^{-1}) for cations.

Traceable standard solutions (Dionex Seven Anions II and Dionex Six Cations II) were used to generate calibration curves for each species of interest, all having correlation coefficients R^2 well above 0.995. The detection limits of the major species (defined as 3 times the standard deviation of blank measurements relative to the methods sensitivity) on a 36 h measurement period were: $0.0003 \mu\text{g m}^{-3}$ for NH_4^+ ($3.2 \mu\text{g L}^{-1}$), $0.001 \mu\text{g m}^{-3}$ for Na^+ ($13.4 \mu\text{g L}^{-1}$), $0.0015 \mu\text{g m}^{-3}$ for K^+ ($19.8 \mu\text{g L}^{-1}$), $0.0002 \mu\text{g m}^{-3}$ for Mg^{2+} ($3.2 \mu\text{g L}^{-1}$), $0.0016 \mu\text{g m}^{-3}$ for Ca^{2+} ($20.6 \mu\text{g L}^{-1}$), $0.0010 \mu\text{g m}^{-3}$ for SO_4^{2-} ($13.2 \mu\text{g L}^{-1}$), $0.0012 \mu\text{g m}^{-3}$ for NO_3^- ($15.1 \mu\text{g L}^{-1}$); and $0.0019 \mu\text{g m}^{-3}$ for Cl^- ($24.9 \mu\text{g L}^{-1}$). Ions concentrations in analysed blank filters (laboratory and field) were subtracted from their corresponding concentrations in the aerosol samples.

The sum of the detected ions, or of the gravimetrically determined mass concentration, over all DLPI stages is hereafter termed “PM₁₀ fraction”, while the sum over impactor stages from 1 to 10 is termed “PM_{2.5} fraction”. Modal diameters of the size segregated aerosols particles or of the analysed ionic components (individual or as a sum) were determined by fitting lognormal distributions.

2.4 Estimation of the aerosols acidity

The thermodynamic model proposed by Fountoukis and Nenes (2007), i.e. ISORROPIA-II (<http://isorro피아.eas.gatech.edu/>), was used to get an estimate of the in-situ potential acidity of our PM_{2.5} fractions. ISORROPIA-II thermodynamic equilibrium

model calculates the gas/liquid/solid equilibrium partitioning of K^+ , Ca^{2+} , Mg^{2+} , NH_4^+ , Na^+ , SO_4^{2-} , NO_3^- , Cl^- and aerosol water content, and it can predict particles pH. Up to now the model has been used in various field campaigns data analysis (Nowak et al., 2006; Fountoukis et al., 2009).

To obtain the best predictions of aerosols pH, ISORROPIA-II was run in the “forward mode” for metastable aerosol state, as preliminary runs of the experimental data in the “reverse mode” did not supply suitable information. In the “metastable” mode the aerosol is assumed to be present only in the aqueous phase, either supersaturated or not (Fountoukis and Nenes, 2007). As model input data we used just aerosol-phase ion concentrations measured by IC, along with relative humidity and temperature data from the Hawk GSM-240 weather station. Actually, in the absence of accompanying gas-phase data required to constrain the thermodynamic models, the accuracy of aerosol pH predictions can be enhanced by using the aerosol concentrations in “forward mode” calculations (Guo et al., 2015; Hennigan et al., 2015), which seem to be less sensitive to measurement errors than the “reverse mode”. Where required, NH_3 data predicted by ISORROPIA-II were used for the interpretation of the results.

2.5 Air mass back trajectories and air mass origin

Air mass back trajectories were calculated using the HYSPLIT 4 model of the NOAA Air Resources Laboratory (Stein et al., 2015; Rolph et al., 2017). Forty-eight hour back trajectories, arriving at the investigated site at 18:00 local time (15:00 UTC), were computed at 500, 1000 and 2000 m altitudes above the ground level. Four major sectors of air masses origin were distinguished, and their contributions are shown in FIG. 1. The most and least frequent sectors were the north-eastern (N-E, 36.6 %) and the south-south-eastern (S-SE, 11.4 %) ones, respectively. The W-SW sector is mainly prevailing during winter, while the N-E sector is most common during summer. The NW sector had a slightly enhanced frequency in winter and summer that according to James (2007), could reflect a possible European monsoon circulation. Events from the S-SE sector, prevailing mainly in spring, carried out marine chemical features highly influenced by the Black Sea. Air masses undertaking faster vertical transport most probably due to the locally/continentally driven buoyancy (Holton, 1979; Seinfeld and Pandis, 1998), travelling above large (long range transport) or short (local) continental areas were also identified. For instance, in April 2016 five sampled events out of a total of eight were highly influenced by fast vertical air mass transport. In these events, air masses from both 500 and 1000 m altitude went down to below 500 meters (brushing the ground surface), with strong impact on the chemical composition of the collected particles (vide infra).

3 Results and discussion

3.1 Variability of PM_{10} and $PM_{2.5}$ mass concentrations

Table 1 shows summary statistics (median, geometric mean, arithmetic mean, standard deviation, minimum and maximum) for PM_{10} and $PM_{2.5}$ mass concentrations at the AMOS site for both working days and weekends. Statistical tests were applied to determine whether there are significant differences among working days and weekends. The Shapiro-Wilk normality test

applied to both PM_{2.5} and PM₁₀ indicated that the entire data-base was normally distributed (detailed statistics are given in Table S 1 from Supplement Material, SM). Moreover, the difference in the mean values of the two groups was not high enough to exclude random sampling variability, thereby suggesting that the differences are not statistically significant. Therefore, local anthropogenic activities seem to bring similar contribution to the aerosol burden in the area on both working days and weekends. However, the PM₁₀ annual mean mass concentration (18.95 µg m⁻³) did not exceed the WHO 20 µg m⁻³ air annual mean value, while the PM_{2.5} annual mean mass concentration (16.92 µg m⁻³) exceeded the 10 µg m⁻³ air annual mean value set by WHO (2006b).

Table 2 presents the annual and/or seasonal arithmetic means of PM₁₀ and PM_{2.5} mass concentrations in Iasi, compared to other European sites (mean ± stdev). The annual averages obtained in the present work show differences in comparison with those reported by Arsene et al. (2011) for the same site. Arsene et al. (2011) have used a SFU system consisting of a 8.0 µm pore size, 47-mm diameter Isopore polycarbonate filter mounted in front of a 0.4 µm pore size, 47-mm diameter Isopore filter. However, the values determined in the present work for the fractions PM_{0.027-1.6} (15.6 ± 8.7 µg m⁻³) and PM_{0.381-1.6} (9.1 ± 5.6 µg m⁻³) are much closer to those reported by Arsene et al. (2011) for PM_{1.5} (10.5 ± 11.2 µg m⁻³). The potential influence on the PM levels of particle size cut-off, differences in sampling site altitude, occurrence of precipitation events, long-range transport phenomena, and air masses buoyancy is presented in detail in Section S 1 of the SM.

FIGURE 2 shows monthly arithmetic mean mass concentrations (± standard deviations) of PM₁₀ and PM_{2.5} in Iasi. The distribution of the PM_{2.5}/PM₁₀ ratio is presented in the same figure. The relative contribution of PM_{2.5} toward PM₁₀ showed low variability amongst the months of the year, with ratios ranging from ~ 0.75 to ~ 1.0. For urban background and/or traffic sites, WHO (2006a) suggests PM_{2.5}/PM₁₀ ratios in the 0.42–0.82 range. Seasonal patterns, with maxima during the cold and minima during the warm seasons, are observed for all of the PM_{2.5}, PM₁₀ and PM_{2.5}/PM₁₀ profiles and might be the combined result of seasonal emissions variations, local- and long-range air transport and dispersion, chemical processes, and deposition (Wang et al., 2016). The maxima of PM_{2.5}/PM₁₀ during the cold seasons are most probably caused by combustion processes as the burning of coal/petroleum for heating purposes enhances secondary aerosols generation (Li et al., 2012). The lower PM_{2.5}/PM₁₀ values during the warm seasons might be due to dust events and to more intense anthropogenic activities near the sampling site (e.g., excavation, construction and building renewal) that would both cause higher loading of coarse particles in the atmosphere. As suggested by Zhang et al. (2001), various land use categories (e.g., grass, crops, mixed farming, shrubs) corroborated with other particle-related characteristics (i.e., particle density, relevant meteorological variables) may enhance the dry deposition of sub-micron particles during the warm seasons and hence their fine/coarse ratio. Another clear seasonal pattern was observed for the mass concentration size distribution (FIG. 3). Over the cold seasons, it had a clear monomodal feature with maximum at 381 nm. In contrast, the warm seasons were characterized by the same dominant fine mode, but also by the occurrence of a super-micron mode between 1.60–2.39 µm. Again, changes in sources contributions and meteorological conditions could account for the observed differences (details in Section S 2 of the SM).

3.2 Ionic balance, seasonality of water soluble ions and stoichiometry of $(\text{NH}_4)_2\text{SO}_4$ and NH_4NO_3

3.2.1 Ionic balance and potential aerosols acidity

The completeness of the ionic balance was checked for the identified and quantified species (F^- , Cl^- , NO_2^- , NO_3^- , PO_4^{3-} , SO_4^{2-} , HCO_2^- , $\text{C}_2\text{H}_3\text{O}_2^-$, $\text{C}_2\text{O}_4^{2-}$, Na^+ , K^+ , NH_4^+ , Mg^{2+} and Ca^{2+}) in both PM_{10} and $\text{PM}_{2.5}$. The slopes in the raw ion chromatography data related to \sum_{cations} vs. \sum_{anions} were < 1 in both $\text{PM}_{2.5}$ and PM_{10} (detailed statistics in Table S 2), pointing to an important cation deficit that was higher in the cold compared to the warm seasons. However, for each sampling event, either cation or anion deficit was observed in various impactor stages. It should also be noted that, at the investigated site, it was even observed $\text{RH} \sim 82\%$ during the cold seasons.

Predicting pH is suggested as the best method to analyse particle acidity (Guo et al., 2015). The ion balance method is usually based upon the principle of electroneutrality, and any deficit in measured cationic compared to anionic charge is assigned to the presence of unmeasured protons (H^+). The reverse occurs for unmeasured hydroxyl (OH^-) (Hennigan et al., 2015) or bicarbonate/carbonate ($\text{HCO}_3^-/\text{CO}_3^{2-}$) (Fountoukis and Nenes, 2007). In the present work, $\text{HCO}_3^-/\text{CO}_3^{2-}$ was assigned as the missing anion (details in Section S 3 for $\text{HCO}_3^-/\text{CO}_3^{2-}$ estimation) while NH_4^+ as the main missing cation (details in Section S 4 for the missing NH_4^+ assumptions). Detailed statistics of the \sum_{cations} vs. \sum_{anions} dependences, with $\text{HCO}_3^-/\text{CO}_3^{2-}$ and missing NH_4^+ included in the ionic balance, is presented in Table S 3.

In an attempt to investigate whether or not the H^+ species would bring an important contribution within the ionic balance, ISORROPIA-II thermodynamic equilibrium model proposed by Fountoukis and Nenes (2007) has been used in the present work (more details about ISORROPIA-II runs in Section S 5 of the SM). We investigated the relationship between ISORROPIA-II predicted aerosol pH and the ionic balance for the present data-base, and the results are presented in FIG. 4a. The data remarkably follow a traditional titration curve, and they also clearly show that many of the analysed particles were \sim neutral (dashed lines at 0). A very important fraction of the investigated samples was in the acidic range ($\text{pH} < 3$ if samples were in cation deficit mode), while the remaining fraction was alkaline (pH slightly above 7 with an anion deficit mode). However, as suggested by Hennigan et al. (2015), small uncertainties in the ionic balance (mainly due to measurement uncertainties and more likely in \sim neutral conditions) may lead to shifts that span over about 10 pH units. Moreover, the sensitivity to changes in the aerosol NH_4^+ concentration has been checked in predicted aerosol pH under forward-mode calculation. As shown in FIG. 4b, it seems that the predicted pH might decrease by 2 % when the ionic balance takes into account NH_4^+ (total) concentration (defined as the sum between that derived from raw IC data and the part estimated by using the rationale of Arsene et al. (2011)). Details on the pH sensitivity tests toward NH_4^+ concentrations are given in Section S 6. In Iasi, north-eastern Romania, an important fraction of the total analysed samples was alkaline while the remaining part was acidic. A more detailed view of the samples pH distribution can be obtained from the data presented in FIGS. 4c,d. It seems that over the warm seasons about 55–56 % of the analysed samples were alkaline ($\text{pH} > 7$) and about 44–45 % were acidic ($\text{pH} < 7$), with the last fraction mainly distributed in the very strong acidity fraction ($\sim 35\%$ of the samples with pH in the 0–3 range, and about 2 % with aerosol pH less than 0). Over the cold seasons only 47 % of the total analysed samples were

alkaline ($\text{pH} > 7$) and 53 % were acidic ($\text{pH} < 7$). The acidity was also mainly distributed in the very strong acidity fraction (~ 43 % of the acidic samples with pH in the 0–3 range). Sulfuric, nitric, hydrochloric and formic acids are the most likely contributors to aerosols pH in the 0–3 range. Note that strongly acidic aerosols affect air quality, health of aquatic and terrestrial ecosystems (especially through acid deposition), as well as atmospheric visibility and climate (Dockery et al., 1996; Gwynn et al., 2000; Hennigan et al., 2015). Possible impacts of strongly acidic aerosols are presented in more detail in Section S 7. Moreover, aerosols acidity can impact the gas–particle partitioning of semi-volatile organic acids. While under strongly acidic conditions (pH 1–3) the pH contribution of organic acids is expected to be negligible as these conditions prevents their dissociation, the scenario may change completely at pH values of 3–7 (vide infra). Under these circumstances, formic acid with $\text{pK}_a = 3.75$ (Bacarella et al., 1955) might give a significant pH contribution to $\sim 7\%$ of the warm-season samples and $\sim 10\%$ of the cold-season ones.

FIGURES 5a,b present the size distribution of averaged aerosol mass, NO_3^- , SO_4^{2-} and NH_4^+ concentrations while FIGS. 5c,d present ISORROPIA-II estimates for pH and H^+ mass concentration distributions, for both the cold (FIGS. 5a,c) and the warm (FIGS. 5b,d) seasons. Clear monomodal distribution seems to be specific for the cold seasons, while for the warm seasons the second mode (1.60–2.39 μm) mass concentration distribution seems to be predominated by NO_3^- . For the 155–612 nm size range, from details presented in FIGS. 5c,d, it is quite clear that $\text{pH} \leq 2$. In the present work, the aerosol H^+ levels inferred indirectly from the ion balance as proposed by Hennigan et al. (2015) showed statistically significant correlation with the H^+ loadings predicted by ISORROPIA-II in the forward mode (Pearson coefficient of 0.72, $p < 0.001$). However, despite the good correlation, there were important discrepancies between the two estimated H^+ levels (intended as absolute values), with those from ISORROPIA-II being considerably lower than those from the ionic balance. The main issue with the model is that it may account only for partial dissociation, while the ionic balance may be affected by the uncertainty due to the propagation of measurement error. The latter may be particularly important in the presence of a slight anion deficit balance, which is interpreted as an H^+ loaded system. Despite the uncertainties in the actual pH values, it is very likely that the 155–612 nm aerosol particles are strongly acidic and that H^+ is mainly contributed by completely dissociated strong acids such as H_2SO_4 and HNO_3 . Contributions from free acidity (dissociated H^+) or total acidity (free H^+ and undissociated H^+ bound to weak acids) is expected to be more important in all other remaining fraction, and especially in the 27.6–94.5 nm particles size range (vide infra). Of course, a higher confidence in the estimate of particles pH would allow better prediction of the chemical behaviour of organics that, if dissociated at relatively low acidities, would significantly contribute to the ion balance.

In the literature there is suggestion that the molar ratio approach may be a proxy for aerosol pH estimation (Hennigan et al., 2015). However, such a procedure is highly susceptible to bias the results, either due to exclusion of minor ionic species or because it does not consider the effects of aerosol water or species activities on particle acidity. In this work, even when the aerosol was inferred to be highly acidic (samples with molar ratio $\text{NH}_4^+ / (\text{Cl}^- + \text{NO}_3^- + 2 \times \text{SO}_4^{2-}) < 0.75$), there was no statistically significant correlation between the cation/anion molar ratio and $[\text{H}^+]$ from either ion balance or model

predictions. Therefore, the molar ratio does not appear to be a suitable tool to infer the acidity of atmospheric particles at the study site, but it could be a good parameter to distinguish between alkaline and acidic particles.

Data on gaseous NH_3 were not available, but the potential relationship was also investigated between $\text{NH}_3/\text{NH}_4^+$ phase partitioning (with NH_3 values predicted by ISORROPIA-II) and particles pH. The hypothesis of phase partitioning equilibrium is justified by the fact that the sampling time-interval (36 h) was much longer than the equilibration time for submicron particles (seconds to minutes; Meng et al., 1995). As previously mentioned, in the present work the number of samples with $\text{pH} < 0$ was significantly lower compared to those with $\text{pH} > 0$. Moreover, ISORROPIA-II predicted that in the 94.5–612 nm size range there would be a significant NH_3 fraction in the gas phase.

The detailed $\text{NH}_3/\text{NH}_4^+$ partitioning as a function of RH is presented below, and considerations on the potential effects on the partitioning brought about by changes in the SO_4^{2-} and NO_3^- concentrations, and by temperature affecting both SO_4^{2-} and NO_3^- production, is given in Section S 8 of the SM. The potential role played by temperature on $\text{NH}_3/\text{NH}_4^+$ partition seems to be minimal, but one should also consider that highly acidic aerosols will affect a variety of processes and definitely the partitioning of HNO_3 to the gas phase, producing low nitrate aerosol levels. ISORROPIA-II runs predicted gas-phase NH_3 concentrations in Iasi as high as 0.52 ± 0.28 (0.46) [mean \pm stdev (median)] $\mu\text{g m}^{-3}$ at $\text{RH} < 40\%$, 0.61 ± 0.26 (0.49) $\mu\text{g m}^{-3}$ at $\text{RH} = 40\text{--}60\%$, and 0.96 ± 0.54 (0.92) $\mu\text{g m}^{-3}$ at $\text{RH} > 60\%$. These warm-season values are smaller than those reported in a modelling study by Backes et al. (2016), who predicted NH_3 abundances as high as 1.6 to 2.4 $\mu\text{g m}^{-3}$ (data extracted from NH_3 concentration for the reference case, i.e., FIG. 3 in Backes et al., 2016, for north-eastern Romania). In contrast, the 0.96 ± 0.54 (0.92) $\mu\text{g m}^{-3}$ value at $\text{RH} > 60\%$, which would be mainly found during the cold seasons, seems to be in reasonable agreement with the ≤ 0.8 $\mu\text{g m}^{-3}$ value modelled by Backes et al. (2016) over winter-time. Moreover, from ISORROPIA-II runs performed at $\text{RH} < 40\%$, it was estimated that $(77.6 \pm 28.4)\%$ or $(79.3 \pm 26.2)\%$ (mean \pm stdev) of the NH_3 predicted by ISORROPIA-II could be present in the gaseous phase (with reference to both NH_4^+ derived from raw IC data, and to the $\text{NH}_4^+(\text{total})$ fraction). Similar but slightly decreasing values were predicted for gas-phase NH_3 as RH increased, namely $(76.5 \pm 30.9)\%$ or $(78.6 \pm 28.2)\%$ (raw IC and $\text{NH}_4^+(\text{total})$, respectively) at $\text{RH} = 40\text{--}60\%$ and $(68.3 \pm 36.7)\%$ or $(74.5 \pm 29.7)\%$ at $\text{RH} > 60\%$.

In other studies, thermodynamic equilibrium calculations predicted that all of the NH_3 was mainly susceptible of partitioning to the particle phase at the equilibrium, and also that > 44 or 51% of the investigated samples presented aerosols $\text{pH} < 0$ (Hennigan et al., 2015). However, it seems that at the investigated Romanian site the atmosphere could be rich enough in NH_3 so as to allow its occurrence on the gas phase while also promoting particle-phase partitioning. The seasonal trends in the NH_3 concentrations derived from ISORROPIA runs for Iasi are reported in FIG. S 1 (Section S 9). The same section reports considerations on possible interrelated emission factors governing the distribution in the NH_3 concentration levels in Iasi.

The ISORROPIA-II data referred to the 155–612 nm size range (regardless of RH) suggested that the aerosol ammonium fraction ($\text{NH}_4^+(\text{NH}_3 + \text{NH}_4^+)$) was over 0.20 irrespective of the calculation procedure (raw IC or $\text{NH}_4^+(\text{total})$). Clear ($\text{NH}_4^+(\text{NH}_3 + \text{NH}_4^+)$) maxima were observed at 381 nm (raw IC data: 0.71 at $\text{RH} < 40\%$, 0.63 at $\text{RH} = 40\text{--}60\%$, and 0.76

at RH > 60 %; $\text{NH}_4^+(\text{total})$, defined as the sum between that derived from raw IC data and the part estimated by using the rationale of Arsene et al. (2011): 0.66 at RH < 40 %, 0.56 at RH = 40–60 %, 0.65 at RH > 60 %). As seen in FIGS. 5c,d, the aerosol pH is very low in the 155–612 nm size range, while it often approaches 8 in the 27.6–94.5 and 612–9940 nm size ranges. Although not presented, in the 155–612 nm size range the aerosol ammonium fraction ($\text{NH}_4^+(\text{NH}_3 + \text{NH}_4^+)$) approaches 1, while in other two size ranges it is very low or close to 0 thereby suggesting the occurrence of gaseous NH_3 .

3.2.2 Seasonality of the major water-soluble ions

Table 3 shows monthly-based statistics for meteorological variables and mass concentrations of PM_{10} , $\text{PM}_{2.5}$ and major water-soluble ions in $\text{PM}_{2.5}$. Compared to the $\text{PM}_{2.5}$ fraction, in the PM_{10} fraction we observed increases in the mass concentrations of the following ions (notation for the % increase: min–max (mean)): 13–80 % (35 %) for Cl^- ; 1–107 % (32 %) for NO_3^- ; 1–170 % (17 %) for SO_4^{2-} ; 38–185 % (63 %) for HCO_3^- ; 14–171 % (41 %) for acetate; 4–136 % (22 %) for formate; 0–294 % (27 %) for oxalate; 16–48 % (32 %) for Na^+ ; 6–58 % (20 %) for K^+ ; 1–105 % (12 %) for $\text{NH}_4^+(\text{total})$; 28–83 % (46 %) for Mg^{2+} , and 33–123 % (61 %) for Ca^{2+} . However, the PM_{10} and $\text{PM}_{2.5}$ mass concentrations fractions show statistically significant correlation with a ratio of 1.1 (Pearson coefficient of 0.99, $p < 0.001$). Higher mass concentrations of specific water-soluble ions (Cl^- , NO_3^- , K^+ , NH_4^+ and, to some extent, SO_4^{2-}) were observed during the cold compared to the warm seasons, probably because of the combination of increased strength of pollution sources and meteorological effects (inducing lower mixing heights or even temperature inversion), or due to different chemical/photochemical processing. Although lowering mixing heights over the cold seasons might increase pollutant concentration in the atmosphere, for some species additional phenomena should be taken into account in order to explain their distribution. For particulate SO_4^{2-} , high concentrations can be observed during winter and autumn but also in summer, and in the latter case they can be due to higher temperature and solar radiation that enhance photochemical reactions and the atmospheric oxidation potential, because of the elevated occurrence of oxidant species such as ozone, hydroxyl and nitrate radicals. These conditions favour the oxidation of SO_2 to particulate SO_4^{2-} . Also particulate $\text{C}_2\text{O}_4^{2-}$ was maximum in summer, possibly due to enhanced photochemical processing. Moreover, the maxima observed for SO_4^{2-} during the cold seasons might be due to the intensification of coal burning for heating purposes. Higher abundances of particulate NO_3^- , SO_4^{2-} , NH_4^+ and K^+ in winter compared to summer are reported for other European (Schwarz et al., 2012; Voutsas et al., 2014) and non-European sites as well (Sharma et al., 2007). Sharma et al. (2007) also suggest a potential role of CaCO_3 in controlling particulate NO_3^- abundance in Kanpur, India. Seasonal variations for selected water-soluble ionic components in $\text{PM}_{2.5}$ are shown in FIGS. 6a-h, while FIG. 6i reports the variation of the mixing layer depth at the investigated site. Fine particulate Cl^- , NO_3^- , K^+ , $\text{NH}_4^+(\text{total})$, and to some extent even SO_4^{2-} , seem to exhibit distinct seasonal variations with maxima during the cold and minima over the warm seasons, which might be related to changes in the mixing layer depth. The summer minima observed for both NO_3^- and NH_4^+ are not surprising, because NH_4NO_3 is volatile and tends to dissociate to gas-phase NH_3 and HNO_3 at high temperatures. Coarse particulate $\text{C}_2\text{O}_4^{2-}$, Ca^{2+} and Na^+ did not show much variation with respect to seasons. However, SO_4^{2-} and $\text{C}_2\text{O}_4^{2-}$ showed similar patterns (implying most probably common sources), and the Ca^{2+} trend suggests prevalent contribution from soil

dust. Higher ion concentrations in winter than in summer are reported by Sharma et al. (2007) for Kanpur (India), while Ianniello et al. (2011) report opposite trends for Beijing (China).

Particulate Cl^- mass concentrations show a clear seasonal pattern, with higher values during the cold than during the warm seasons (FIG. 6a). The chloride mass concentration in both $\text{PM}_{2.5}$ and PM_{10} had a statistically significant correlation with RH, temperature (only for PM_{10} fraction), particle loading and mixing layer depth (detailed statistics in Table S 4). The chloride maxima during the cold seasons might be the result of increased coal burning for heating purposes or of the use of NaCl in winter on icy/snowy roads. These observations are in agreement with other studies in eastern European sites (Arsene et al., 2011; Alastuey et al., 2016). However, the Cl^- mass concentration follows a similar pattern as that of K^+ (tracer of biomass burning), thereby suggesting that over the cold seasons wood burning might become an important heating source (Christian et al., 2010; Akagi et al., 2011).

Also nitrate shows cold-season maxima and warm-season minima (see Table 3 and FIG. 6b). The inset distribution presented within NO_3^- seasonal variation (FIG. 6b) suggests that, in summer, the coarse PM fraction can bring significant contributions to the aerosol atmospheric burden of nitrate. In our work, fine particulate NO_3^- mass concentrations varied from 0.31 to 3.62 $\mu\text{g m}^{-3}$ (Table 3) and these data are in very good agreement with those predicted for Europe in a modelling study performed by Backes et al. (2016). The data obtained in the present work over the cold seasons ($3.62 \pm 1.10 \mu\text{g m}^{-3}$ in January, February, December as the coldest months of the year, and $2.65 \pm 0.38 \mu\text{g m}^{-3}$ over January, February, March, October, November, and December) seem to be in reasonably good agreement with those predicted for Europe by Backes et al. (2016). In contrast, the $0.59 \pm 0.30 \mu\text{g m}^{-3}$ NO_3^- concentration in $\text{PM}_{2.5}$ measured over the warm seasons (including the April month characterised by predominant air-mass buoyancy, and decreasing down to $0.44 \pm 0.12 \mu\text{g m}^{-3}$ if the April month is excluded) is lower than that predicted by Backes et al. (2016) (abundances as high as $0.8 \mu\text{g m}^{-3}$ over summer). Similarly to the NH_4^+ case, this might reflect the susceptibility of NO_3^- to be transferred to the gas phase over the warm seasons.

The NO_3^- mass concentrations in both $\text{PM}_{2.5}$ and PM_{10} had a statistically significant correlation with RH, temperature, mixing layer depth and particles loading (Table 3, detailed statistics in Table S 4). However, it has to be observed that highly acidic aerosols expected over all seasons have the potential to affect the partitioning of HNO_3 to the gas phase, producing low nitrate aerosol levels. Guo et al. (2015) also report low nitrate aerosol levels during summer. Moreover, NO_3^- heterogeneous formation (i.e., condensation or absorption of NO_2 in moist aerosols or N_2O_5 oxidation and HNO_3 condensation) generally relates to RH and the particulate loading (Wang et al., 2006; Ianniello et al., 2011). At the investigated site, this process might be of similar importance as the gas-particle conversion, which implies oxidation of precursor gases, such as NO_x , to nitrate via HNO_3 formation and involving photochemical processes. The high concentration of NO_3^- during the cold seasons might also be caused by higher NH_3 atmospheric levels from yet unaccounted sources, which could neutralize gas-phase H_2SO_4 and HNO_3 to produce ammonium salts (vide infra). Reactive nitrogen species are emitted to the atmosphere mainly in the forms of NO_x (from transport or power generation) and NH_3 (agriculture). In Iasi, the animal husbandry sector (open and closed barns, manure storage/spreading) is most likely an important NH_3 source. Moreover, the high relative humidity observed in the cold seasons could offer suitable conditions for significant fractions of

HNO₃ and NH₃ to be dissolved in humid particles, therefore enhancing particulate-phase NO₃⁻ and NH₄⁺ (Pathak et al., 2009, 2011; Ianniello et al., 2010; Sun et al., 2010). From measurements performed in October 2004 in Beijing, China, Kai et al. (2007) also concluded that high RH, stable atmosphere and high NH₃ levels can enhance transformation of NO_x into NO₃⁻. Particulate SO₄²⁻ maxima are observable during both cold and warm seasons. However, the particulate SO₄²⁻ mass concentrations showed statistically significant correlation with the measured meteorological parameters only at a 68 % confidence level (detailed statistics in Table S 4). The data presented in FIG. 6c show that the seasonal trend of the monthly SO₄²⁻ mean mass concentrations is not as clear as that of NO₃⁻ and NH₄⁺, which might suggest the occurrence of regional SO₄²⁻ sources as well (Wang et al., 2016). Moreover, high RH (in Iasi, especially during cold months) may aid the conversion of SO₂ to SO₄²⁻ (Kadowaki, 1986), with a significant enhancement of SO₄²⁻ production rate in aqueous phase (Sharma et al., 2007). However, the oxidation of SO₂ to sulfate may be induced not only by H₂O₂ in the aqueous phase, but also by gas-phase radical hydroxyl (Vione et al., 2003). This issue can explain the PM sulfate maxima during the warm seasons because of higher sunlight irradiance and temperature (Stelson and Seinfeld, 1982; Stockwell and Calvert, 1983; Kadowaki, 1986; Wang et al., 2005).

The data reported in Table 3 and FIG. 6f show that particulate NH₄⁺(total) has a clear seasonal pattern with maxima during the cold and minima over the warm seasons, in agreement with reports at other European (Schwarz et al., 2012; Bressi et al., 2013; Tositti et al., 2014; Voutsas et al., 2014) or non-European sites (Sharma et al., 2007; Wang et al., 2016). This behaviour is opposite to that reported by Ianniello et al. (2011). The cold-season maxima and warm-season minima we observed can be due to the effect of variations in the mixing layer depth, combined with gas-phase transfer of NH₄NO₃ to NH₃ and HNO₃ as temperature increases. In our dataset, NH₄⁺(total) varied from 0.8 to 2.09 µg m⁻³, a much lower range than that reported by Meng et al. (2011) for a more polluted site (Beijing, China, with concentrations varying between 4.73 to 9.04 µg m⁻³ among various seasons). However, the data we measured in the cold season (2.03 ± 0.30 µg m⁻³ over January, February and December; 1.65 ± 0.23 µg m⁻³ over January, February, March, October, November and December) seem to be in reasonable agreement with those predicted for Europe by Backes et al. (2016). In contrast, the 0.90 ± 0.09 µg m⁻³ NH₄⁺(total) measured concentration over the warm seasons is much lower than that predicted by Backes et al. (2016), and the discrepancy might actually reflect the limitation of the experimental measurement techniques concerning NH₄NO₃ volatility. Moreover, the NH₄⁺(total) mass concentration correlated significantly with RH and particle loading in both the PM_{2.5} and PM₁₀ fractions, and it anticorrelated significantly with temperature and mixing layer depth (detailed statistics in Table S 4). The PM_{2.5} fraction showed statistically significant correlation also with the mixing depth (Pearson coefficient higher than 0.67, p = 0.016). The seasonal variation of particulate NH₄⁺(total) follows especially those of particulate NO₃⁻ and Cl⁻, which would indicate that most probably NH₄⁺(total) largely originates from neutralization between NH₃, HNO₃ and HCl (Wang et al., 2006), or that the cited particulate species derive from similar gas-to-particle processes (Huang et al., 2010). Although in the present work gaseous NH₃ was not measured, ISORROPIA-II runs predicted that the atmosphere was often in a gaseous ammonia-rich state, independently of the RH values ([NH₃]/([HNO₃] + [HCl]) >> 1).

At the investigated site, $\text{C}_2\text{O}_4^{2-}$ and SO_4^{2-} show similar behaviour and the $\text{C}_2\text{O}_4^{2-}$ maxima during summer may suggest photochemical and/or biogenic contributions to its abundance (Laongsri and Harrison, 2013). The Na^+ ion, tracer of sea-salt or NaCl aerosols, shows higher concentrations during spring when one has a predominant long-range transport of air masses from the S-SE sector, with contributions from natural sources and especially sea-spray aerosols from the Black Sea.

5 Particulate K^+ mass concentrations also show a clear seasonal pattern, with higher values during the cold compared to the warm seasons (FIG. 6e). This phenomenon could be due to increased wood burning combined with a limited mixing layer depth. However, particulate K^+ mass concentrations also had some maxima when one expects intense agricultural biomass burning for field clearing (i.e., April, July, and September). The K^+ mass concentrations follow a similar pattern as Cl^- (Pearson coefficient of 0.79, $p = 0.002$) but a different one compared to SO_4^{2-} . Therefore, we suggest that intense wood

10 burning may be a common source for K^+ and Cl^- species in the study area (Christian et al., 2010; Akagi et al., 2011). High mass concentrations of Ca^{2+} and Mg^{2+} (with Mg^{2+} shown in Table 3 but not in FIG. 6), as soil/dust tracers, were observed especially during spring and summer. Over these seasons, lower precipitation frequency and high wind speed contribute to the observed behaviour. During the cold seasons, low wind speeds might prevent mineral dust resuspension and produce low values for these ions. However, Mg^{2+} and Ca^{2+} as mineral ions did not correlate with either $\text{PM}_{2.5}$ or PM_{10} ,

15 which suggests that inorganic particles would be mainly produced by NH_3 -triggered secondary processes.

3.2.3 Stoichiometry of $(\text{NH}_4)_2\text{SO}_4$, NH_4NO_3 and NH_4Cl

Table 4 presents the correlation matrix (Pearson coefficients) for the major ionic species (Cl^- , NO_3^- , SO_4^{2-} , CH_3COO^- , HCOO^- , $\text{C}_2\text{O}_4^{2-}$, HCO_3^- , Na^+ , NH_4^+ (total), K^+ , Mg^{2+} , Ca^{2+}) in $\text{PM}_{2.5}$, for both the cold (Table 4.a) and the warm seasons (Table 4.b). Despite similar correlations in PM_{10} as well, $\text{PM}_{2.5}$ was selected for the correlation matrix analysis because of

20 higher representativeness. For the cold seasons there are significant correlations (at the 99.9 % confidence level) among many chemical pairs, suggesting an important occurrence of $(\text{NH}_4)_2\text{SO}_4$, NH_4NO_3 and $(\text{NH}_4)_2\text{C}_2\text{O}_4$. In the warm seasons, $(\text{NH}_4)_2\text{SO}_4$, $\text{Mg}(\text{NO}_3)_2$, and NaCl seem to be the most important. However, $\text{Ca}(\text{HCO}_3)_2$ might play a role during both cold and warm seasons. Over the cold seasons, K^+ shows statistically significant correlation with many inorganic (NO_3^- , Cl^- and SO_4^{2-}) and organic (HCOO^- and $\text{C}_2\text{O}_4^{2-}$) anions, thereby suggesting that at least some of these species might have common

25 biomass burning sources (Ianniello et al., 2011 and references therein). However, in the case of SO_4^{2-} and NO_3^- the most likely explanation would rather be the use of both coal and wood for burning, as well as the effect of the mixing layer depth. In the ambient atmosphere, inorganic ammonium salts such as NH_4HSO_4 , $(\text{NH}_4)_2\text{SO}_4$, NH_4NO_3 and NH_4Cl are known to be produced by gas-to-particle conversion processes. In the present work, from the ionic balance analysis the NH_4^+ ion was assigned as the most critical parameter in the chemical composition analysis of aerosol particles (with 274 analysed samples,

30 i.e., about one quarter of the total, being highly deficient in cations). FIGURES 7a,b present the relationship between the molar concentrations of fine particulate NH_4^+ (i.e., from raw IC data and also in the total form estimated under the assumptions from Arsene et al., 2011) and that of particulate SO_4^{2-} for both the cold (FIG. 7a) and warm (FIG. 7b) seasons. Correlations between particulate NH_4^+ and SO_4^{2-} are statistically significant in both cases (detailed statistics in Table S 5).

During cold and warm seasons, the $[\text{NH}_4^+]/(2 \times [\text{SO}_4^{2-}])$ molar ratio was either ~ 1 (raw IC data), or $(\text{NH}_4^+(\text{total}) \text{ values})$ equal to 1.76 (cold seasons) and 1.02 (warm seasons). These data suggest the existence of enough NH_3 for the complete neutralization of H_2SO_4 , and also a predominance of particulate $(\text{NH}_4)_2\text{SO}_4$ in agreement with the observations of Ianniello et al. (2011). Moreover, as shown in Table 4, for particulate SO_4^{2-} and $\text{NH}_4^+(\text{total})$ the correlation was statistically significant (with Pearson coefficients of 0.96, $p < 0.001$ for cold and 0.97, $p < 0.001$ for warm seasons), thereby suggesting that $(\text{NH}_4)_2\text{SO}_4$ could be formed from $\text{H}_2\text{SO}_4(\text{g})$ and $\text{NH}_3(\text{g})$ in either case. However, the 1.76 value for the $[\text{NH}_4^+](\text{total})/(2 \times [\text{SO}_4^{2-}])$ molar ratio during the cold seasons will indicate that there should still be particulate NH_4^+ potentially available for combination with other anions (or the existence of enough excess ammonia to neutralize acidic species such as HNO_3 and HCl). Zhao et al. (2016) report a $[\text{NH}_4^+]/(2 \times [\text{SO}_4^{2-}])$ molar ratio of 1.54 ($R^2 = 0.63$), indicating the complete neutralization of H_2SO_4 and a predominance of $(\text{NH}_4)_2\text{SO}_4$ in sulfate salts during the cold seasons.

Unfortunately, at present, no measured NH_3 values are available for the interest site but it is still believed that, in the atmosphere of Iasi, sufficient gas-phase NH_3 occurs to promote both the homogeneous and heterogeneous formation of nitrate salts in the collected aerosol particles. The NH_4NO_3 formation routes might involve either the homogeneous reaction between gaseous HNO_3 and NH_3 (Ianniello et al., 2011), or the heterogeneous reaction between NH_3 and the products formed upon hydrolysis of N_2O_5 that could be present on the surface of the pre-existing moist aerosols under relatively high humidity (Pathak et al., 2011; Shon et al., 2013). Actually, gaseous NH_3 can influence both the inorganic ions and the aqueous-phase H^+ distribution in aerosols. The concentration of H^+ in aqueous aerosols is mainly determined by the balance of the acidic ionic components with the basic ones. During both cold and warm seasons, about half or slightly more than half of the collected samples were found alkaline with pH values fluctuating between 7 and 8. The remaining samples were acidic and with pH values ranging mainly from 1 to 3. Zhao et al. (2016) report that, on average, a + 25 % perturbation in the NH_3 level could lead to a 0.14 unit pH increase, and a – 25 % perturbation could cause a 0.23 unit pH decrease. They concluded that sufficient NH_3 was frequently present in wintertime atmosphere, and also that the fine collected particulates were almost fully neutralized by NH_3 .

FIGURES 7c,d,e,f show the relationships between the fine-particulate molar concentrations of (i) NH_4^+ and the sum of SO_4^{2-} and NO_3^- (FIGS. 7c,d), and (ii) NH_4^+ and the sum of SO_4^{2-} , NO_3^- and Cl^- (FIGS. 7e,f), for both cold and warm seasons. From details given in FIGS. 7c,d,e,f it can be easily observed that NH_4^+ , with both calculation methods (IC and total), was in deficit over the cold and warm seasons. Under these circumstances, it is believed that both particulate NO_3^- and Cl^- could be associated with other alkaline species or be part of acidic aerosol. Because the neutralising capacity of NH_4^+ toward SO_4^{2-} , NO_3^- and Cl^- acidic species might give a rough indication on the potential particles acidity (Li et al., 2015), from FIGS. 7c,d,e,f it is quite clear that at the study site, if NH_4^+ derived from raw IC data is used, the neutralisation ratios in the investigated particles are less than unity. This suggests that the atmospheric particles are most likely acidic, and also that a more complex chemistry is ongoing involving the HNO_3 and HCl species. However, when $\text{NH}_4^+(\text{total})$ is used, the neutralisation ratio approaches 1 and suggests a possibly complete neutralization of particles acidity. From details in FIGS. 7e,f it can be easily seen that actually the available NH_4^+ is not enough to compensate for other species. However, it should

be noted that Cl^- is not significantly influencing the neutralization of particles acidity. In a study performed by Zhao et al. (2016) the authors reported a $[\text{NH}_4^+]/(2 \times [\text{SO}_4^{2-}] + [\text{NO}_3^-])$ molar ratio of 0.86 ($R^2 = 0.78$) and an $[\text{NH}_4^+]/(2 \times [\text{SO}_4^{2-}] + [\text{NO}_3^-] + [\text{Cl}^-])$ molar ratio of 0.60 ($R^2 = 0.86$). Details presented in FIGS. 7c,d clearly show that when $\text{NH}_4^+(\text{total})$ is taken into account, a complete neutralization of H_2SO_4 and HNO_3 can be achieved during the cold seasons (FIG. 7c). In contrast, during the warm seasons (FIG. 7d) the molar ratio is slightly lower than 1 (i.e., 0.95). According to Seinfeld and Pandis (1998), during the warm seasons the high temperature and the low relative humidity would be favourable for NH_4^+ to reach a minimum concentration, because it is mainly transformed into NH_3 . Actually, temperature values above 25°C , such as those often encountered at the investigated site over the warm seasons, are known to prevent formation of particulate NH_4NO_3 (Adams et al., 1999). Under these circumstances, a considerable decrease in the $[\text{NH}_4^+](\text{total})/([\text{NO}_3^-] + 2 \times [\text{SO}_4^{2-}])$ molar ratio is to be expected during warm seasons. The cold-season temperature and relative humidity at the investigated site were, respectively, $5.3 \pm 3.9^\circ\text{C}$ and $(65.3 \pm 12.8)\%$. Coherently, the data presented in Table 4 show that the $(\text{NO}_3^-, \text{NH}_4^+(\text{total}))$ pair has significant correlation (Pearson coefficient of 0.98, $p < 0.001$) only during the cold seasons, while during the warm seasons (temperature and relative humidity of, respectively $18.9 \pm 3.8^\circ\text{C}$ and $40.5 \pm 7.7\%$) the correlation is very poor as increasing temperature and decreasing relative humidity limit the production of the NH_4NO_3 aerosol (Matsumoto and Tanaka 1996; Utsunomiya and Wakamatsu 1996; Alastuey et al., 2004).

In the atmosphere, both H_2SO_4 and HNO_3 are known to compete for the reaction with NH_3 to form $(\text{NH}_4)_2\text{SO}_4$ and NH_4NO_3 . As presented in Sect. 3.2.2, at the investigated site a reduction in both in NO_3^- and SO_4^{2-} was observed over the warm seasons and this may cause a further increase in gas-phase NH_3 . It is also interesting to observe that the reaction rate constant of $(\text{NH}_4)_2\text{SO}_4$ aerosol formation is similar to the rate constant of NH_4NO_3 formation (Harrison and Kitto, 1992; Pandolfi et al., 2012; Behera et al., 2013), and both are much higher than the rate constant between NH_3 and HCl (Behera and Sharma, 2012). This issue probably dictates the competition of any of the particulate SO_4^{2-} , NO_3^- and Cl^- for the available NH_4^+ . Usually, when a sufficient amount of NH_3 is available for neutralization of H_2SO_4 and HNO_3 , fine-mode $(\text{NH}_4)_2\text{SO}_4$ and NH_4NO_3 will be formed via reactions R1 (Cziczo et al., 1997; Zhang et al., 2015) and R2 (Fountoukis and Nenes, 2007; Zhang et al., 2015),



In contrast, in NH_3 -limited environments, coarse-mode NO_3^- is formed through reaction R3 involving Mg^{2+} (but not Ca^{2+}):



During the warm seasons, however, higher concentrations of $(\text{NH}_4)_2\text{SO}_4$ compared to NH_4NO_3 are expected because $(\text{NH}_4)_2\text{SO}_4$ is less volatile than NH_4NO_3 (Utsunomiya and Wakamatsu, 1996). Moreover, NH_4NO_3 will be formed only when excess NH_3 is available to react with HNO_3 . A modelling study by Backes et al. (2016) suggests that a reduction of NH_3 emissions by 50 % may lead to a 24 % reduction of the total $\text{PM}_{2.5}$ concentrations in northwest Europe, mainly due to reduced formation of NH_4NO_3 . However, the NH_3 concentration in the atmosphere over Europe seems to be high enough to saturate the reaction forming $(\text{NH}_4)_2\text{SO}_4$ particles, even in a scenario of reduced NH_3 levels, while on the contrary it is not

high enough to saturate the reaction with HNO_3 to form NH_4NO_3 particles. A reduced formation of NH_4NO_3 particles may lead to an increase in gas-phase HNO_3 during winter. In our study, results from ISORROPIA-II thermodynamic model foresee an increase of gas-phase HNO_3 at higher RH values during cold seasons. Higher levels of gas-phase HNO_3 may increase its condensation onto existing particles such as sodium chloride (NaCl), and the replacement of Cl^- with NO_3^- may enhance the concentration of HCl in the atmosphere (similar processes are described in Arsene et al., 2011).

In the atmosphere, additional non-volatile species containing nitrate and chloride might also be present, thus we investigated the potential of fine-particulate NO_3^- and Cl^- to be chemically bound to Ca^{2+} , Mg^{2+} , K^+ or Na^+ . The free NO_3^- and Cl^- concentrations, defined as the fractions of excess nitrate and chloride that are not bound to alkali or alkaline earth metals, were estimated for both the cold and warm seasons according to the concept described in Ianniello et al. (2011). Zero or negative values of free NO_3^- and Cl^- imply that NH_4NO_3 and NH_4Cl are not present. Estimated free NO_3^- and Cl^- concentrations showed similar contributions in both the $\text{PM}_{2.5}$ and PM_{10} fractions. Over the cold seasons we calculated $(6.5 \pm 7.9) \times 10^{-3} \mu\text{mol m}^{-3}$ ($0.4 \pm 0.5 \mu\text{g m}^{-3}$) for NO_3^- , and negative values for free Cl^- ; over the warm seasons we had $(1.6 \pm 1.8) \times 10^{-3} \mu\text{mol m}^{-3}$ ($0.1 \pm 0.1 \mu\text{g m}^{-3}$) for NO_3^- , and again negative values for free Cl^- (data provided as mean \pm stdev). This result suggests the potential presence of NH_4NO_3 , especially during the cold seasons, but it excludes the occurrence of NH_4Cl . During the cold seasons, particulate NO_3^- didn't show correlation with either Ca^{2+} or Mg^{2+} , but it showed significant correlation with K^+ ($r = 0.85$, $p < 0.001$, see Table 4), which indicates the possible formation of the non-volatile KNO_3 salt along with NH_4NO_3 . Over the warm seasons, fine particulate NO_3^- didn't show correlation with K^+ , but it showed significant correlation with Na^+ and Mg^{2+} (respectively, $r = 0.71$, $p < 0.001$ and $r = 0.86$, $p < 0.001$), indicating possible formation of non-volatile NaNO_3 and $\text{Mg}(\text{NO}_3)_2$ but not of $\text{Ca}(\text{NO}_3)_2$ salts. Moreover, in the warm seasons the fine-particulate NO_3^- also showed statistically significant correlation with HCO_3^- ($r = 0.63$, $p < 0.001$), which suggests a prevalence of particulate NO_3^- formation via the mineral route over the homogeneous reactions. The interaction between NO_3^- and Mg^{2+} could increase in importance during the warm seasons because, as NH_4^+ is not available, neutralization of HNO_3 could occur on coarse soil particles rich in Mg^{2+} (Matsumoto and Tanaka, 1996; Utsunomiya and Wakamatsu, 1996; Alastuey et al., 2004).

From the literature it is known that species such as $(\text{NH}_4)_2\text{SO}_4$ and NH_4HSO_4 , at room temperature, uptake water (deliquesce) at RH values of, respectively, $(79 \pm 1) \%$ and 39% (Cziczo et al., 1997). The $(\text{NH}_4)_2\text{SO}_4$ aerosol particles might remain in "metastable" or supersaturated state liquid phase until a very low RH (crystallization point, RH around 33%) is reached (only thereafter a solid might be formed). In contrast, for NH_4HSO_4 it has been shown that the solid phase is difficult to be formed. In the present work, it is very likely that only over July (RH of 32.95 %), August (RH of 37.12 %) and September (RH of 31.56 %) the formation of solid $(\text{NH}_4)_2\text{SO}_4$ or NH_4HSO_4 could occur.

Pure NH_4NO_3 deliquesces at 62 % RH and there is suggestion that sometime even at 8 % RH the crystallization point is not reached (Dougle et al., 1998). According to suggestions from the literature, only during months when the ambient RH is lower than the relative humidity at deliquescence (RHD), the NH_4NO_3 is considered as a solid (Seinfeld and Pandis, 1998). In the present work, from March to October the ambient RH was always lower than the RHD and NH_4NO_3 could thus be assumed to be in equilibrium with the solid phase. Within all the other months, from the estimated RHD values there is the

possibility that NH_4NO_3 is in equilibrium with the aqueous phase and deliquescent particles. However, in the investigated site, solid NH_4NO_3 could be formed almost all over the year either due to the very complex chemical composition of the collected particles, or due to abundant contribution of organic carbon to the particles mass concentration (Dougle et al., 1998). Formation of NH_4NO_3 over the warm seasons has been reported also by Ianniello et al. (2011) but under different conditions. For deliquesced particles there is suggestion that most of the fine particulate NO_3^- occurs as an internal mixture with SO_4^{2-} , and also that HNO_3 can easily be absorbed into the droplets (Huang et al., 2010). In specific circumstances, the fine particulate NO_3^- can be formed from HNO_3 and NH_3 through heterogeneous reactions on fully neutralized fine particulate SO_4^{2-} , which is abundant in urban areas (Stockwell et al., 2000). In the present work, a statistically significant correlation between SO_4^{2-} and NO_3^- was observed during the cold seasons in the $\text{PM}_{2.5}$ fraction ($r = 0.91$, $p < 0.001$). High concentrations of NO_3^- were found in the presence of elevated RH levels (significant correlation: $r = 0.84$, $p < 0.001$), while SO_4^{2-} concentrations were high over the entire RH range (non-significant correlation: $r = 0.44$, $p = 0.177$). These results can be interpreted as nitrate being produced on pre-existing sulfate aerosols, which could provide sufficient surface area and water content for the heterogeneous reactions to occur. Although the formation of fine particulate NO_3^- can take place via reaction (R2), in particular circumstances and especially at high RH values, the amounts of the gaseous precursors such as NH_3 and HNO_3 may have relatively little influence on the fine-particulate NO_3^- formation (Markovic et al., 2011). The salt NH_4Cl is known to be 2–3 times more volatile than NH_4NO_3 , as HCl is more volatile than HNO_3 . Moreover, at $\text{RH} < 75\text{--}85\%$, particulate NH_4Cl is in equilibrium with the gaseous compounds (Ianniello et al., 2011 and references therein). Coherently, during the cold seasons particulate NH_4^+ (total) showed a statistically significant correlation with particulate Cl^- (Pearson coefficient of 0.73, $p < 0.001$), but during the warm seasons the correlation was very poor. Finally, only during the cold seasons significant correlations were observed between fine particulate Cl^- and SO_4^{2-} (Pearson coefficient of 0.59, $p < 0.001$) and between fine particulate Cl^- and RH (Pearson coefficient of 0.71, $p = 0.010$). Usually, high concentrations of fine particulate Cl^- and SO_4^{2-} were found at high levels of RH (35–83 %). Under these circumstances, the amount of gaseous precursors is believed to have relatively little influence on the formation of fine particulate Cl^- . If formed, NH_4Cl is most probably generated from HCl and NH_3 through heterogeneous reactions on neutralised sulfate particles. However, in the present work, estimation of free Cl^- suggests that no Cl^- was available to be bound with other chemical species (i.e., NH_4^+) apart from alkali or alkaline earth metals, thereby excluding a significant occurrence of NH_4Cl (especially over the warm seasons).

3.3 Relative ionic contribution in size resolved aerosol particles from Iasi and potential influence of long-range transport phenomena on particles size distribution

FIGURES 8a,b,c,d present, as monthly based averages, the relative contributions of identified and quantified water-soluble ions to total detected components in fractions grouped in four stages, i.e., 0.0276–0.0945 μm size range (FIG. 8a), 0.155–0.612 μm size range (FIG. 8b), 0.946–2.39 μm size range (FIG. 8c) and 3.99–9.94 μm size range (FIG. 8d). From details presented in FIG. 8a, for the 0.0276–0.0945 μm fraction there is important contribution of formate, acetate and oxalate that

may actually indicate a possible important role of organic acids in secondary organic aerosols formation. Higher values of these components over the warm seasons may suggest an enhancement in the role of biogenic emission sources. Important contributions are brought by SO_4^{2-} , $\text{NH}_4^+(\text{total})$, K^+ and even by the (unexpectedly high) HCO_3^- . However, high particulate HCO_3^- is also evident for the 0.946–2.39 μm (FIG. 8c) and 3.99–9.94 μm size range (FIG. 8d) fractions. The 0.155–0.612 μm fraction (FIG. 8b) seems to be mainly constituted by SO_4^{2-} , NO_3^- and $\text{NH}_4^+(\text{total})$, with very small contributions from other ions.

The seasonal variation observed mainly for SO_4^{2-} and NO_3^- might suggest an enhancement of photo-oxidative processes over the warm seasons. The 0.946–2.39 μm (FIG. 8c) and 3.99–9.94 μm size range (FIG. 8d) fractions have a non-homogeneous chemical composition dominated mainly by HCO_3^- , NO_3^- and organics. Among all the analysed ions in the investigated period, in the PM_{10} fraction SO_4^{2-} was the most abundant with $(26.0 \pm 4.3) \%$ contribution, followed by NO_3^- $(26.0 \pm 10.7 \%)$, $\text{NH}_4^+(\text{total})$ $(15.0 \pm 3.4 \%)$, organics including acetate, formate and oxalate $(12.2 \pm 3.7 \%)$ and HCO_3^- $(10 \pm 7.7 \%)$. Similarly, in the $\text{PM}_{2.5}$ fraction SO_4^{2-} was again the most abundant $(28.9 \pm 5.6 \%)$ followed by NO_3^- $(19.6 \pm 12.1 \%)$, $\text{NH}_4^+(\text{total})$ $(16.6 \pm 3.2 \%)$, organics including acetate, formate and oxalate $(11.4 \pm 4.0 \%)$ and HCO_3^- $(8.0 \pm 6.8 \%)$. In both the PM_{10} and the $\text{PM}_{2.5}$ fractions, the largest contribution of SO_4^{2-} was observed in June 2016 with, respectively, $(34.6 \pm 10.9 \%)$ and $(40.8 \pm 11.0 \%)$. During the cold seasons, particulate SO_4^{2-} and NO_3^- contributions were, respectively, $(23.6 \pm 2.3 \%)$ and $(28.6 \pm 4.9 \%)$ for PM_{10} , and $(25.5 \pm 2.9 \%)$ and $(30.1 \pm 5.8 \%)$ for $\text{PM}_{2.5}$. During the warm seasons, the SO_4^{2-} and NO_3^- contributions, were, respectively, $(28.5 \pm 4.7 \%)$ and $(10.1 \pm 4.8 \%)$ for PM_{10} , and $(32.4 \pm 5.6 \%)$ and $(9.2 \pm 5.4 \%)$ for $\text{PM}_{2.5}$. Wonaschutz et al. (2015) report for Vienna (Austria) NO_3^- contributions of 31.3 % during winter and of 6.9 % during summer.

Particulate Ca^{2+} and HCO_3^- , as dust tracer ions, brought a significant contribution especially over the warm seasons $(43.8 \pm 11.2 \%$ in PM_{10} and $37.8 \pm 12.3 \%$ in $\text{PM}_{2.5}$ in August 2016), suggesting that Ca^{2+} and HCO_3^- mostly originate from soil dust re-suspension during the dry seasons. In 2016, spring was the season with predominant air masses undertaking long-range transport from the S-SE sector (see FIG. 1), thereby suggesting the presence of sea-spray aerosols from the Black Sea or other marine areas. The highest contributions from sea-spray aerosols tracers (i.e., Na^+ and Mg^{2+} , Masiol et al., 2012) were actually recorded in April (5.8 % for Na^+ and 0.7 % for Mg^{2+}). Although the most abundant ions are SO_4^{2-} , NO_3^- and $\text{NH}_4^+(\text{total})$, organics (including acetate, formate and oxalate) might also bring significant contributions $((17.3 \pm 4.4) \%$ in PM_{10} and $18.2 \pm 5.1 \%$ in $\text{PM}_{2.5}$ in July 2016, much higher than that reported by Arsene et al., 2011, for Iasi). The difference might reflect either an inversion of the photochemistry taking place at the investigated location, or differences in the sampling efficiency between the two studies.

FIGURES 9a,b,c,d show the size distributions of seasonal averaged mass concentrations for Cl^- , NO_3^- , SO_4^{2-} , NH_4^+ (FIGS. 9a,b) and K^+ , Na^+ , Mg^{2+} , Ca^{2+} (FIGS. 9c,d). While during the cold seasons NO_3^- , SO_4^{2-} , NH_4^+ and K^+ reside mainly in the fine mode with maxima at $\sim 381 \text{ nm}$, all the other ions (i.e., Cl^- , Na^+ , Mg^{2+} , Ca^{2+}) have major contributions in the super-micron mode (maxima between 1.6–2.39 μm). Over the cold seasons, clear evidences were obtained of the occurrence of chloride in a bimodal distribution. During the warm seasons only SO_4^{2-} and K^+ presented clear maxima at 381 nm, while all

the other identified/quantified species had more important contributions in the super-micron mode. For SO_4^{2-} , a larger modal diameter in the cold compared to the warm seasons is most likely due to hygroscopic growth under high RH, and/or to increased secondary aerosol production (lower temperatures facilitate condensation). Secondary aerosol mass from aqueous-phase reactions may also play a role (Wonaschutz et al., 2015). The maxima observed in the coarse mode could also be explained considering that heterogeneous chemistry on dust particles might act as a source for some particulate species (Wang et al., 2012).

While particulate NO_3^- over the cold seasons presented monomodal distributions in the sub-micron size range (maxima at 381 nm), over the warm seasons a second mode was observed with maxima in the 1.60-2.39 μm size range. Such a size distribution suggests that NO_3^- during the warm seasons is produced by adsorption of HNO_3 on sea salt and soil particles (Park et al., 2004). According to Karydis et al. (2016), particulate NO_3^- is not associated only with NH_4^+ in the fine mode. Light metal ions such as Ca^{2+} , Mg^{2+} , Na^+ , and K^+ , which mainly occur in the coarse mode, can be associated with NO_3^- and affect its partitioning into the aerosol phase. Dust effects on the distribution of particulate species might include a decrease of fine-mode NH_4^+ and a shift of particulate NO_3^- from the fine to the coarse mode (Wang et al., 2012). In addition, the presence of significant levels of NO_3^- , Cl^- , Mg^{2+} , Ca^{2+} and Na^+ in the coarse fraction might suggest that NO_3^- possibly originates upon reaction of HNO_3 with MgCO_3 , CaCO_3 or NaCl . Similar patterns were identified in Vienna, Austria (Wonaschutz et al., 2015) and in Prague, Czech Republic (Schwarz et al., 2012). Significant amounts of particulate NO_3^- formed upon reaction of HNO_3 with CaCO_3 on soil-derived particles have also been observed and reported (Yao et al., 2003; Sharma et al., 2007). Moreover, sea-salt aerosols may also undergo chemical transformation of NaCl into NaNO_3 during transport (Schwarz et al., 2012).

The size distributions of particulate K^+ reflect the occurrence of one dominant fine mode (with maxima at 381 nm) during both the cold and the warm seasons, and of a second less important mode during the warm seasons (with maxima in the 0.946–1.6 μm range). Such behaviour most likely reflects contributions from biomass burning all over the year (Schmidl et al., 2008; Pachon et al., 2013). For both Ca^{2+} and Mg^{2+} ions, clear monomodal mass distributions with maxima in the 1.6 to 2.39 μm size range were observed over the investigated period. Over the warm seasons, Ca^{2+} accounts for $(7.0 \pm 2.9) \%$ of the PM_{10} fraction and for $(5.5 \pm 2.9) \%$ of the $\text{PM}_{2.5}$ fraction, while over the cold seasons it accounts for only $(3.0 \pm 0.6) \%$ of the PM_{10} and $(2.2 \pm 0.5) \%$ of the $\text{PM}_{2.5}$ fraction. These observations indicate that the impact from soil dust re-suspension could be more important during the warm (dry) seasons. Mineral dust may also explain the higher coarse fraction of Mg^{2+} (mineral source being MgCO_3).

Clear evidences were obtained in this work that air-mass origin highly influences the aerosol chemical composition at the investigated site. Annual averaged sector contributions, in terms of PM long-range transport, are shown in FIG. S 2 while the seasonal contributions of PM and particulate inorganic/organic ions associated with different air mass origins are reported as Radar charts in FIG. S 3 (within Section S 10). FIG. S 4 (within Section S 10) highlights the % distributions for the identified-quantified ions and the gaseous concentrations of NH_3 , HNO_3 and HCl for selected investigated events, predicted by ISORROPIA-II. Wonaschutz et al. (2015) suggested that in Vienna, Austria, air-mass origin is the most important factor

for bulk PM concentrations, chemical composition of the coarse fraction ($> 1.5 \mu\text{m}$) and mass size distribution, while it is less important for the chemical composition of the fine fraction ($< 1.5 \mu\text{m}$). Although Iasi is located far from the Mediterranean or Black Sea, over the warm seasons the sea-salt chloride contribution to the aerosol budget in the area is not entirely excluded (Arsene et al., 2011). Moreover, dust particles originating from the Sahara are acknowledged as travelling across the tropical Atlantic Ocean ($10\text{--}90 \mu\text{g m}^{-3}$) and across the Mediterranean, affecting air quality in southern Europe ($10\text{--}60 \mu\text{g m}^{-3}$) (Karydis et al., 2016). In the present work, particulate Na^+ and Cl^- ions as tracers of sea-salt aerosols (Tositti et al., 2014) were mainly observed in conditions predominated by contributions from air masses arriving in Iasi from S-SE directions. However, one of the most interesting collected events was that of 9th–11th April 2016. For this event, the PM_{10} fraction mass concentration was as high as $43.9 \mu\text{g m}^{-3}$, a value which is about two times higher than the average of the total events. These conditions were highly influenced by air masses originating from both the Saharan desert and the Mediterranean Sea. As shown in FIG. 10a, the size distributions of particulate Na^+ , Ca^{2+} , Mg^{2+} , Cl^- ions and their mass concentrations present a highly dominating mode with maxima at $2.39 \mu\text{m}$. For this event, the (Ca^{2+} , Mg^{2+}) and (Na^+ , Cl^-) pairs showed statistically significant correlations (respectively, $r = 0.94$, $p < 0.001$ and $r = 0.85$, $p < 0.001$), suggesting common contributions from mineral Saharan dust (Ca^{2+} , Mg^{2+}) and from sea-salt marine aerosols (Na^+ , Cl^-). Moreover, FIG. 10a clearly shows that Na^+ , Ca^{2+} , Mg^{2+} and Cl^- make a very significant contribution to the total aerosol mass in the super-micron mode, with the maxima at $2.39 \mu\text{m}$.

In April 2016, an interesting behaviour was also observed for the averaged mass size distributions of particulate NH_4^+ , NO_3^- , SO_4^{2-} and Mg^{2+} (FIG. 10b). This month is highly affected by the atmospheric air masses buoyancy phenomenon, as shown by trajectories analysis for selected events and, while particulate NH_4^+ and SO_4^{2-} were mainly residing in the fine mode with clear maxima at 381 nm , NO_3^- and Mg^{2+} also presented a predominant mode in the $1.6\text{--}2.39 \mu\text{m}$ fraction. Such distributions, corroborated with meteorological conditions, would actually suggest a possible heterogeneous formation route for SO_4^{2-} (Wang et al., 2012). In contrast, the adsorption of HNO_3 on mineral dust and sea-salt particles (Karydis et al., 2016) would become more important for NO_3^- .

4 Conclusions

- 25 The atmospheric concentrations of particulate species including acetate, formate, fluoride, chloride, nitrite, nitrate, phosphate, sulfate, oxalate, sodium, potassium, ammonium, magnesium, and calcium were measured over 2016 at an urban site in Iasi, north-eastern Romania. The measurements were carried out by means of a cascade Dekati Low-Pressure Impactor (DLPI), performing aerosol size classification in 13 specific fractions evenly distributed over the $0.0276\text{--}9.94 \mu\text{m}$ size range.
- 30 The entire data set was analysed to investigate the seasonal variations in fine particulate species and the meteorological effects, and to examine the contributions of local and regional sources. ISORROPIA-II thermodynamic model runs were

used to estimate the pH values of the collected atmospheric particles, as on the present data-base it was the best method to analyse particles acidity.

Within the aerosol mass concentration, the identified ions mass brings contributions as high as 40.6 % with the rest being unaccounted yet. Fine particulate Cl^- , NO_3^- , NH_4^+ and K^+ exhibited clear seasonal variations with minima during the warm seasons, mainly due to cold-season enhancement in the emission sources, changes in the mixing layer depth and specific meteorological conditions (e.g., higher RH values prevailing in Iasi during the cold seasons). Fine particulate SO_4^{2-} did not show much variation with respect to seasons. The measured concentrations of NH_4^+ and NO_3^- in fine-mode ($\text{PM}_{2.5}$) aerosols were in reasonably good agreement with modelled values for the cold seasons but not for the warm seasons. This observation reflects the susceptibility of NH_4NO_3 aerosols to be lost due to volatility.

Clear evidences were obtained that NH_4^+ in $\text{PM}_{2.5}$ was primarily associated with SO_4^{2-} and NO_3^- . However, indirect ISORROPIA-II estimations showed that the atmosphere of Iasi might be ammonia-rich during both cold and warm seasons, so that enough NH_3 would be present to neutralise the H_2SO_4 , HNO_3 and HCl acidic components and to generate fine particulate ammonium salts, in the form of $(\text{NH}_4)_2\text{SO}_4$, NH_4NO_3 and NH_4Cl . Significant amounts of fine-particulate NO_3^- were in fact detected during the cold seasons. The presence of possibly large amounts of NH_3 , the domination of $(\text{NH}_4)_2\text{SO}_4$ over NH_4NO_3 and NH_4Cl , and the high relative humidity conditions in the cold seasons (likely leading to dissolution of a significant fraction of atmospheric HNO_3 and NH_3) are among the most important driving forces enhancing the fine-particulate NO_3^- and NH_4^+ distribution in the investigated site.

Most probably, gaseous NH_3 is not only a precursor of NH_4^+ formation, but it also affects the occurrence of NO_3^- and eventually Cl^- in $\text{PM}_{2.5}$ via neutralisation processes. The chemical composition data-base concerning $\text{PM}_{2.5}$ (and PM_{10}), combined with predictions from ISORROPIA-II run in the forward mode, allow us to suggest that NH_3 was most probably present in sufficiently high concentration to promote fine particle acidity neutralisation, during both the cold and the warm seasons. Although it is known that running ISORROPIA-II in the forward mode, with only aerosol concentrations as input may result in a bias in the predicted pH due to the repartitioning of ammonia in the model, this approach was the only one that allowed for a reasonable interpretation of the obtained results.

Over the warm seasons, ~ 35 % of the total analysed samples presented pH values in the very strong acidity fraction (0–3 pH units range), while over the cold seasons the fraction of samples in this pH range was ~ 43 %. However, while during the warm seasons ~ 24–25 % of the acidic samples were in the 1–2 pH range (reflecting mainly contributions from very strong inorganic acids), over the cold seasons a ~ 40 % fraction in the 1–3 pH range would reflect possible contributions from other acidic type species (i.e., organics). The observed changes in aerosols acidity could potentially impact the gas–particle partitioning of semi-volatile organic acids.

Acknowledgements

The authors acknowledge the financial support provided by UEFISCDI within the PN-III-P4-ID-PCE-2016-0299 (AI-FORECAST), PN-II-PCE-2011-3-0471 (EVOLUTION-AIR) and PN-II-RU-TE-2014-4-2461 (SOS-AROMATIC) projects. European Union's Horizon 2020 research and innovation programme, through the EUROCHAMP-2020 Infrastructure Activity Grant (grant agreement No 730997) and Chemical On-Line cOmpoSition and Source Apportionment of fine aerosols COLOSSAL grant (CA16109), is gratefully acknowledged. The authors acknowledge also the NOAA Air Resources Laboratory (ARL) for the provision of the HYSPLIT transport and dispersion model and/or READY website (<http://www.ready.noaa.gov>) used in this publication.

References

- 10 Adams, P. J., Seinfeld, J. H., and Koch, D. M.: Global concentration of tropospheric sulfate, nitrate and ammonium aerosol simulated in a general circulation model, *J. Geophys. Res.*, 104, 13791–13823, doi:10.1029/1999JD900083, 1999.
- Akagi, S. K., Yokelson, R. J., Wiedinmyer, C., Alvarado, M. J., Reid, J. S., Karl, T., Crounse, J. D., and Wennberg, P.O.: Emission factors for open and domestic biomass burning for use in atmospheric models, *Atmos. Chem. Phys.*, 11, 4039–4072, doi:10.5194/acp-11-4039-2011, 2011.
- 15 Aksoyoglu, S., Ciarelli, G., El-Haddad, I., Baltensperger, U., Prevot, A. S. H.: Secondary inorganic aerosols in Europe: sources and the significant influence of biogenic VOC emissions, especially on ammonium nitrate, *Atmos. Chem. Phys.*, 17, 7757–7773, doi:10.5194/acp-17-7757-2017, 2017.
- Alastuey, A., Querol, X., Rodríguez, S., Plana, F., Lopez-Soler, A., Ruiz, C., and Mantilla, E.: Monitoring of atmospheric particulate matter around sources of inorganic secondary inorganic aerosol, *Atmos. Environ.*, 38, 4979–4992, doi:10.1016/j.atmosenv.2004.06.026, 2004.
- 20 Alastuey, A., Querol, X., Aas, W., Lucarelli, F., Perez, N., Moreno, T., Cavalli, F., Areskoug, H., Balan, V., Catrambone, M., Ceburnis, D., Cerro, J. C., Conil, S., Gevorgyan, L., Hueglin, C., Imre, K., Jaffrezo, J. L., Leeson, S. R., Mihalopoulos, N., Mitosinkova, M., O'Dowd, C. D., Pey, J., Putaud, J. P., Riffault, V., Ripoll, A., Sciare, J., Sellegri, K., Spindler, G., and Yttri, K. E.: Geochemistry of PM₁₀ over Europe during the EMEP intensive measurement periods in summer 2012 and winter 2013, *Atmos. Chem. Phys.*, 16, 6107–6129, doi:10.5194/acp-16-6107-2016, 2016.
- Aneja, V. P., Chauhan, J. P., and Walker, J. T.: Characterization of atmospheric ammonia emissions from swine waste storage and treatment lagoons, *J. Geophys. Res.*, 105, 11535–11545, doi:10.1029/2000JD900066, 2000.
- Arsene, C., Olariu, R. I., and Mihalopoulos, N.: Chemical composition of rainwater in the north-eastern Romania, Iasi region (2003-2006), *Atmos. Environ.*, 41, 9452–9467, doi:10.1016/j.atmosenv.2007.08.046, 2007.
- 30 Arsene, C., Olariu, R. I., Zarmas, P., Kanakidou, M., and Mihalopoulos, N.: Ion composition of coarse and fine particles in Iasi, north-eastern Romania. Implications for aerosols chemistry in the area, *Atmos. Environ.*, 45, 906–916, doi:10.1029/2000JD900066, 2011.

- Athanasopoulou, E., Tombrou, M., Pandis, S. N., and Russell, A. G.: The role of sea-salt emissions and heterogeneous chemistry in the air quality of polluted coastal areas, *Atmos. Chem. Phys.*, 8, 5755–5769, doi:10.5194/acp-8-5755-2008, 2008.
- Bacarella, A. L., Grunwald, E., Marshall, H. P., and Purlee, E. L.: The potentiometric measurement of acid dissociation constants and pH in the system methanol-water. pK_a values for carboxylic acids and anilinium ions, *J. Org. Chem.*, 20, 747–762, doi:10.1021/jo01124a007, 1955.
- Backes, A. M., Aulinger, A., Bieser, J., Matthias, V., and Quante, M.: Ammonia emissions in Europe, part II: How ammonia emission abatement strategies affect secondary aerosols, *Atmos. Environ.*, 126, 153–161, doi:10.1016/j.atmosenv.2015.11.039, 2016.
- 10 Bardouki, H., Liakakou, H., Economou, C., Sciare, J., Smolik, J., Zdimal, V., Eleftheriadis, K., Lazaridis, M., Dye, C., and Mihalopoulos, N.: Chemical composition of size-resolved atmospheric aerosols in the eastern Mediterranean during summer and winter, *Atmos. Environ.*, 37, 195–208, doi: 10.1016/S1352-2310(02)00859-2, 2003.
- Behera, S. N. and Sharma, M.: Transformation of atmospheric ammonia and acid gases into components of $PM_{2.5}$: an environmental chamber study, *Environ. Sci. Pollut. Res.*, 19, 1187–1197, doi:10.4209/aaqr.2012.11.0328, 2012.
- 15 Behera, S. N., Betha, R., and Balasubramanian, R.: Insights into chemical coupling among acidic gases, ammonia and secondary inorganic aerosols, *Aerosol Air Qual. Res.*, 13, 1282–1296, doi:10.1007/s11356-011-0635-9, 2013.
- Bressi, M., Sciare, J., Gherzi, V., Bonnaire, N., Nicolas, J. B., Petit, J. E., Moukhtar, S., Rosso, A., Mihalopoulos, N., and Feron, A.: A one-year comprehensive chemical characterisation of fine aerosol ($PM_{2.5}$) at urban, suburban and rural background sites in the region of Paris (France), *Atmos. Chem. Phys.*, 13, 7825–7844, doi:10.5194/acp-13-7825-2013, 2013.
- 20 Brook, R. D.: Cardiovascular effects of air pollution, *Clin. Sci.*, 115, 175–187, doi: 10.1042/CS20070444, 2008.
- Christian, T. J., Yokelson, R. J., Cardenas, B., Molina, L. T., Engling, G., and Hsu, S. C.: Trace gas and particle emissions from domestic and industrial biofuel use and garbage burning in central Mexico, *Atmos. Chem. Phys.*, 10, 565–584, doi:10.5194/acp-10-565-2010, 2010.
- Clegg, S. L., Brimblecombe, P., and Wexler, A. S.: Thermodynamic model of the system $H^+ - NH_4^+ - SO_4^{2-} - NO_3^- - H_2O$ at tropospheric temperatures, *J. Phys. Chem. A*, 102, 2137–2154, doi:10.1021/jp973042r, 1998.
- 25 Cziczo, D. J., Nowak, J. B., Hu, J. H., and Abbatt, J. P. D.: Infrared spectroscopy of model tropospheric aerosols as a function of relative humidity: observation of deliquescence and crystallization, *J. Geophys. Res.*, 102, 18843–18850, doi:10.1029/97JD01361, 1997.
- Directive 2008/50/EC of the European Parliament and of the Council of 21 May 2008 on ambient air quality and cleaner air for Europe, *Official Journal L* 152, 11/06/2008, pp. 0001–0044, 2008.
- 30 Dockery, D. W., Cunningham, J., Damokosh, A. I., Neas, L. M., Spengler, J. D., Koutrakis, P., Ware, J. H., Raizenne, M., and Speizer, F. E.: Health effects of acid aerosols on North American children: respiratory symptoms, *Environ. Health Perspect.*, 104 (5), 500–505, 1996.

- Dominici, F., Peng, D. K., Bell, M. L., Pham, L., McDermott, A., Zeger, S. L., and Samet, J. M.: Fine particulate air pollution and hospital admission for cardiovascular and respiratory diseases, *JAMA*, 295, 1127–1134, doi:10.1001/jama.295.10.1127, 2006.
- Dougle P. G., Veeffkind J. P., and ten Brink, H. M.: Crystallisation of mixtures of ammonium nitrate, ammonium sulfate and soot, *J. Aerosol Sci.*, 29, 3, 375–386, doi:10.1016/S0021-8502(97)10003-9, 1998.
- EEA Report, European Environment Agency Report, Air quality in Europe-2015 report, ISSN 1977–8449, Report No. 5, 2015.
- Fang, T., Guo, H., Zeng, L., Verma, V., Nenes, A., and Weber, R. J.: Highly acidic ambient particles, soluble metals, and oxidative potential: A link between sulfate and aerosol toxicity, *Environ. Sci. Technol.*, 51, 2611–2620, doi:10.1021/acs.est.6b06151, 2017.
- Fountoukis, C. and Nenes, A.: ISORROPIA II: a computationally efficient thermodynamic equilibrium model for K^+ – Ca^{2+} – Mg^{2+} – NH_4^+ – Na^+ – SO_4^{2-} – NO_3^- – Cl^- , and H_2O aerosols, *Atmos. Chem. Phys.*, 7, 4639–4659, doi:10.5194/acp-7-4639-2007, 2007.
- Fountoukis, C., Nenes, A., Sullivan, A., Weber, R., Van Reken, T., Fischer, M., Matias, E., Moya, M., Farmer, D., and Cohen, R. C.: Thermodynamic characterization of Mexico City aerosol during MILAGRO 2006, *Atmos. Chem. Phys.*, 9, 2141–2156, doi:10.5194/acp-9-2141-2009, 2009.
- Freney, E., Sellegri, K., Canonaco, F., Colomb, A., Borbon, A., Michoud, V., Doussin, J. F., Crumeyrolle, S., Amarouche, N., Pichon, J. M., Bourianne, T., Gomes, L., Prevot, A. S. H., Beekmann, M., and Schwarzenboeck, A.: Characterizing the impact of urban emissions on regional aerosol particles: airborne measurements during the MEGAPOLI experiment, *Atmos. Chem. Phys.*, 14, 1397–1412, doi:10.5194/acp-14-1397-2014, 2014.
- Gerasopoulos, E., Koulouri, E., Kalivitis, N., Kouvarakis, G., Sarrikoski, S., Makela, T., Hillamo, R., and Mihalopoulos, N.: Size-segregated mass distribution of aerosols near Eastern Mediterranean: seasonal variability and comparison with AERONET columnar size-distributions, *Atmos. Chem. Phys.*, 7, 2551–2561, doi:10.5194/acp-7-2551-2007, 2007.
- Guo, H., Xu, L., Bougiatioti, A., Cerully, K. M., Capps, S. L., Hite, J. R., Carlton, A. G., Lee, S. H., Bergin, M. H., Ng, N. L., Nenes, A., and Weber, R. J.: Particle water and pH in the southeastern United States, *Atmos. Chem. Phys.*, 15, 5211–5228, doi: 10.5194/acp-15-5211-2015, 2015.
- Guo, H., Sullivan, A. P., Campuzano-Jost, P., Schroder, J. C., Lopez-Hilfiker, F. D., Dibb, J. E., Jimenez, J. L., Thornton, J. A., Brown, S. S., Nenes, A., and Weber, R. J.: Fine particle pH and the partitioning of nitric acid during winter in the northeastern United States, *J. Geophys. Res.: Atmos.*, 121, 10355–10376, doi: 10.1002/2016JD025311, 2016.
- Gwynn, R. C., Burnett, R. T., and Thurston, G. D.: A time-series analysis of acidic particulate matter and daily mortality and morbidity in the Buffalo, New York, region, *Environ. Health Perspect.* 108 (2), 125–133, 2000.
- Harrison, R. M. and Kitto, A. M. N.: Estimation of the rate constant for the reaction of acid sulfate aerosol with NH_3 gas from atmospheric measurements, *J. Atmos. Chem.*, 15, 133–143, doi:10.1007/BF00053755, 1992.

- Hasheminassab, S., Daher, N., Saffari, A., Wang, D., Ostro, B. D., and Sioutas, C.: Spatial and temporal variability of sources of ambient fine particulate matter (PM_{2.5}) in California, *Atmos. Chem. Phys.*, 14, 12085–12097, doi:10.5194/acp-14-12085-2014, 2014.
- Hennigan, C. J., Izumi, J., Sullivan, A. P., Weber, R. J., and Nenes, A.: A critical evaluation of proxy methods used to estimate the acidity of atmospheric particles, *Atmos. Chem. Phys.*, 15, 2775–2790, doi:10.5194/acp-15-2775-2015, 2015.
- Hitzenberger, R., Ctyroky, P., Berner, A., Tursic, J., Podkrajsek, B., and Grgic, I.: Size distribution of black (BC) and total carbon (TC) in Vienna and Ljubljana, *Chemosphere*, 65, 2106–2113, doi:10.1016/j.chemosphere.2006.06.042, 2006.
- Holton, J. R.: *An Introduction to Dynamic Meteorology*, 4th ed., Academic Press, New York, 1979.
- Huang, X. F., He, L. Y., Hu, M., Canagaratna, M. R., Sun, Y., Zhang, Q., Zhu, T., Xue, L., Zeng, L. W., Liu, X. G., Zhang, Y. H., Jayne, J. T., Ng, N. L., and Worsnop, D. R.: Highly time-resolved chemical characterization of atmospheric submicron particles during 2008 Beijing Olympic Games using an Aerodyne High-Resolution Aerosol Mass Spectrometer, *Atmos. Chem. Phys.*, 10, 8933–8945, doi:10.5194/acp-10-8933-2010, 2010.
- Ianniello, A., Spataro, F., Esposito, G., Allegrini, I., Rantica, E., Ancora, M. P., Hu, M., and Zhu, T.: Occurrence of gas phase ammonia in the area of Beijing (China), *Atmos. Chem. Phys.*, 10, 9487–9503, doi:10.5194/acp-10-9487-2010, 2010.
- Ianniello, A., Spataro, F., Esposito, G., Allegrini, I., Hu, M., and Zhu, T.: Chemical characteristics of inorganic ammonium salts in PM_{2.5} in the atmosphere of Beijing (China), *Atmos. Chem. Phys.*, 11, 10803–10822, doi:10.5194/acp-11-10803-2011, 2011.
- Ichim, L., Vlaicu, M., Draxineanu, A., and Alexandru, C.: Populatia Romaniei pe localitati la 1 Ianuarie 2016, in *INS 2016*, Iagar, E.M., Pisica, S., Baltateanu, L., (eds.), ISSN: 2066–2181, Institutul National de Statistica, Romania, pp. 130, 2016.
- IPCC, 2013: Summary for Policymakers, in: *Climate Change 2013: The Physical Science Basis. Contribution of Working Group I to the Fifth Assessment Report of the Intergovernmental Panel on Climate Change* [Stocker, T. F., Qin, D., Plattner, G. K., Tignor, M., Allen, S. K., Boschung, J., Nauels, A., Xia, Y., Bex, V., Midgley P.M., (eds.)], Cambridge University Press, Cambridge, United Kingdom and New York, NY, USA, pp. 1–30, doi:10.1017/CBO9781107415324.004, 2013.
- ISORROPIA Main Page: <http://isorro피아.eas.gatech.edu/>, last access: 11 July 2017.
- James, P. M.: An objective classification method for Hess and Brezowsky Grosswetterlagen over Europe, *Theor. Appl. Climatol.*, 88, 17–42, doi:10.1007/s00704-006-0239-3, 2007.
- Jang, M., Czoschke, N. M., Lee, S., and Kamens, R. M.: Heterogeneous atmospheric aerosol production by acid-catalyzed particle-phase reactions, *Science*, 298, 814–817, doi:10.1126/science.1075798, 2002.
- Kadowaki, S.: On the nature of the atmospheric oxidation processes of SO₂ to sulfate and of NO₂ to nitrate on the basis of diurnal variations of sulfate, nitrate, and other pollutants in an urban area, *Environ. Sci. Technol.*, 20, 1249–1253, doi:10.1021/es00154a009, 1986.
- Kai, Z., Yuesi, W., Tianxue, W., Yousef, M., and Frank, M.: Properties of nitrate, sulfate and ammonium in typical polluted atmospheric aerosols (PM₁₀) in Beijing, *Atmos. Res.*, 84, 67–77, doi:10.1016/j.atmosres.2006.05.004, 2007.

- Karydis, V. A., Tsimpidi, A. P., Lei, W., Molina, L. T., and Pandis, S. N.: Formation of semivolatile inorganic aerosols in the Mexico City Metropolitan Area during the MILAGRO campaign, *Atmos. Chem. Phys.*, 11, 13305–13323, doi:10.5194/acp-11-13305-2011, 2011.
- Karydis, V. A., Tsimpidi, A. P., Pozzer, A., Astitha, M., and Lelieveld, J.: Effects of mineral dust on global atmospheric nitrate concentrations, *Atmos. Chem. Phys.*, 16, 1491–1509, doi:10.5194/acp-16-1491-2016, 2016.
- Keene, W. C., Pszenny, A. A. P., Maben, J. R., Stevenson, E., and Wall, A.: Closure evaluation of size-resolved aerosol pH in the New England coastal atmosphere during summer, *J. Geophys. Res.*, 109, D23307, doi:10.1029/2004JD004801, 2004.
- Kocak, M., Mihalopoulos, N., and Kubilay, N.: Contributions of natural sources to high PM₁₀ and PM_{2.5} events in the eastern Mediterranean, *Atmos. Environ.*, 41, 3806–3818, doi:10.1016/j.atmosenv.2007.01.009, 2007.
- Laongsri, B. and Harrison, R. M.: Atmospheric behaviour of particulate oxalate at UK urban background and rural sites, *Atmos. Environ.*, 71, 319–326, doi:10.1016/j.atmosenv.2013.02.015, 2013.
- Lelieveld, J., Evans, J. S., Fnais, M., Giannadaki, D., and Pozzer, A.: The contribution of outdoor air pollution sources to premature mortality on a global scale, *Nature*, 525, 367–371, doi:10.1038/nature15371, 2015.
- Li, W., Shi, Z., Zhang, D., Zhang, X., Li, P., Feng, Q., Yuan, Q., and Wang, W.: Haze particles over a coal-burning region in the China Loess Plateau in winter: three flight missions in December 2010, *J. Geophys. Res.*, 117, D12306, doi:10.1029/2012JD017720, 2012.
- Li, T. C., Yuan, C. S., Lo, K. C., Hung, C. H., Wu, S. P., and Tong, C.: Seasonal variation and chemical characteristics of atmospheric particles at Three Islands in the Taiwan Street, *Aerosol Air Qual. Res.*, 15, 2277–2290, doi:10.4209/aaqr.2015.03.0153, 2015.
- Markovic, M. Z., Hayden, K. L., Murphy, J. G., Makar, P. A., Ellis, R. A., Chang, R. Y. W., Slowik, J. G., Mihele, C., and Brook, J.: The effect of meteorological and chemical factors on the agreement between observations and predictions of fine aerosol composition in southwestern Ontario during BAQS-Met, *Atmos. Chem. Phys.*, 11, 3195–3210, doi:10.5194/acp-11-3195-2011, 2011.
- Masiol, M., Squizzato, S., Ceccato, D., Rampazzo, G., and Pavoni, B.: Determining the influence of different atmospheric circulation patterns on PM₁₀ chemical composition in a source apportionment study, *Atmos. Environ.*, 63, 117–124, doi:10.1016/j.atmosenv.2012.09.025, 2012.
- Matsumoto, K. and Tanaka, H.: Formation and dissociation of atmospheric particulate nitrate and chloride: an approach based on phase equilibrium, *Atmos. Environ.*, 30, 639–648, doi:10.1016/1352-2310(95)00290-1, 1996.
- Meng, Z. Y., Seinfeld, J. H., Saxena, P., and Kim, Y. P.: Atmospheric gas - aerosol equilibrium IV. Thermodynamics of carbonates, *Aerosol Sci. Technol.*, 23, 131–154, doi:10.1080/02786829508965300, 1995.
- Meng, Z. Y., Lin, W. L., Jiang, X. M., Yan, P., Wang, Y., Zhang, Y. M., Jia, X. F., and Yu, X. L.: Characteristics of atmospheric ammonia over Beijing, China, *Atmos. Chem. Phys.*, 11, 6139–6151, doi:10.5194/acp-11-6139-2011, 2011.
- Meskhidze, N., Chameides, W. L., Nenes, A., and Chen, G.: Iron mobilization in mineral dust: Can anthropogenic SO₂ emissions affect ocean productivity?, *Geophys. Res. Lett.*, 30, 2085, doi: 10.1029/2003GL018035, 2003.

- Metzger, S., Mihalopoulos, N., and Lelieveld, J.: Importance of mineral cations and organics in gas-aerosol partitioning of reactive nitrogen compounds: case study based on MINOS results, *Atmos. Chem. Phys.*, 6, 2549–2567, doi:10.5194/acp-6-2549-2006, 2006.
- Nenes, A., Pilinis, C., and Pandis, S. N.: Continued development and testing of a new thermodynamic aerosol module for urban and regional air quality models, *Atmos. Environ.*, 33, 1553–1560, doi:10.1016/S1352-2310(98)00352-5, 1999.
- Nowak, J. B., Huey, L. G., Russell, A. G., Tian, D., Neuman, J. A., Orsini, D., Sjostedt, S. J., Sullivan, A. P., Tanner, D. J., Weber, R. J., Nenes, A., Edgerton, E., and Fehsenfeld, F. C.: Analysis of urban gas phase ammonia measurements from the 2002 Atlanta Aerosol Nucleation and Real-Time Characterization Experiment (ANARChE), *J. Geophys. Res.*, 111, D17308, doi: 10.1029/2006JD007113, 2006.
- Olariu, R. I., Vione, D., Grinberg, N., and Arsene C.: Applications of liquid chromatographic techniques in the chemical characterization of atmospheric aerosols, *J. Liq. Chromatogr. Related Technol.*, 38, 322–348, doi:10.1080/10826076.2014.941256, 2015.
- Ostro, B., Malig, B., Broadwin, R., Basu, R., Gold, E. B., Bromberger, J. T., Derby, C., Feinstein, S., Greendale, G. A., Jackson, E. A., Kravitz, H. M., Matthews, K. A., Sternfeld, B., Tomey, K., Green, R. R., and Green, R.: Chronic PM_{2.5} exposure and inflammation: determining sensitive subgroups in mid-life women, *Environ. Res.*, 132, 168–175, doi: 10.1016/j.envres.2014.03.042, 2014.
- Pachon, J. E., Weber, R. J., Zhang, X., Mulholland, J. A., and Russell, A. G.: Revising the use of potassium (K) in the source apportionment of PM_{2.5}, *Atmos. Pollut. Res.*, 4, 14–21, doi: 10.5094/APR.2013.002, 2013.
- Pandolfi, M., Amato, F., Reche, C., Alastuey, A., Otjes, R. P., Blom, M. J., and Querol, X.: Summer ammonia measurements in a densely populated Mediterranean city, *Atmos. Chem. Phys.*, 12, 7557–7575, doi:10.5194/acp-12-7557-2012, 2012.
- Park, R. J., Jacob, D. J., Field, B. D., Yantosca, R. M., and Chin, M.: Natural and transboundary pollution influences on sulfate-nitrate-ammonium aerosols in the United States: implications for policy, *J. Geophys. Res.*, 109, D15204, doi:10.1029/2003JD004473, 2004.
- Pathak, R. K., Wu, W. S., and Wang, T.: Summertime PM_{2.5} ionic species in four major cities of China: nitrate formation in an ammonia-deficient atmosphere, *Atmos. Chem. Phys.*, 9, 1711–1722, doi: 10.1016/S1352-2310(98)00352-5, 2009.
- Pathak, R. K., Wang, T., and Wu, W. S.: Nighttime enhancement of PM_{2.5} nitrate in ammonia-poor atmospheric conditions in Beijing and Shanghai: Plausible contributions of heterogeneous hydrolysis of N₂O₅ and HNO₃ partitioning, *Atmos. Environ.*, 45, 1183–1191, doi:10.1016/j.atmosenv.2010.09.003, 2011.
- Pope, C. A., Burnett, R. T., Thurston, G. D., Thun, M. J., Calle, E. E., Krewski, D., and Godleski, J. J.: Cardiovascular mortality and long-term exposure to particulate air pollution: epidemiological evidence of general pathophysiological pathways of disease, *Circulation*, 109, 71–77, doi: 10.1161/01.CIR.0000108927.80044.7F, 2004.
- Prinn, R. G.: The cleansing capacity of atmosphere, *Annu. Rev. Environ. Resour.*, 28, 29, doi:10.1146/annurev.energy.28.011503.163425, 2003.

- Querol, X., Alastuey, A., Ruiz, C. R., Artinano, B., Hansson, H. C., Harrison, R. M., Buringh, E., ten Brink, H. M., Lutz, M., Bruckmann, P., Straehl, P., and Schneider, J.: Speciation and origin of PM₁₀ and PM_{2.5} in selected European cities, *Atmos. Environ.*, 38, 6547–6555, doi:10.1016/j.atmosenv.2004.08.037, 2004.
- Ramanathan, V., Crutzen, P. J., Kiehl, J. T., and Rosenfeld, D., Aerosols, climate, and the hydrological cycle, *Science*, 294, 2119–2124, doi:10.1126/science.1064034, 2001.
- Ravishankara, A. R.: Heterogeneous and multiphase chemistry in the troposphere, *Science*, 276, 1058–1065, doi:10.1126/science.276.5315.1058, 1997.
- Rolph, G., Stein, A., and Stunder, B.: Real-time Environmental Applications and Display sYstem: READY, *Environmental Modelling and Software*, 95, 210–228, doi:10.1016/j.envsoft.2017.06.025, 2017.
- Sandrini, S., Van Pinxteren, D., Giulianelli, L., Herrmann, H., Poulain, L., Facchini, C. M., Gilardoni, S., Rinaldi, M., Paglione, M., Turpin, B. J., Pollini, F., Bucci, S., Zanca, N., and Decesari, S.: Size-resolved aerosol composition at an urban and a rural site in the Po Valley in summertime: Implications for secondary aerosol formation, *Atmos. Chem. Phys.*, 16 (17), 10879–10897, doi:10.5194/acp-16-10879-2016, 2016.
- Schmidl, C., Marr, I. L., Caseiro, A., Kotianova, P., Berner, A., Bauer, H., Kasper-Giebla A., and Puxbaum, H.: Chemical characterisation of fine particle emissions from wood stove combustion of common woods growing in mid-European Alpine regions, *Atmos. Environ.*, 42, 126–141, doi:10.1016/j.atmosenv.2007.09.028, 2008.
- Schwarz, J., Chi, X., Maenhaut, W., Civis, M., Hovorka, J., and Smolik, J.: Elemental and organic carbon in atmospheric aerosols at downtown and suburban sites in Prague, *Atmos. Res.*, 90, 287–302, doi:10.1016/j.atmosres.2008.05.006, 2008.
- Schwarz, J., Stefancova, L., Maenhaut, W., Smolik, J., and Zdimal, V.: Mass and chemically speciated size distribution of Prague aerosol using an aerosol dryer - The influence of air mass origin, *Sci Total. Environ.*, 437, 348–362, doi:10.1016/j.scitotenv.2012.07.050, 2012.
- Seinfeld, J. H. and Pandis, S. N.: *Atmospheric Chemistry and Physics: From Air Pollution to Climate Change*, Wiley: New York, 1998.
- Sharma, M., Kishore, S., Tripathi, S. N., and Behera, S. N.: Role of atmospheric ammonia in the secondary particulate matter: a study at Kanpur, India, *J. Atmos. Chem.*, 58, 1–17, doi:10.1007/s10874-007-9074-x, 2007.
- Shon, Z., Ghosh, S., Kim, K., Song, S., Jung, K., and Kim, N.: Analysis of water-soluble ions and their precursor gases over diurnal cycle, *Atmos. Res.*, 132-133, 309–321, doi:10.1016/j.atmosres.2013.06.003, 2013.
- Sicard, P., Lesne, O., Alexandre, N., Mangin, A., and Collomp, R.: Air quality trends and potential health effects e development of an aggregate risk index, *Atmos. Environ.*, 45, 5, 1145–1153, doi:10.1016/j.atmosenv.2010.12.052, 2011.
- Stein, A. F., Draxler, R. R., Rolph, G. D., Stunder, B. J. B., Cohen, M. D., and Ngan, F.: NOAA's HYSPLIT atmospheric transport and dispersion modeling system, *Bull. Am. Meteorol. Soc.*, 96, 2059–2077, doi:10.1175/BAMS-D-14-00110.1, 2015.
- Stelson, A. W. and Seinfeld, J. H.: Relative humidity and pH dependence of the vapour pressure of ammonium nitrate-nitric acid solutions at 25 °C, *Atmos. Environ.*, 16, 993–1000, doi:10.1016/0004-6981(82)90185-8, 1982.

- Stockwell, W. R. and Calvert, J. G.: The mechanism of the HO-SO₂ reaction, *Atmos. Environ.*, 17, 2231–2235, doi:10.1016/0004-6981(83)90220-2, 1983.
- Stockwell, W. R., Watson, J. G., Robinson, N. F., Steiner, W., and Sylte, W.: The ammonium nitrate particle equivalent of NO_x emissions for wintertime conditions in Central California's San Joaquin Valley, *Atmos. Environ.*, 34, 4711–4717, doi:10.1016/S1352-2310(00)00148-5, 2000.
- Sun, J., Zhang, Q., Canagaratna, M. R., Zhang, Y., Ng, N. L., Sun, Y., Jayne, J. T., Zhang, X., Zhang, X., and Worsnop, D. R.: Highly time- and size-resolved characterization of submicron aerosol particles in Beijing using an Aerodyne Aerosol Mass Spectrometer, *Atmos. Environ.*, 44, 131–140, doi:10.1016/j.atmosenv.2009.03.020, 2010.
- Sutton, M. A., Howard, C. M., Erismann, J. W., Billen, G., Bleeker, A., Grennfelt, P., van Grinsven, H., and Grizzetti, B.: The European Nitrogen Assessment: Sources, Effects and Policy Perspectives, Cambridge University Press, 2011.
- Tolis, E. I., Saraga, D. E., Lytra, M. K., Papathanasiou, A. C., Bougaidis, P. N., Prekas-Patronakis, O. E., Ioannidis, I. I., and Bartzis, J. G.: Concentration and chemical composition of PM_{2.5} for a one-year period at Thessaloniki, Greece: a comparison between city and port area, *Atmos. Environ.*, 113, 197–207, doi:10.1016/j.atmosenv.2015.05.014, 2015.
- Tositti, L., Brattich, E., Masiol, M., Baldacci, D., Ceccato, D., Parmeggiani, S., Stracquadanio, M., and Zappoli, S.: Source apportionment of particulate matter in a large city of southeastern Po Valley (Bologna, Italy), *Environ. Sci. Pollut. Res.*, 21, 872–890, doi:10.1007/s11356-013-1911-7, 2014.
- Trebs, I., Metzger, S., Meixner, F. X., Helas, G., Hoffer, A., Andreae, M. O., Moura, M. A. L., da Silva Jr., R. S., Rudich, Y., Falkovich, A. H., Artaxo, P., and Slanina, J.: The NH₄⁺–NO₃[–]–Cl[–]–SO₄^{2–}–H₂O aerosol system and its gas phase precursors at a pasture site in the Amazon Basin: How relevant are mineral cations and soluble organic acids?, *J. Geophys. Res.*, 110, D07303, doi:10.1029/2004JD005478, 2005.
- Tsai, Y. I. and Cheng, M. T.: Visibility and aerosol chemical compositions near the coastal area in Central Taiwan, *Sci. Total Environ.*, 231, 37–51, doi:10.1016/S0048-9697(99)00093-5, 1999.
- Tursic, J., Podkrajsek, B., Grgic, I., Ctyroky, P., Berner, A., Dusek, U., and Hitzenberger, R.: Chemical composition and hygroscopic properties of size-segregated aerosol particles collected at the Adriatic coast of Slovenia, *Chemosphere*, 63, 1193–1202, doi:10.1016/j.chemosphere.2005.08.040, 2006.
- Utsunomiya, A. and Wakamatsu, S.: Temperature and humidity dependence on aerosol composition in the northern Kyushu, Japan, *Atmos. Environ.*, 30, 2379–2386, doi:10.1016/1352-2310(95)00350-9, 1996.
- Vione, D., Maurino, V., Minero, C., Pelizzetti, E.: The atmospheric chemistry of hydrogen peroxide: A Review, *Ann. Chim. (Rome)*, 93, 477–488, 2003.
- Voutsas, D., Samara, C., Manoli, E., Lazarou, D., and Tzoumaka, P.: Ionic composition of PM_{2.5} at urban sites of northern Greece: secondary inorganic aerosol formation, *Environ. Sci. Pollut. Res.*, 21, 4995–5006, doi:10.1007/s11356-013-2445-8, 2014.
- Wang, Y., Zhuang, G., Tang, A., Yuan, H., Sun, Y., Chen, Sh., and Zheng, A.: The ion chemistry and the source of PM_{2.5} aerosol in Beijing, *Atmos. Environ.*, 39, 3771–3784, doi:10.1016/j.atmosenv.2005.03.013, 2005.

- Wang, Y., Zhuang, G., Zhang, X., Huang, K., Xu, C., Tang, A., Chen, J., and Zheng, A.: The ion chemistry, seasonal cycle, and sources of PM_{2.5} and TSP aerosol in Shanghai, *Atmos. Environ.*, 40, 2935–2952, doi:10.1016/j.atmosenv.2005.12.051, 2006.
- Wang, K., Zhang, Y., Nenes, A., and Fountoukis, C.: Implementation of dust emission and chemistry into the Community Multiscale Air Quality modeling system and initial application to an Asian dust storm episode, *Atmos. Chem. Phys.*, 12, 10209–10237, doi:10.5194/acp-12-10209-2012, 2012.
- Wang, H.L., Qiao, L.P., Lou, S.R., Zhou, M., Ding, A.J., Huang, H.Y., Chen, J.M., Wang, Q., Tao, S.K., Chen, C.H., Li, L., and Huang, C.: Chemical composition of PM_{2.5} and meteorological impact among three years in urban Shanghai, China, *J. Clean. Prod.*, 112, 1302–1311, doi:10.1016/j.jclepro.2015.04.099, 2016.
- Wexler, A.S. and Clegg, S. L.: Atmospheric aerosol models for systems including the ions H⁺, NH₄⁺, Na⁺, SO₄²⁻, NO₃⁻, Cl⁻, Br⁻, and H₂O, *J. Geophys. Res.*, 107, 4207, doi:10.1029/2001JD000451, 2002.
- WHO 2006a, Health Risks of Particulate Matter from Long-range Transboundary Air Pollution, E88189. European Centre for Environment and Health, WHO Regional Office for Europe, Denmark, 2006.
- WHO 2006b, WHO Air quality guidelines for particulate matter, ozone, nitrogen dioxide and sulphur dioxide, Global update 2005, Summary of risk assessment, WHO/SDE/PHE/ OEH/06.02, Geneva, Switzerland, 2006.
- Wonaschutz, A., Demattio, A., Wagner, R., Burkart, J., Zikova, N., Vodicka, P., Ludwig, W., Steiner, G., Schwarz, J., and Hitztenberger, R.: Seasonality of new particle formation in Vienna, Austria - Influence of air mass origin and aerosol chemical composition, *Atmos. Environ.*, 118, 118–126, doi:10.1016/j.atmosenv.2015.07.035, 2015.
- Yao, X. H., Lau, A. P. S., Fang, M., Chan, C. K., and Hu, M.: Size distributions and formation of ionic species in atmospheric particulate pollutants in Beijing, China: 1 - inorganic ions, *Atmos. Environ.*, 37, 2991–3000, doi:10.1016/S1352-2310(03)00255-3, 2003.
- Zhang, L. M., Gong, S. L., Padro, J., and Barrie, L.: A size segregated particle dry deposition scheme for an atmospheric aerosol module, *Atmos. Environ.*, 35, 549–560, doi:10.1016/S1352-2310(00)00326-5, 2001.
- Zhang, R., Wang, G., Guo, S., Zamora, M. L., Ying, Q., Lin, Y., Wang, W., Hu, M., and Wang, Y.: Formation of urban fine particulate matter, *Chem. Rev.*, 115, 3803–3855, doi:10.1021/acs.chemrev.5b00067, 2015.
- Zhao, M., Wang, S., Tan, J., Hua, Y., Wu, D., and Hao, J.: Variation of urban atmospheric ammonia pollution and its relation with PM_{2.5} chemical property in winter of Beijing, China, *Aerosol Air Qual. Res.*, 16, 1378–1389, doi:10.4209/aaqr.2015.12.0699, 2016.

Table 1: Basic statistics for the PM₁₀ and PM_{2.5} fractions mass concentrations determined over the investigated period (n = 84 sampling events) in Iasi, north-eastern Romania.

Statistical parameter	PM ₁₀ (μg m ⁻³)			PM _{2.5} (μg m ⁻³)		
	Working day	Weekend	Annual	Working day	Weekend	Annual
Mean	19.25	18.60	18.95	17.31	16.47	16.92
Median	16.05	17.26	16.35	14.01	15.43	14.51
Geomean	16.90	16.91	16.90	14.86	14.83	14.84
Stdev	10.05	8.62	9.35	9.92	8.11	9.07
Min	5.56	7.11	5.56	5.08	6.30	5.08
Max	42.65	44.84	44.84	41.57	43.91	43.91

Table 2: Annual and/or seasonal arithmetic means of the PM₁₀ and PM_{2.5} fraction mass concentrations in Iasi, north-eastern Romania, and other various European sites (mean ± stdev).

Site	Category	Sampling aagl* (m)	Sampling period	PM _{2.5} (µg m ⁻³)	PM ₁₀ (µg m ⁻³)	Reference
Iasi (Romania)	urban	35	2016	16.9±9.1	18.9±9.3	This work
				14.0±7.1 (warm)	16.8±8.3 (warm)	
				21.3±13.0 (cold)	22.6±13.1 (cold)	
				15.6±8.7**	-	
				9.1±5.5 [#]	-	
Iasi (Romania)	urban	25	2007–2008	10.5±11.2	38.3±25.4	Arsene et al., 2011 ^a
Paris (France)	urban background	20	2009–2010	14.8±9.6	–	Bressi et al., 2013
Northern Europe (SE12)	EMEP and 4 regional background sites	–	2012–2013	–	3–8	Alastuey et al., 2016 ^b
North-western Europe (IE321)					10–15 (S); ~ 35 (W)	
Central western Europe (FR09)					10–15 (S); ~ 25 (W)	
Central Europe (DE44)					20–25 (S); 25–30 (W)	
Eastern Europe (SK06,HU02)					10–15 (S); 15–25 (W)	
Eastern Europe (MD13)					~ 25 (S); 25–30 (W)	
South western Europe (ES22)					20–25 (S); 5–10 (W)	
Central southern Europe (IT01)					25–35 (S); 20–25 (W)	
South eastern Europe (GR02)					~ 25 (S); 35–40 (W)	
Thessaloniki (Greece)	urban	7	2011–2012	37.7±15.7	–	Tolis et al., 2015
Thessaloniki (Greece)	urban	3	2011–2012	21.5±8.3 (warm) 33.9±19.3 (cold)	–	Voutsas et al., 2014 ^c
Finokalia (Greece)	remote coastal	~ 5	2004–2006	18.2	30.8	Gerasopoulos et al., 2007
Bologna (Italy)	urban background	courtyard	2005–2006	31.6±21.0	44.5±24.2	Tositti et al., 2014
Venice (Italy)	semi-rural coastal	–	2007–2008	–	22.5±12.9	Masiol et al., 2012
Prague (Czech)	urban	12-25	2004–2005	–	33±13	Schwarz et al., 2008

Note: * sampling altitude above ground level, **PM_{0.027-1.6} and [#]PM_{0.381-1.6} annual values given for discussion and comparison purposes with Arsene et al. (2011) study, ^athe total (coarse + fine) and the fine fractions reported (coarse fraction - particles of AED > 1.5 µm and fine fractions - particles of AED < 1.5 µm); ^bS–summer (8 June–12 July 2012), W–winter (11 January–8 February 2013); ^caveraged value of warm and cold seasons data (error propagation method for uncertainty estimation); SE12–Aspvreten (Sweden); IE321–Mace Head (Ireland); FR09–Revin (France); DE44–Melpitz (Germany), SK06–Starina (Slovak Republic), HU02–K-Puszt (Hungary), MD13–Leova II (Moldavian Republic), ES22–Montsec (Spain); IT01–Montelibretti (Italy), GR02–Finokalia (Greece).

Table 3: Monthly averages of meteorological variables, PM₁₀, PM_{2.5} fractions and of water soluble ions mass concentrations ($\mu\text{g m}^{-3}$) in PM_{2.5} aerosol particles from Iasi, north-eastern Romania. Data are presented as mean \pm stdev (median).

Month	January	February	March	April	May	June	July	August	September	October	November	December
WS (m/s)	6.41 \pm 4.89 (5.60)	7.34 \pm 4.74 (6.80)	6.49 \pm 4.79 (5.70)	6.41 \pm 5.05 (5.60)	5.45 \pm 4.44 (4.90)	6.07 \pm 4.36 (5.70)	6.28 \pm 5.00 (5.40)	5.37 \pm 4.72 (4.70)	4.67 \pm 3.73 (4.40)	7.17 \pm 4.57 (6.80)	5.72 \pm 4.92 (4.90)	3.77 \pm 3.76 (3.20)
AT (°C)	-1.06 \pm 4.71 (-1.42)	5.86 \pm 1.98 (6.61)	6.50 \pm 3.49 (5.35)	13.65 \pm 4.15 (14.48)	15.65 \pm 3.25 (15.70)	21.05 \pm 4.75 (20.46)	23.27 \pm 3.05 (24.58)	21.86 \pm 2.13 (21.21)	18.20 \pm 5.57 (20.30)	10.03 \pm 5.11 (7.86)	7.41 \pm 5.86 (6.23)	2.77 \pm 2.41 (2.56)
RH (%)	71.27 \pm 15.86 (69.57)	68.20 \pm 6.97 (68.27)	46.30 \pm 27.50 (37.88)	44.43 \pm 13.19 (47.27)	50.32 \pm 15.88 (47.47)	46.63 \pm 16.69 (43.99)	32.95 \pm 7.58 (33.97)	37.12 \pm 13.14 (35.50)	31.56 \pm 14.10 (28.71)	54.30 \pm 10.58 (49.64)	69.92 \pm 22.10 (72.41)	81.85 \pm 13.22 (82.85)
RHD (%)	78.66 \pm 3.61 (78.83)	73.54 \pm 1.38 (73.01)	73.14 \pm 2.34 (73.86)	68.59 \pm 2.49 (68.02)	67.37 \pm 1.92 (67.30)	64.38 \pm 2.54 (64.62)	63.16 \pm 1.62 (62.46)	63.88 \pm 1.13 (64.21)	65.98 \pm 3.16 (64.71)	70.87 \pm 3.17 (72.17)	72.61 \pm 3.81 (73.27)	75.71 \pm 1.73 (75.85)
n*	5	5	8	8	9	8	5	9	7	7	7	6
PM _{2.5}	23.39 \pm 11.65 (26.19)	21.30 \pm 8.37 (20.65)	16.10 \pm 5.31 (14.98)	15.29 \pm 8.34 (11.67)	8.98 \pm 3.78 (6.88)	11.45 \pm 5.61 (9.19)	16.15 \pm 11.12 (14.19)	14.00 \pm 4.27 (13.70)	17.36 \pm 5.60 (17.77)	12.71 \pm 4.81 (13.29)	16.93 \pm 13.09 (12.04)	30.94 \pm 9.51 (24.55)
PM ₁₀	24.25 \pm 11.99 (27.86)	22.11 \pm 8.50 (21.43)	17.25 \pm 5.28 (16.08)	18.22 \pm 11.08 (13.18)	12.11 \pm 4.43 (14.25)	14.33 \pm 6.98 (10.24)	19.05 \pm 11.57 (16.00)	16.59 \pm 5.52 (16.17)	19.76 \pm 6.87 (20.20)	15.13 \pm 5.81 (16.49)	18.13 \pm 13.58 (13.49)	32.08 \pm 9.44 (26.12)
Cl ⁻	0.32 \pm 0.15 (0.34)	0.35 \pm 0.10 (0.37)	0.14 \pm 0.10 (0.10)	0.21 \pm 0.16 (0.15)	0.14 \pm 0.08 (0.13)	0.14 \pm 0.08 (0.14)	0.20 \pm 0.11 (0.18)	0.26 \pm 0.15 (0.31)	0.19 \pm 0.06 (0.18)	0.38 \pm 0.24 (0.32)	0.24 \pm 0.24 (0.19)	0.55 \pm 0.19 (0.64)
NO ₃ ⁻	3.54 \pm 1.93 (4.14)	3.21 \pm 1.36 (3.14)	2.42 \pm 1.09 (2.43)	1.36 \pm 0.86 (1.22)	0.47 \pm 0.28 (0.41)	0.31 \pm 0.17 (0.26)	0.31 \pm 0.11 (0.30)	0.41 \pm 0.17 (0.33)	0.69 \pm 0.41 (0.57)	1.25 \pm 0.82 (1.13)	1.88 \pm 1.27 (2.12)	3.62 \pm 1.10 (4.07)
SO ₄ ²⁻	2.76 \pm 1.66 (2.49)	2.58 \pm 0.91 (2.50)	2.03 \pm 0.71 (2.15)	1.96 \pm 0.75 (1.82)	1.70 \pm 0.81 (1.53)	2.39 \pm 1.31 (2.32)	2.04 \pm 0.98 (1.58)	2.22 \pm 0.76 (2.04)	2.15 \pm 0.84 (2.18)	1.96 \pm 1.00 (2.05)	1.17 \pm 0.27 (1.16)	2.16 \pm 0.69 (2.33)
CH ₃ COO ⁻	0.51 \pm 0.31 (0.45)	0.79 \pm 0.50 (0.63)	0.30 \pm 0.18 (0.29)	0.84 \pm 0.36 (0.82)	0.64 \pm 0.44 (0.49)	0.58 \pm 0.34 (0.57)	0.82 \pm 0.53 (0.48)	0.69 \pm 0.71 (0.57)	0.70 \pm 0.26 (0.60)	0.80 \pm 0.28 (0.89)	0.46 \pm 0.33 (0.43)	0.59 \pm 0.12 (0.54)
HCOO ⁻	0.07 \pm 0.05 (0.06)	0.06 \pm 0.03 (0.06)	0.09 \pm 0.09 (0.05)	0.15 \pm 0.20 (0.07)	0.04 \pm 0.02 (0.05)	0.05 \pm 0.03 (0.04)	0.12 \pm 0.11 (0.07)	0.08 \pm 0.02 (0.08)	0.09 \pm 0.02 (0.10)	0.09 \pm 0.04 (0.08)	0.03 \pm 0.02 (0.04)	0.07 \pm 0.02 (0.07)
C ₂ O ₄ ²⁻	0.08 \pm 0.06 (0.08)	0.08 \pm 0.04 (0.08)	0.08 \pm 0.04 (0.07)	0.08 \pm 0.05 (0.08)	0.06 \pm 0.04 (0.06)	0.09 \pm 0.06 (0.08)	0.12 \pm 0.09 (0.10)	0.14 \pm 0.05 (0.15)	0.10 \pm 0.08 (0.11)	0.06 \pm 0.06 (0.04)	0.02 \pm 0.02 (0.02)	0.10 \pm 0.04 (0.09)
HCO ₃ ⁻	0.39 \pm 0.12 (0.43)	0.48 \pm 0.24 (0.39)	0.39 \pm 0.20 (0.36)	0.65 \pm 0.67 (0.39)	0.32 \pm 0.17 (0.38)	0.64 \pm 0.56 (0.45)	0.51 \pm 0.24 (0.56)	2.23 \pm 1.95 (1.73)	0.63 \pm 0.18 (0.60)	0.25 \pm 0.17 (0.24)	0.25 \pm 0.34 (0.10)	0.35 \pm 0.25 (0.42)
Na ⁺	0.14 \pm 0.05 (0.13)	0.17 \pm 0.08 (0.16)	0.12 \pm 0.08 (0.10)	0.41 \pm 0.31 (0.41)	0.19 \pm 0.14 (0.10)	0.13 \pm 0.05 (0.12)	0.13 \pm 0.08 (0.12)	0.18 \pm 0.09 (0.17)	0.14 \pm 0.09 (0.11)	0.25 \pm 0.16 (0.26)	0.12 \pm 0.15 (0.08)	0.17 \pm 0.09 (0.16)
NH ₄ ⁺ _{total}	2.07 \pm 1.08 (2.39)	1.94 \pm 0.70 (1.97)	1.48 \pm 0.58 (1.57)	0.93 \pm 0.25 (0.96)	0.80 \pm 0.29 (0.67)	0.90 \pm 0.36 (0.86)	0.94 \pm 0.40 (0.78)	0.84 \pm 0.16 (0.82)	0.97 \pm 0.23 (0.92)	1.10 \pm 0.48 (1.22)	1.17 \pm 0.57 (1.25)	2.09 \pm 0.49 (2.37)
K ⁺	0.54 \pm 0.25 (0.67)	0.48 \pm 0.20 (0.44)	0.27 \pm 0.12 (0.25)	0.30 \pm 0.13 (0.27)	0.26 \pm 0.16 (0.15)	0.28 \pm 0.16 (0.24)	0.37 \pm 0.21 (0.31)	0.31 \pm 0.11 (0.32)	0.45 \pm 0.14 (0.48)	0.41 \pm 0.13 (0.41)	0.43 \pm 0.32 (0.36)	0.71 \pm 0.18 (0.65)
Mg ²⁺	0.03 \pm 0.01 (0.03)	0.03 \pm 0.02 (0.03)	0.02 \pm 0.02 (0.01)	0.04 \pm 0.04 (0.02)	0.01 \pm 0.00 (0.01)	0.02 \pm 0.02 (0.02)	0.02 \pm 0.00 (0.01)	0.05 \pm 0.04 (0.03)	0.02 \pm 0.01 (0.02)	0.03 \pm 0.02 (0.03)	0.01 \pm 0.01 (0.01)	0.03 \pm 0.01 (0.03)
Ca ²⁺	0.21 \pm 0.07 (0.22)	0.27 \pm 0.08 (0.26)	0.22 \pm 0.07 (0.19)	0.28 \pm 0.24 (0.21)	0.15 \pm 0.05 (0.17)	0.30 \pm 0.25 (0.22)	0.25 \pm 0.12 (0.23)	0.92 \pm 0.84 (0.65)	0.30 \pm 0.08 (0.31)	0.15 \pm 0.08 (0.15)	0.16 \pm 0.17 (0.10)	0.20 \pm 0.12 (0.20)
pH _{total}	4.20 \pm 2.32 (2.88)	4.17 \pm 2.53 (3.27)	3.94 \pm 2.81 (2.51)	3.88 \pm 2.97 (1.80)	3.95 \pm 3.10 (2.82)	4.14 \pm 2.92 (2.27)	4.58 \pm 2.87 (4.26)	5.06 \pm 2.73 (7.14)	4.24 \pm 3.19 (3.55)	4.25 \pm 2.75 (3.60)	3.86 \pm 2.55 (2.54)	4.12 \pm 2.16 (2.87)

Note: * n represent the number of aerosol sample events collected each month

Table 4: Correlation matrix (Pearson coefficients) for major ionic species (Cl^- , NO_3^- , SO_4^{2-} , CH_3COO^- , HCOO^- , $\text{C}_2\text{O}_4^{2-}$, HCO_3^- , Na^+ , NH_4^+ (total), K^+ , Mg^{2+} , Ca^{2+}) in fine aerosol particles from Iasi, north-eastern Romania, both for cold (a) and warm (b) seasons.

(a)	$\text{PM}_{2.5}$ (cold)	Cl^-	NO_3^-	SO_4^{2-}	CH_3COO^-	HCOO^-	$\text{C}_2\text{O}_4^{2-}$	HCO_3^-	Na^+	NH_4^+ (total)	K^+	Mg^{2+}	Ca^{2+}
	Cl^-	1.00	0.75	0.59	0.56	0.57	0.71	0.22	0.49	0.73	0.80	0.35	0.04
	NO_3^-		1.00	0.91	0.37	0.74	0.87	0.13	0.04	0.98	0.85	0.00	0.06
	SO_4^{2-}			1.00	0.43	0.72	0.87	0.05	0.02	0.96	0.72	0.07	0.11
	CH_3COO^-				1.00	0.56	0.63	0.13	0.17	0.45	0.47	0.01	0.03
	HCOO^-					1.00	0.85	0.04	0.01	0.76	0.65	0.12	0.09
	$\text{C}_2\text{O}_4^{2-}$						1.00	0.23	0.08	0.89	0.76	0.16	0.17
	HCO_3^-							1.00	0.56	0.17	0.05	0.76	0.98
	Na^+								1.00	0.03	0.06	0.83	0.50
	NH_4^+ (total)									1.00	0.82	0.08	0.12
	K^+										1.00	0.08	0.09
	Mg^{2+}											1.00	0.66
	Ca^{2+}												1.00
(b)	$\text{PM}_{2.5}$ (warm)	Cl^-	NO_3^-	SO_4^{2-}	CH_3COO^-	HCOO^-	$\text{C}_2\text{O}_4^{2-}$	HCO_3^-	Na^+	NH_4^+ (total)	K^+	Mg^{2+}	Ca^{2+}
	Cl^-	1.00	0.57	0.10	0.81	0.37	0.08	0.81	0.87	0.02	0.76	0.83	0.63
	NO_3^-		1.00	0.34	0.02	0.14	0.17	0.63	0.71	0.23	0.08	0.86	0.39
	SO_4^{2-}			1.00	0.01	0.66	0.76	0.17	0.05	0.97	0.43	0.03	0.01
	CH_3COO^-				1.00	0.32	0.11	0.30	0.07	0.11	0.55	0.05	0.08
	HCOO^-					1.00	0.58	0.32	0.01	0.66	0.59	0.02	0.01
	$\text{C}_2\text{O}_4^{2-}$						1.00	0.58	0.04	0.71	0.46	0.01	0.15
	HCO_3^-							1.00	0.45	0.06	0.13	0.12	0.99
	Na^+								1.00	0.11	0.19	0.76	0.38
	NH_4^+ (total)									1.00	0.49	0.12	0.12
	K^+										1.00	0.02	0.03
	Mg^{2+}											1.00	0.81
	Ca^{2+}												1.00

FIGURE captions

FIGURE 1: Sectors contributions identified from classification of 2-day back trajectories of air masses ending at Iasi and representative backward trajectories of long and short range transport, Black Sea influence and African dust (shown trajectories correspond to sampling events).

FIGURE 2: Patterns of the monthly arithmetic mean concentrations and standard deviations in the PM_{10} , $PM_{2.5}$ and $PM_{2.5}/PM_{10}$ variables at Iasi, north-eastern Romania.

FIGURE 3: Size distribution histograms of aerosol particles mass concentration gravimetrically determined over both the cold and warm seasons.

FIGURE 4: Distribution of the aerosol pH predicted by ISORROPIA-II (forward mode) vs. the ion balance (a), sensitivity of aerosol pH predicted with the model to small changes in the input aerosol NH_4^+ concentration (b) and bar chart distribution in aerosol pH over the warm and cold season both for NH_4^+ derived from raw IC data (c) and NH_4^+ (total) (d).

FIGURE 5: Size distribution of averaged aerosol mass, NO_3^- , SO_4^{2-} and NH_4^+ concentrations over cold (a) and warm (b) seasons accompanied by the size distribution of ISORROPIA-II estimated pH and H^+ mass concentration over both the cold (c) and the warm (d) seasons.

FIGURE 6: Seasonal variations for selected water-soluble ionic components in the $PM_{2.5}$ fraction (a-h) and variation of the mixing layer depth at the investigated site (i). The inset distribution presented within NO_3^- seasonal variation reflects the contribution of the coarse fraction over the warm seasons. The horizontal black line represents the mean, the horizontal colored line – the median, the box – the 25–75% percentiles, the length of the whiskers plot – the 10 and 90% of observed concentrations, circles – outliers).

FIGURE 7: Regression analysis of the $[NH_4^+]$ vs. $(2 \times [SO_4^{2-}])$ (a, b), $[NH_4^+]$ vs. $([NO_3^-] + 2 \times [SO_4^{2-}])$ (c,d) and $[NH_4^+]$ vs. $([Cl^-] + [NO_3^-] + 2 \times [SO_4^{2-}])$ (e,f) dependences specific for $PM_{2.5}$ particles.

FIGURE 8: The relative contributions, as monthly-based averages, of identified and quantified water soluble ions to total detected components in the 0.0276–0.0945 μm (a), 0.155–0.612 μm (b), 0.946–2.39 μm (c) and 3.99–9.94 μm (d) size range grouped fractions.

FIGURE 9: Size distributions of seasonal averaged mass concentrations for Cl^- , NO_3^- , SO_4^{2-} , NH_4^+ (a,b) and K^+ , Na^+ , Mg^{2+} , Ca^{2+} (c,d) ions in atmospheric aerosols from Iasi, both during the cold and, respectively, the warm seasons.

FIGURE 10: Evidences of long range transport contributions from Saharan dust within the size distribution of particulate Na^+ , Ca^{2+} , Mg^{2+} , Cl^- ions and aerosol mass (a) and of air masses buoyancy phenomena within the size distribution of particulate NH_4^+ , NO_3^- , SO_4^{2-} , Mg^{2+} ions and aerosol mass (b).

FIGURE 1

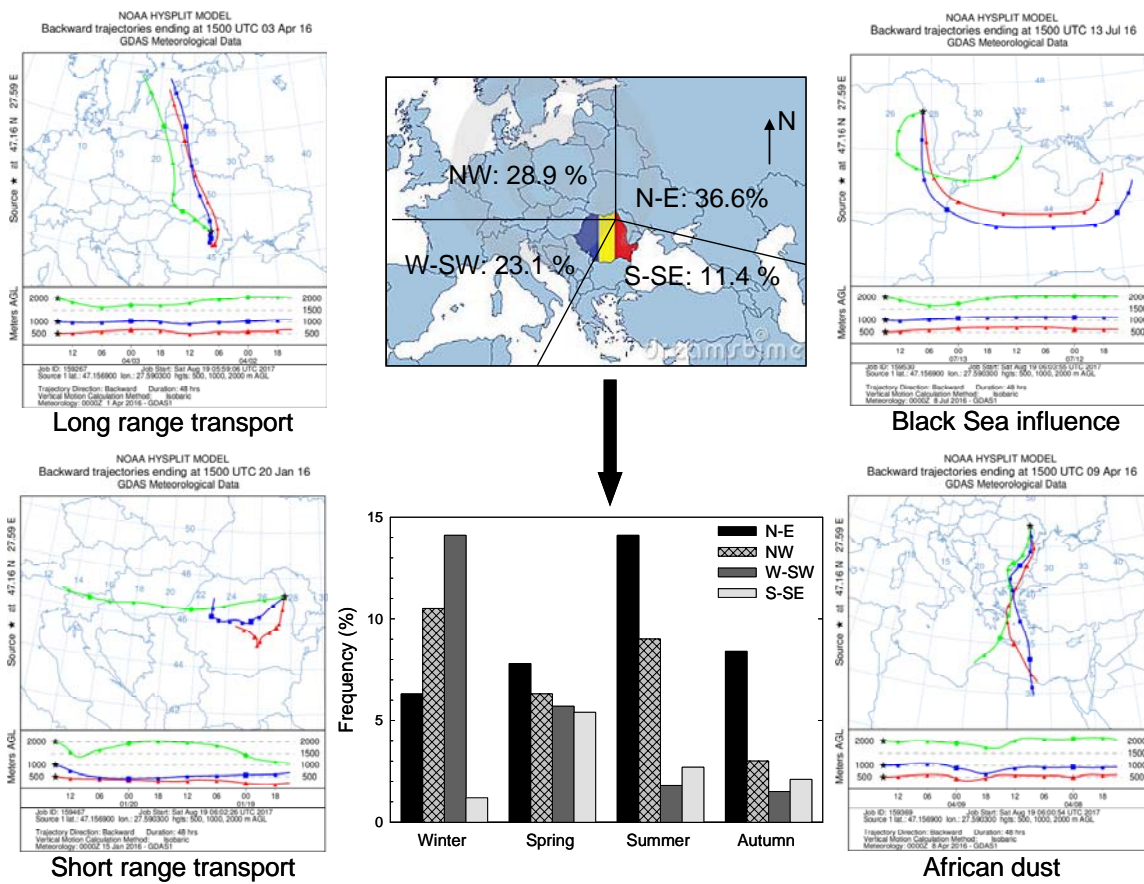


FIGURE 2

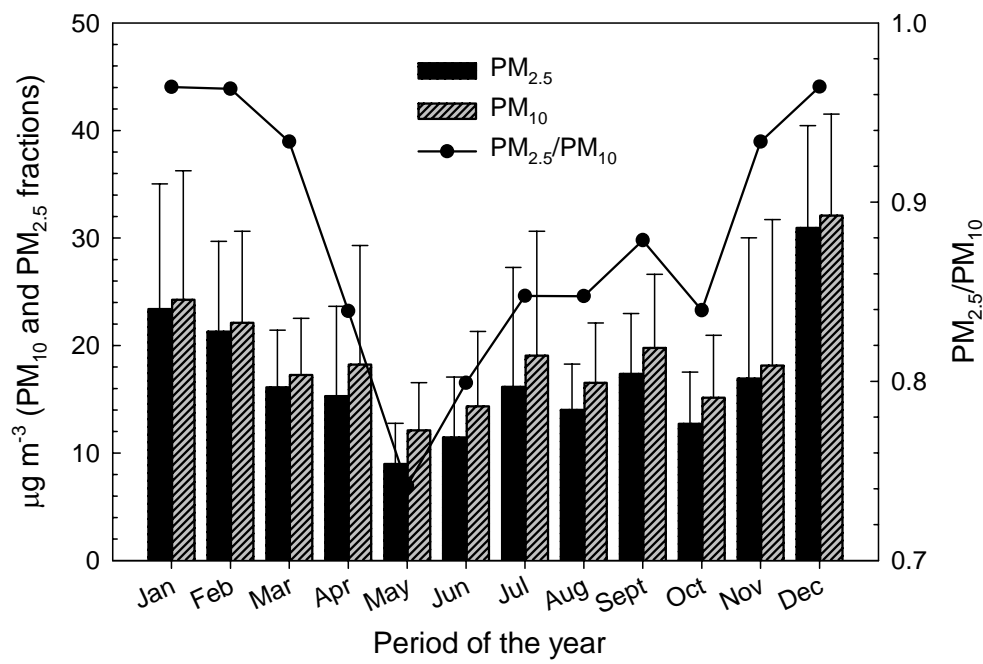


FIGURE 3

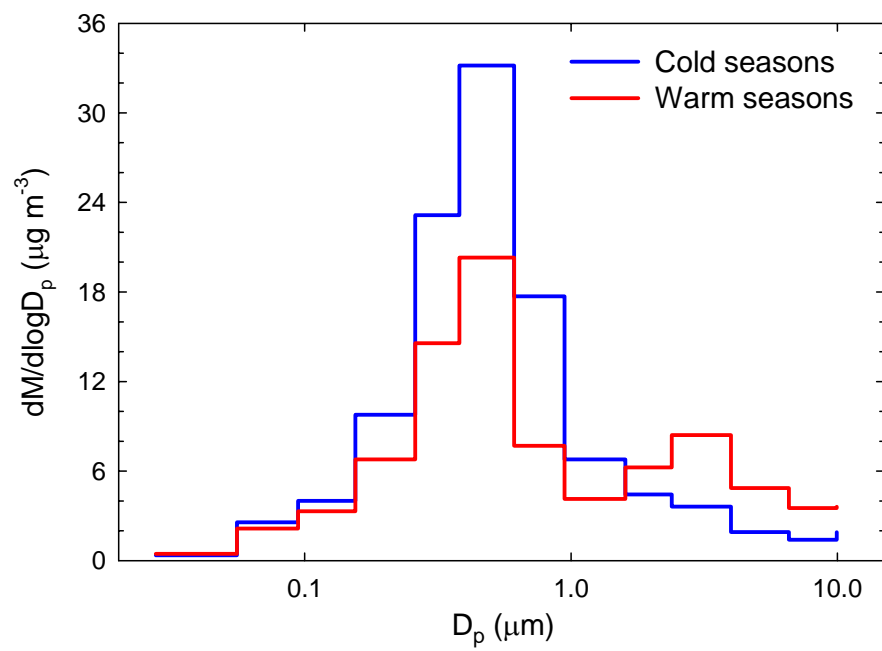


FIGURE 4

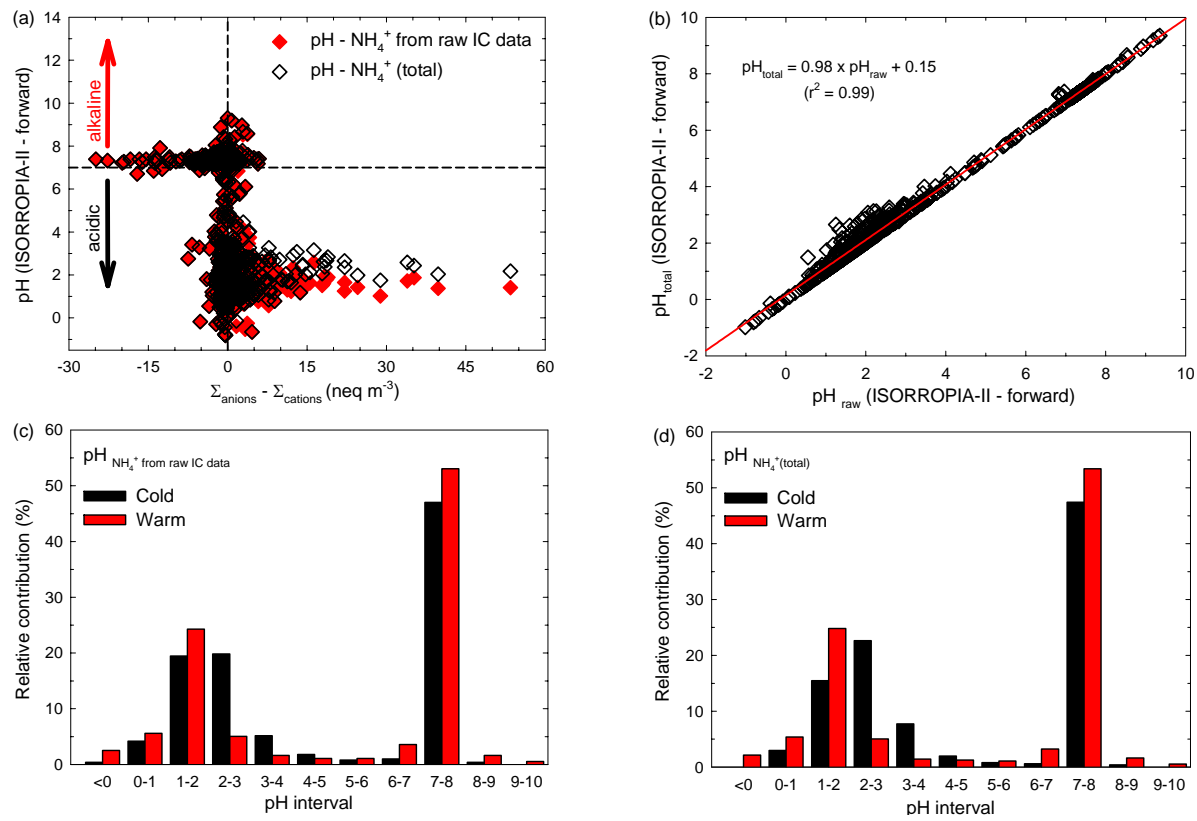


FIGURE 5

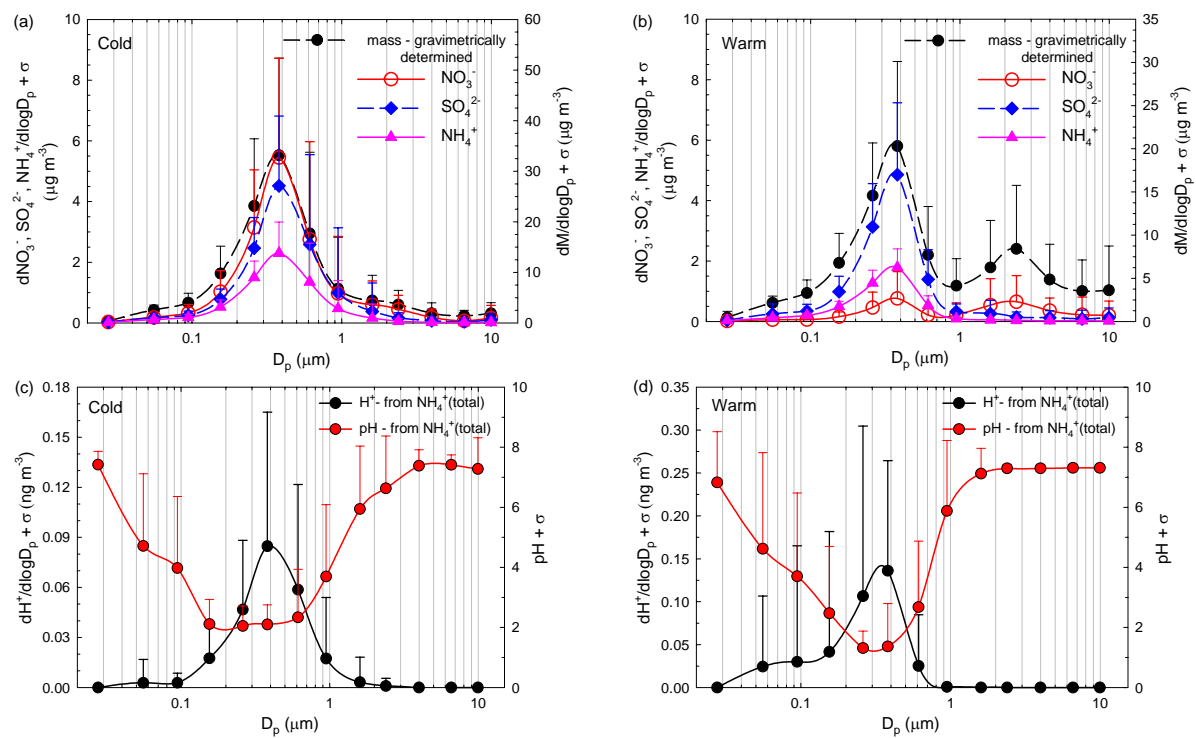


FIGURE 6

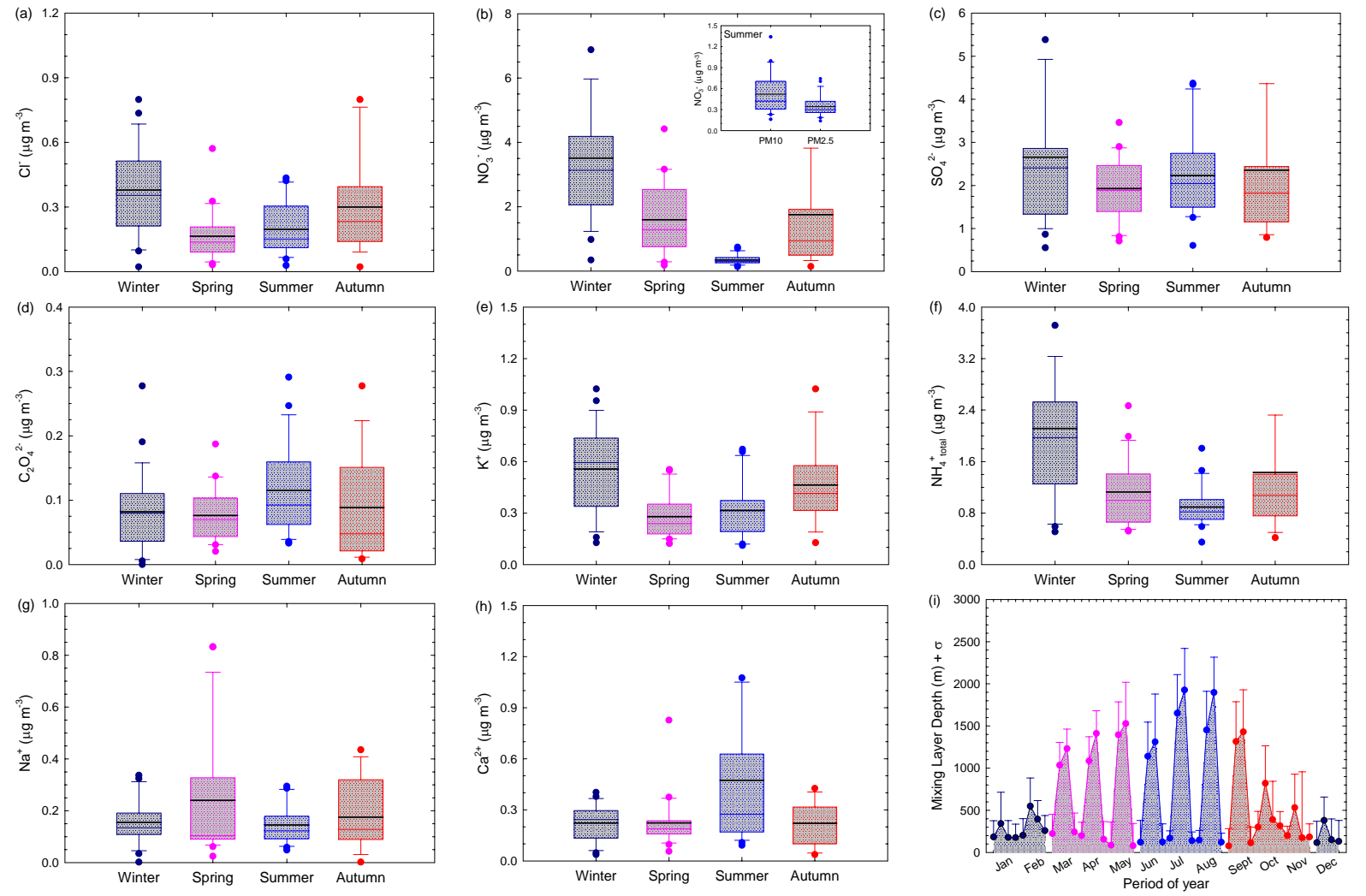


FIGURE 7

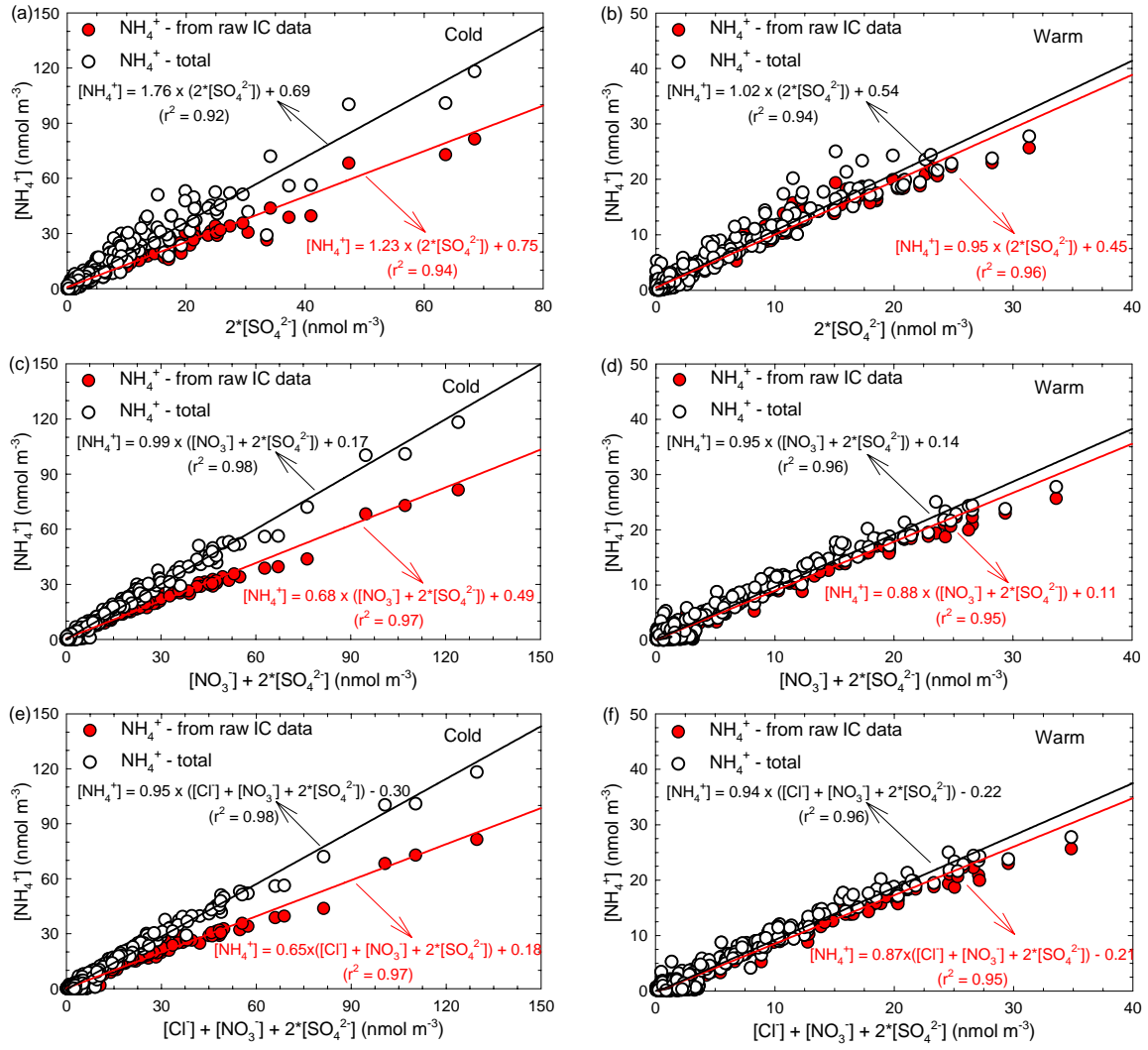


FIGURE 8

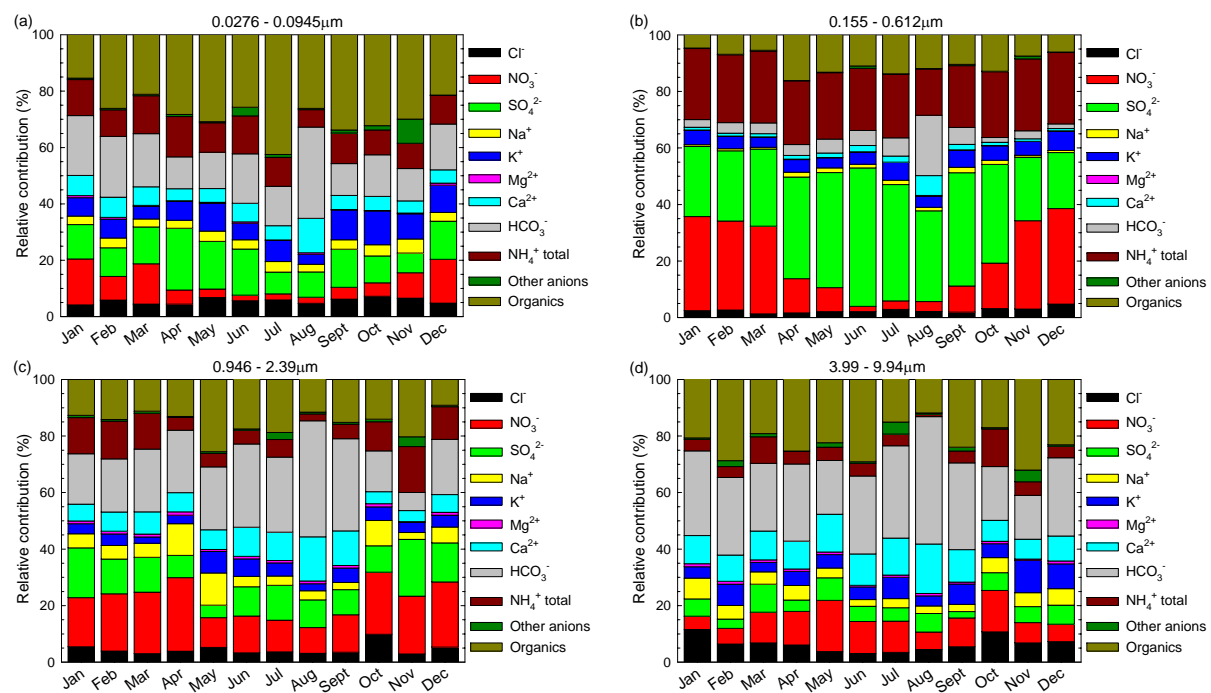


FIGURE 9

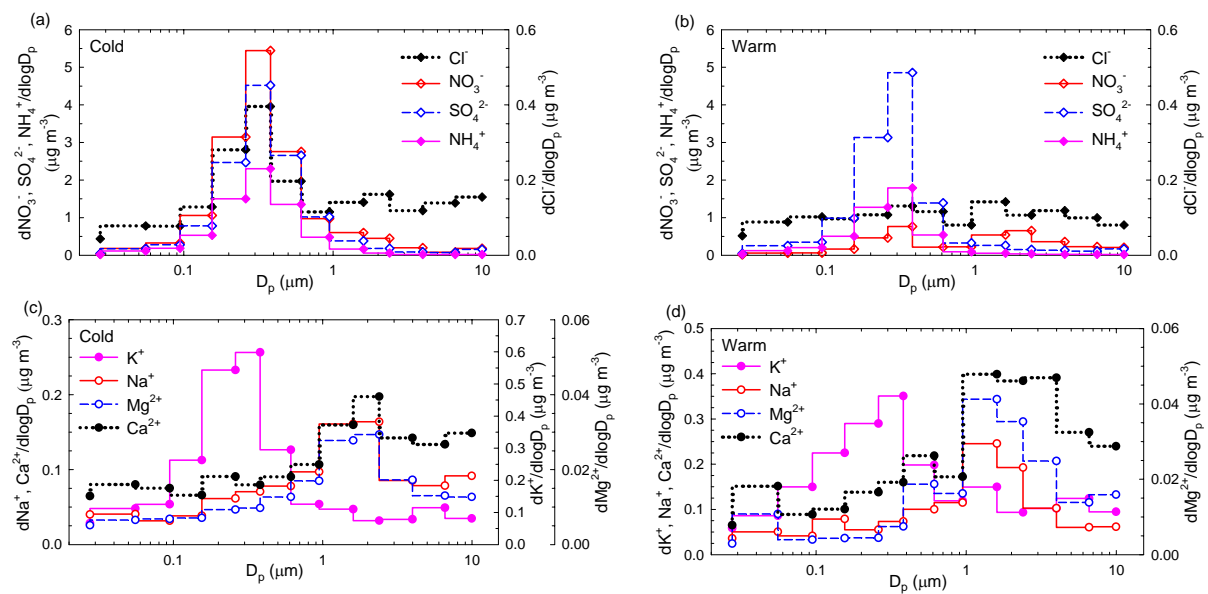
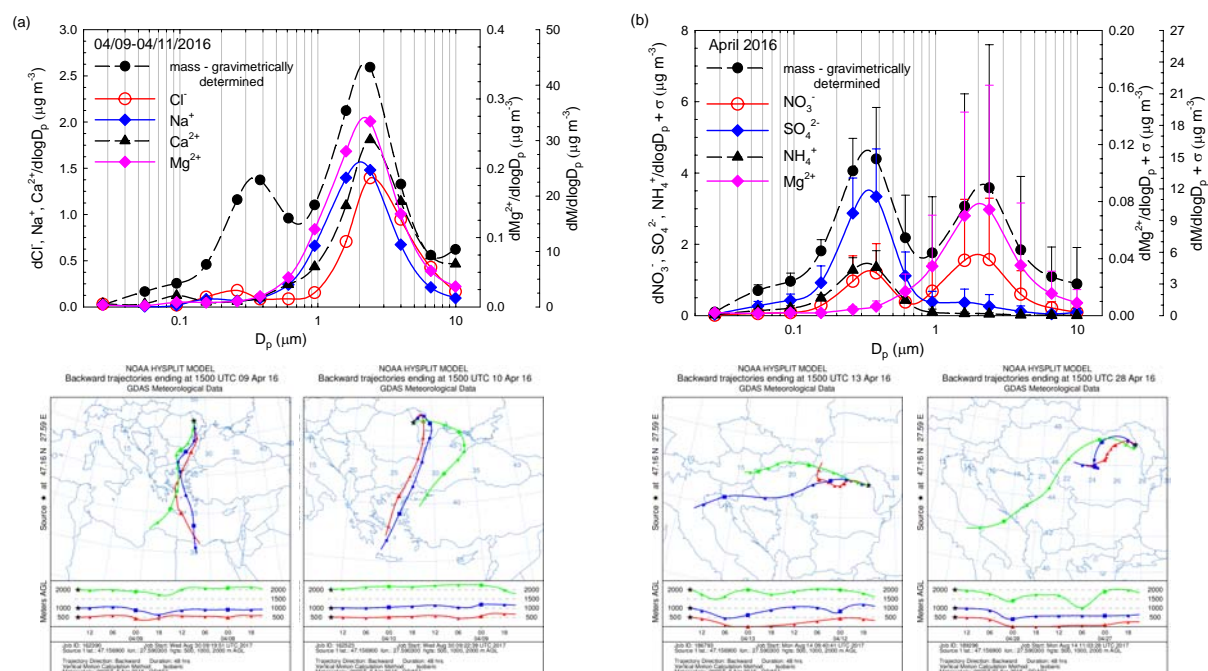


FIGURE 10



Chemical characteristics of size resolved atmospheric aerosols in Iasi, north-eastern Romania. Nitrogen-containing inorganic compounds controlling aerosols chemistry in the area

Alina Giorgiana Galon-Negru¹, Romeo Iulian Olariu^{1,2}, Cecilia Arsene^{1,2}

¹"Alexandru Ioan Cuza" University of Iasi, Faculty of Chemistry, Department of Chemistry, 11 Carol I, 700506 Iasi, Romania

²"Alexandru Ioan Cuza" University of Iasi, Integrated Centre of Environmental Science Studies in the North Eastern Region, 11 Carol I, Iasi 700506, Romania

Correspondence to: Cecilia Arsene (carsene@uaic.ro); Phone number: +40-232-201354; Fax: +40-232-201313; Postal address: Cecilia Arsene, "Alexandru Ioan Cuza" University of Iasi, Faculty of Chemistry, Department of Chemistry, 11 Carol I, 700506 Iasi, Romania

Table S 1: Detailed statistics for the PM₁₀ and PM_{2.5} fractions mass concentrations determined over the investigated period (n = 84 sampling events) in Iasi, north-eastern Romania.

Applied test	PM _{2.5}		PM ₁₀	
	p-value	Confidence level (%)	p-value	Confidence level (%)
Shapiro-Wilk normality test	0.546	95	0.682	95
t-test	0.987	95	0.998	95

Section S 1

Possible explanations for the differences/similarities between afore mentioned studies might be seen as a result of the contributions brought from various factors. As shown below the differences in the PM mass concentrations reported in Galon et al. and those reported in Arsene et al. (2011) might be only slightly controlled by changes in the particle size cut-off and/or by the difference in sampling site altitude (25 m in Galon et al. vs. 35 m in Arsene et al. (2011)) which is too small to account for the difference in PM concentrations.

In Arsene et al. (2011) study, aerosol sampling has been undertaken by using a stacked filter unit (SFUs) consisting of a 8.0 µm pore size 47-mm diameter Isopore polycarbonate filter mounted in front of a 0.4 µm pore size 47-mm diameter Isopore filter. According to details in Arsene et al. (2011) and references included therein, the 50% cut-point diameter (D50) of the 8.0 µm pore size filter was estimated to be of the order on 1.5 ± 0.2 µm aerodynamic equivalent diameter (AED). Consequently, particles collected on the 8 µm pore size filters, with a diameter larger than 1.5 µm AED, were referring to the aerosol coarse fraction, while the particles collected on the 0.4 µm pore size filters were attributed to particles with a diameter below 1.5 µm AED. In Galon et al. work aerosols samples were collected on 25 mm in diameter ungreased aluminum filters using a cascade Dekati Low-Pressure Impactor (DLPI), operating at a flow rate of 29.85 L min^{-1} . Enhanced

sampling efficiency of the DLPI unit used in Galon et al. work, with regard to fine and ultrafine particles, has been observed in comparison with the SFU unit reported by Arsene et al. (2011). Parallel DLPI and SFU sampling runs (performed within January–July 2016) showed that the DLPI unit could collect in average with $\sim 6 \mu\text{g m}^{-3}$ more particles than the SFU system and this observation allowed us suggesting that most probably the operational limits of the SFU system with regard to fine and ultrafine particles could suppress to some extent the values reported by Arsene et al. (2011).

The difference observed between the PM_{10} mass concentration, i.e. $18.9 \pm 9.3 \mu\text{g m}^{-3}$, reported by Galon et al. and the PM_{total} mass concentration, i.e. $38.3 \pm 25.4 \mu\text{g m}^{-3}$, reported by Arsene et al. (2011) might actually be the result of sampling in different years with emission sources of various prevalence. Implementation of environmental quality management systems in various sectors with anthropogenic activity may account for that (e.g. attempts given by the local administrative sector in settling down soil- or road-resuspended dust especially over the warm seasons by wetting the roads, protecting areas with intense building activities, etc.).

Regarding other literature available values, in a study from 2016, Alastuey et al. (2016) report for PM_{10} concentrations in Moldova (the closest point to our sampling site), values as high as $\sim 25 \mu\text{g m}^{-3}$ over summer and of $\sim 25\text{--}30 \mu\text{g m}^{-3}$ over winter period, yielding an annual averaged value of $\sim 27.5 \mu\text{g m}^{-3}$ which is much higher than the $18.9 \mu\text{g m}^{-3}$ value reported in the present work, for Iasi, north-eastern Romania. However, the elevated concentrations observed at the eastern sites were attributed to regional or local sources (Alastuey et al., 2016). In Alastuey et al. (2016) the author reports only the altitude above sea level (i.e. 156 m for Moldova's location) and the sampling a.g.l. is not mentioned. It might be that in Alastuey et al. (2016) study if the Moldavian sampling location was assigned as an EMEP site than the sampling a.g.l. was settled in agreement with an EC Directive recommending an a.g.l. of ~ 4 or 8 m. It is believed that the difference observed between Galon et al. site (i.e. $18.9 \pm 9.3 \mu\text{g m}^{-3}$) in comparison with other European sites might actually reflect that sampling altitude would be an important controlling factor to the atmospheric aerosol burden at a site.

In Iasi, north-eastern Romania, mass concentrations in the 5 to $10 \mu\text{g m}^{-3}$ range, for the PM_{10} and $\text{PM}_{2.5}$ fractions were especially observed in samples collected after raining events (i.e., May, June, August, and October). Such behaviour would be expected since particles from the atmosphere might be efficiently removed by precipitation (Arsene et al., 2011). However, during events with strong natural or anthropogenic contributions the PM_{10} and $\text{PM}_{2.5}$ mass concentrations exceeded the averages observed at AMOS. For example, an event collected in April 2016, from 9th to 11th, with $34.3 \mu\text{g m}^{-3}$ in $\text{PM}_{2.5}$ and $43.9 \mu\text{g m}^{-3}$ in PM_{10} , was actually highly influenced by the long range transport phenomena of African dust and marine aerosols from the Black and Aegean/Mediterranean seas (i.e., event described in detail later in the text). For other events, the exceeding fine fraction mass concentrations are believed to be a result of more variable sources (combustion, biogenic, local mineral dust, meteorological factors, etc.).

Section S 2

Beside changes in sources contributions, changes in meteorological conditions (i.e. relative humidity (RH) and wind speed (WS)) might induce distinct behaviour in the seasonal distribution of the PM. While at the investigated site over the warm

seasons RH values varied in the range of ~ 30–50% and in the cold seasons in the range of ~ 45–80% we expect that at these RH values particles have proper meteorological conditions to grow. There is suggestion that in the 0 to 98% RH range, the number median diameter (NMD) may increase two-fold (from 0.018 to 0.036 μm) with the range of geometric standard deviation (σ_g) for the particle size distributions in the 1.53–2.06 range and with the larger number median diameter (NMD) having the smaller σ_g . Moreover, the authors suggest that the smaller particles grew proportionately more than the larger one (Sinclair et al., 1974).

As presented in FIG. 3 in Galon et al. work, in the 0.0556–0.946 μm particles size range, higher $dM/d\log D_p$ values over the cold seasons toward those specific for the warm seasons might actually reflect a cumulative effect induced by the contribution of the sub-micron growth particles due to higher RH values during the cold seasons. Shifts in particles diameter distribution toward higher values are expected in this case.

The observed 1.60–2.39 μm supermicrone mode is most probably a result of a more significantly contribution brought by large particles mainly associated with dust resuspension due to higher wind speeds. Although over the warm seasons averaged wind speed showed similar value to that specific for the cold seasons, monthly standard deviation toward the mean values suggested much larger dispersion. During the warm seasons, storms and rapid wind gusts are known as often engaging important quantities of dust carrying especially particles of larger diameter.

Table S 2: Detailed statistics of linear regression analysis for \sum_{cations} and \sum_{anions} determined for raw ion chromatography data in the $\text{PM}_{2.5}$ and PM_{10} fractions over the total investigated period, cold and warm seasons, in Iasi, north-eastern Romania.

	$\text{PM}_{2.5}$				PM_{10}			
	$\sum_{\text{cations}}/\sum_{\text{anions}}$ ratio	r	p-value	Confidence level (%)	$\sum_{\text{cations}}/\sum_{\text{anions}}$ ratio	r	p-value	Confidence level (%)
Total period	0.69	0.94	< 0.001	99.9	0.70	0.94	< 0.001	99.9
Cold seasons	0.67	0.98	< 0.001	99.9	0.68	0.98	< 0.001	99.9
Warm seasons	0.84	0.87	< 0.001	99.9	0.86	0.86	< 0.001	99.9

Note: r–Pearson coefficient

Section S 3

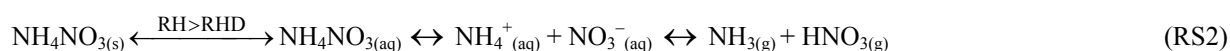
The missing $\text{HCO}_3^-/\text{CO}_3^{2-}$ has been estimated as suggested by Arsene et al. (2007) while the rationale previously proposed by Arsene et al. (2011) has been used to estimate the missing NH_4^+ . Within the $\text{NH}_4^+(\text{total})$ fraction (defined as the sum between that derived from raw IC data and the part estimated by using the rationale of Arsene et al. (2011)), the correction for the missing NH_4^+ accounted for about 21.65 ± 25.70 % for the warm seasons while for the cold seasons the correction accounted for about 46.05 ± 18.43 %. However, when estimated missing NH_4^+ has been taken into account a significant improvement in the overall ionic balance (\sum_{cations} vs. \sum_{anions}) was observed for both the $\text{PM}_{2.5}$ and the PM_{10} fractions (detailed statistics in Table S 3).

Section S 4

During sampling, perturbations in the gas to particle equilibrium may occur with evaporation of semi-volatile NH_4NO_3 and NH_4Cl salts from the fine particles collected on the front filters and fluctuations during sampling in temperature, relative humidity and/or pressure drop across the filters might highly affect the measurements of these species especially in urban environments (Pathak and Chan, 2005; Ianniello et al., 2011). Moreover, the total concentration of ammonium salts in $\text{PM}_{2.5}$ is usually described as a sum of the measurements both for non-volatile (unevolved) and volatile (evolved) fine particulate species (Ianniello et al., 2011). Since in the present work during sampling neither denuders nor backup-filters were used, sampling artefacts of semi-volatile NH_4NO_3 and NH_4Cl species are not completely excluded. Although presented data are reliable from the instrumental analysis point of view, limitations related to potential unmeasured species especially due to sampling procedure (during and after) should always be taken into account (i.e. potential NH_4^+ , NO_3^- and Cl^- evolving from the filters as a result of NH_4NO_3 and NH_4Cl dissociations).

In Galon-Negru et al. manuscript the completeness degree of the ionic balance for the identified and quantified species in both the PM_{10} and $\text{PM}_{2.5}$ fractions was checked and quite often slopes lower than unity in the $\sum \text{cations}$ vs. $\sum \text{anions}$ dependences were observed in both cases indicating important cation deficit in the ionic balance. As mentioned in the manuscript, per sampled events either cation or anion deficit has been observed in various stages. For similar behavior in Arsene et al. (2011) a detailed rationale has been proposed in order to explain/estimate either missing anions or cations within the ionic budget (under subsections 3.3 Role of inter-particle and gas-particle interactions in establishing fine and coarse fractions chemical composition and 3.4 The ionic balance in the coarse and fine fractions of Arsene et al. (2011) paper). As given in Arsene et al. (2011), meteorological conditions favourable to generate deliquesced particles in the form of $\text{NH}_4\text{NO}_{3(\text{aq})}$ and $\text{NH}_4\text{Cl}_{(\text{aq})}$ may exist in Iasi, north-eastern Romania, with deliquesced particles being formed under conditions of relative humidity at deliquescence (RHD), a parameter which is defined as the relative humidity at which deliquescence is completed.

While in Arsene et al. (2011) high RH values were representative for the warm seasons it seems that in Galon-Negru et al. manuscript high RH values, and hence representative conditions for deliquescence to occur, were mainly prevailing during the cold seasons. As suggested in Arsene et al. (2011) under deliquescence conditions, deliquesced particles may lead to the formation of aqueous droplets by a process favouring formation of internal mixture from externally mixed particles, which actually results in changes in the activities of semi-volatile species. According to Pathak and Chan (2005) in mixed collected particles the gas-particle equilibrium will tend to re-establish by mass exchange between the gas and particulate phases. Moreover, if deliquesced particles are formed under favourable meteorological conditions, then the following reactions can occur during inter-particle or gas-particle interactions:





with (RS1), (RS2), (RS5) being responsible for artefacting ammonium measured concentrations. While, actually, reactions (RS1) and (RS2) would be responsible for negative ammonium artefacts, reaction (RS5) would involve absorption of ammonia on aqueous droplets with positive artefacts. The competition between (RS1), (RS2) and (RS5) reactions will strongly depend on meteorological conditions directly related to RH, RHD and temperature but also on chemical species abundances. According to Pathak and Chan (2005) in ammonium reach environments, reaction (RS5) would be responsible on highly contributing artefacts in NH_4^+ and H^+ distribution, especially due to acidity neutralisation by the existent ammonia. In their work, Arsene et al. (2011) proposed a detailed rationale for a potential estimation of the unmeasured NH_4^+ fraction induced most probable by the reactions inducing negative artefacts and significantly occurring during sampling. In Galon-Negru et al. work this unmeasured NH_4^+ has been called “missing NH_4^+ ” and for its estimation Arsene et al. (2011) rationale has been used.

Table S 3: Detailed statistics of linear regression analysis for \sum_{cations} and \sum_{anions} determined when estimated missing NH_4^+ has been taken into account, in the $\text{PM}_{2.5}$ and PM_{10} fractions over the total investigated period, cold and warm seasons, in Iasi, north-eastern Romania.

	$\text{PM}_{2.5}$				PM_{10}			
	$\sum_{\text{cations}}/\sum_{\text{anions}}$ ratio	r	p-value	Confidence level (%)	$\sum_{\text{cations}}/\sum_{\text{anions}}$ ratio	r	p-value	Confidence level (%)
Total period	0.95	0.98	< 0.001	99.9	0.95	0.98	< 0.001	99.9
Cold seasons	0.97	0.99	< 0.001	99.9	0.98	0.99	< 0.001	99.9
Warm seasons	0.87	0.96	< 0.001	99.9	0.86	0.96	< 0.001	99.9

Note: r–Pearson coefficient

Section S 5

Additional information about ISORROPIA-II runs performed in the present work

The model helps deriving (even under constraints) either information related to potential H^+ concentration in the aerosol particles (implicitly also on aerosols pH) or to the liquid water content (if a liquid phase exists), and computed concentrations of gas–phase semi-volatile compounds in equilibrium with the aerosol (e.g., NH_3 , HNO_3 , and HCl) (Hennigan et al., 2015). Although use of ISORROPIA-II model runs in forward mode with only aerosol-phase input is highly susceptible for debate, Guo et al. (2015) report also about use of the model under these specific conditions. It seems that under these circumstances the model is less sensitive to measurement error than the reverse mode. However, in Guo’s et al. (2015) work, pHs reported for SCAPE were corrected for the identified bias and the values were increased by 1 to simplify the correction. Although there is suggestion that in thermodynamic model calculation (a region where the thermodynamic predictions, and assumption of equilibrium, become more accurate) only data with RH exceeding 60 % might be considered (Moya et al., 2002), in the present work ISORROPIA-II was applied over the entire set of data-base regardless RH values (in 2016, at the investigated site, July, August and September were the months with $\text{RH} < 40\%$). However, the model was also

run at additional 5 to 10 % RH (to that experimentally recorded) in order to check RH potential influence on the envisaged estimations. It has been observed that a change in the RH value with 5 or 10 % would result actually in a pH change with about 2 and, respectively, 3 %. Since in the present work, organic species have been taken into account in the ionic balance it is believed that the bias in the estimated species (especially NH_4^+ and $\text{HCO}_3^-/\text{CO}_3^{2-}$) is minimized and implicitly that in inferred H^+ by ISORROPIA-II thermodynamic model.

For the present data-base, ISORROPIA-II model was run in “forward mode” for metastable aerosol. Runs were performed both for NH_4^+ derived from raw IC data and also for the situation when missing ionic species have been indirectly estimated and taken into account ($\text{NH}_4^+(\text{total})$ and $\text{HCO}_3^-/\text{CO}_3^{2-}$ estimated as previously presented). For Iasi, north-eastern Romania, when ISORROPIA-II estimated H^+ has been taken into account the improvement in the overall ionic balance (in comparison with that derived by considering the $\text{NH}_4^+(\text{total})$ fraction) was almost insignificant with an ~ 2 % increase on the \sum_{cations} vs. \sum_{anions} ratio, observed in both the $\text{PM}_{2.5}$ and PM_{10} fractions. However, over the warm seasons it seems that neither $\text{NH}_4^+(\text{total})$ fraction option nor the one taking into account ISORROPIA-II estimated H^+ concentrations do not lead to a close to 1 ionic balance, with ratios varying between 0.84 and 0.88 for the $\text{PM}_{2.5}$ fraction and 0.84 to 0.87 for the PM_{10} fraction. Such observation would not suggest high uncertainty in the accuracy of the ionic species measured values but most probably that some volatile cation species (e.g., amines) were not measured.

Section S 6

Actually, for about 19 % of the data the aerosol pH differed by less than 1.0 pH unit when $\text{NH}_4^+(\text{total})$ concentrations (defined as the sum between that derived from raw IC data and the part estimated by using the rationale of Arsene et al. (2011)) increased in comparison with NH_4^+ derived from raw IC data (a (35.65 ± 24.92) % increase in NH_4^+ concentration for the entire data-base, a (21.65 ± 25.7) % increase for the warm seasons and a (46.05 ± 18.43) % (mean \pm stdev) increase for the cold seasons). Such change in NH_4^+ concentrations is not unexpected since this is assigned as a highly volatile compound, with high susceptibility to be lost by evaporation. As shown in the text, meteorological parameters (i.e., RH) could play an important role within NH_4^+ distribution in both during the warm and the cold seasons. In other studies, higher evaporation rates are reported for summer when compared to winter, but during winter low RH values were prevailing (Ianniello et al., 2011; Zhao et al., 2016). Ianniello et al. (2011) report for example that in Beijing, China, about 35 % of fine particulate NH_4^+ was susceptible to evaporate from the sampling filters during winter while about 53 % of fine particulate NH_4^+ was susceptible to evaporate during summer. For the same location, Zhao et al. (2016) report NH_4^+ loss of 6 % and higher losses of NO_3^- and Cl^- .

Section S 7

In the Introduction section of Galon-Negru et al. work it has been already stated that “Particles acidity might influence transition metals solubility and enhance aerosols toxicity and atmospheric nutrient delivered through atmospheric deposition in marine areas (Meskhidze et al., 2003; Fang et al., 2017).”. Particles pH is known to affect the solubility of trace metals

(such as Fe) found in aerosols (Meskhidze et al., 2003; Fang et al., 2017), with lower pH dissolving metal oxides and converting them to soluble metal sulfates (Oakes et al., 2012), conditions which would significantly change the aerosol environmental impacts. As presented in Guo et al., (2016), while at global level metal mobility will mainly affect nutrient distributions with important impacts on productivity, carbon sequestration, and oxygen levels in the ocean, at regional scales soluble transition metals seem mainly to enhance aerosol toxicity or their oxidative potential. Through SO_4^{2-} contributions to aerosols acidity and the historical record of associations between so-called particle “strong acidity” and adverse health effects, Fang et al. (2017) suggest that SO_4^{2-} linkages to health are most probably determined by SO_4^{2-} role in acid dissolution of primary metals commonly found in ambient particles, while Tsagkogeorgas et al. (2017) suggest that on a regional to global scale the acidification of fresh water and forest ecosystems is most probable caused by wet and dry deposition of SO_2 and SO_4^{2-} particles.

Epidemiological studies have often reported adverse health outcomes associated with strong aerosols acidity (Dockery et al., 1996; Gwynn et al., 2000; Lelieveld et al., 2015). In “Measuring aerosol damage to the atmosphere” (http://ec.europa.eu/research/infocentre/article_en.cfm?artid=31296, 28 October 2013), “Arsene says the high aerosol levels are probably linked to the high rate of various pulmonary diseases registered at the Clinic of Pulmonary Diseases in Iasi. These include cases like chronic obstructive pulmonary diseases (COPD), pneumonia, asthma (allergy, rhinitis), bronchiectasis (sometimes associated with bacterial infection) and tuberculosis often detected in the area.”. The claim is not a result of a systematic work on an epidemiological study in Iasi, north-eastern Romania, but it represents a general observation of Arsene after performing research work with specialists and medical doctors in the field of pulmonary diseases (Cernat et al., 2011).

Moreover, upon our knowledge there is a single report, mentioned by Arsene et al. (2007), referring to indirect evidences of acid rain impacts in Iasi region, north-eastern Romania. In the performed study, Arsene et al. (2007) calculated high wet deposition fluxes for ions of anthropogenic origin in the $\text{SO}_4^{2-} > \text{NO}_3^- > \text{NH}_4^+$ order. The determined values, although among the highest, were in generally in good agreement with values reported for other north European sites (such as those for Poland, the Czech Republic, etc.). In the analysed raining events, air masses crossing very large continental areas (N and E sectors) brought the highest contribution in terms of fluxes for ionic species such as Ca^{2+} while the NW and W sectors brought more significant contributions for anthropogenic related elements (SO_4^{2-} , NO_3^- , NH_4^+). Arsene et al. (2007) suggested that in the rainwater, higher fluxes of these elements for the NW and W sectors, when compared with other geographical sectors, was most probably also a result of important local influences, as the sampling site was located east side of the Oriental Carpathians chain that could constrain, to some extent, the pollution plume transported from western Europe. Arsene et al. (2007) report that the pH of the analysed rainwater events was 5.92 (volume weighted mean average, VWM) suggesting a sufficient load of alkaline components neutralizing rainwater acidity. Moreover, the authors suggested that on average, 97 % of the acidity in the collected rainwater samples was mostly neutralized by CaCO_3 and NH_3 .

Section S 8

Regarding meteorological parameters, i.e. RH and temperature, in Galon-Negru et al. work is shown that over the cold season's high RH values and low temperatures were prevailing while over the warm seasons these parameters showed opposite trends. In the work of Ianniello et al. (2011), related to chemical characteristics of inorganic ammonium salts in PM_{2.5} in the atmosphere of Beijing (China), the relationship between partitions of specific nitrogen-containing inorganic species towards various parameters has been investigated. The prevailing conditions over the two investigated time-periods, i.e. 23 January – 14 February 2007 and from 2 to 34 August 2007, showed higher RH values over the summer (high temperatures) and lower RH values over the winter (low temperatures).

Ianniello et al. (2011) treats in a very complex manner the relationship existent between particulate species such as SO₄²⁻, NO₃⁻, Cl⁻ and NH₄⁺, and possible partition routes in the NH₃/NH₄⁺ system. Gas-to-particle conversion (photochemical processing) or heterogeneous processes are assigned as important sources contributing to particulate NO₃⁻ abundances in the atmosphere. The authors claim that while NO₂ conversion to NO₃⁻ through photochemical processing during the winter season is expected to contribute to NO₃⁻ abundance over this period of the year, the heterogeneous formation (through condensation or absorption of NO₂ in moist aerosols) generally relates to relative humidity and the particulate atmospheric loading (Ianniello et al., 2011). The existence of large amounts of particulate NO₃⁻, observed in summer by Ianniello et al., 2011, was considered as unexpected since NH₄NO₃ is semi-volatile and tends to dissociate and remain in the gas phase under high temperatures. Ianniello et al., (2010) report 6 times higher NH₃ concentrations in summer than in winter, with temperatures ranging from 1 to 14 °C in winter and 22 to 35 °C in summer periods. Under these circumstances high concentrations of fine particulate NO₃⁻ in summer period were attributed to the existence of higher concentrations of NH₃ in the atmosphere, available to neutralise not only H₂SO₄ but also HNO₃ from the atmosphere. In addition, at the high RH values (daily mean in the 35 to 90 % range) reported in Ianniello et al. (2011) study significant fraction of HNO₃ and NH₃ were considered to be dissolved in humid particles, with enhanced distribution of fine particulate NO₃⁻ and NH₄⁺ in the atmosphere.

In Galon-Negru et al. work particulate NH₄⁺ showed higher values during the cold seasons when compared to the warm seasons and its variation coincide with those of fine particulate NO₃⁻ and Cl⁻. Although such behaviour would indicate that NH₄⁺ was largely originating from the neutralization between ammonia and acidic species such as HNO₃ and HCl, as shown under Subsection 3.2.3 (Stoichiometry of (NH₄)₂SO₄, NH₄NO₃ and NH₄Cl), the most important contribution was most probably brought by H₂SO₄ species. However, the very similar pattern observed for NO₃⁻, Cl⁻ and NH₄⁺ suggest that these species were representative for likely internally mixed particles and came most probably from similar gas-to-particle processes (Huang et al., 2010). Galon et al. report for SO₄²⁻ comparable concentrations during both the summer and winter seasons, and Backes et al. (2016a) suggest that the formation of SO₄²⁻ particles is not limited by NH₃ in any season. During the warm seasons, higher temperatures and solar radiation intensity, enhancing the photochemical activity and the atmospheric oxidation potential, is also enhancing the oxidation rate of SO₂ to particulate SO₄²⁻, but during the cold seasons wood burning might become an important source of SO₄²⁻.

At high RH values, and especially for deliquescent particles, there is suggestion that most of the fine particulate NO_3^- exists as an internal mixture with SO_4^{2-} , so that HNO_3 can be easily absorbed into the droplets, a process considerably reducing the thermodynamic dissociation constant for NH_4NO_3 (Zhang et al., 2000; Ianniello et al., 2011). Under these circumstances it is supposed that fine particulate NO_3^- can be formed from HNO_3 and NH_3 through heterogeneous reactions on fully neutralised fine particulate SO_4^{2-} (a process which has been taken into account also in Galon et al. work, under the Subsection 3.2.3). In Galon et al. work significant correlation has been observed between SO_4^{2-} and NO_3^- . These two measured parameters showed significant correlation with the RH, with high concentrations in SO_4^{2-} or NO_3^- being formed at high RH values. Such behaviour would allow us suggesting that NO_3^- is being produced on preexisting SO_4^{2-} aerosols, which could provide sufficient area and aerosol water content for the heterogeneous reaction to occur should be available.

Markovic et al. (2011) show that at high RH, the amount of the gaseous precursors, such as NH_3 and HNO_3 , have relatively little influence on the formation of fine particulate nitrate. Ianniello et al. (2011) concluded also that in summer period, with high prevailing RH values, almost on all days the meteorological conditions were favourable for the formation of NH_4NO_3 at Beijing site.

In Galon et al. work, regarding gaseous NH_3 values such as those derived from ISORROPIA, it should be pointed out that its estimated concentration was much higher than that of HNO_3 and HCl in gas phase. During the cold seasons the $[\text{NH}_3]/([\text{HNO}_3] + [\text{HCl}])$ ratio is as high as 2.0 ± 0.6 for RH values $< 40\%$, 3.6 ± 2.0 for RH values in the $40\text{--}60\%$ range, and 3.0 ± 1.4 for RH values $> 60\%$ RH. During the warm seasons, for similar RH groups, the ratio takes the 4.9 ± 1.9 , 4.6 ± 1.4 and 9.1 ± 6.2 values. Ianniello et al. (2011) report a $[\text{NH}_3]/([\text{HNO}_3] + [\text{HCl}])$ ratio of 27.90 ± 12.70 for winter season and of 54.06 ± 20.60 for the summer period. The authors are finally claiming that the atmosphere of their interest location was ammonia-rich in gas phase over both investigated seasons.

Moreover, for the specific conditions referring to Galon et al. work, the authors have observed that by analysing the events for similar RH groups, but for cold and warm seasons separately, the $\text{NH}_3/\text{NH}_4^+$ partition didn't enhance significantly. During the cold seasons over the three RH investigated groups, the fractions of the NH_3 , HCl and HNO_3 present in the gaseous form have taken in average the 71.4 ± 4.7 , 4.4 ± 0.3 and $24.0 \pm 4.8\%$ values. Over the warm seasons for the previously mention species the fractions present in the gaseous form have taken in average the 83.1 ± 3.4 , 6.6 ± 0.6 and $10.3 \pm 3.4\%$ values.

Section S 9

Backes et al. (2016a,b) present in some of their publication seasonal distributions in NH_3 emissions under static- and dynamic-time profile (STP and DTP) scenarios. While the STP scenario lacks dynamic, meteorology dependent or specific differences in policies or intensity of animal husbandry, the DTP scenario takes into account potential meteorological variables (such as wind speed and surface temperature) influence on the distribution of the annual emissions. However, while under the STP scenario, the annual time series of NH_3 showed one annual peak in spring (March), in the DTP scenario NH_3 concentrations show two annual peaks, one in spring (May) and one in autumn (September). The authors underline that

implementation of the DTP resulted in a shift from seasonal average winter NH_3 emissions to summer emissions. According to Backes et al. (2016a), high NH_3 concentrations are known to appear in proximity to emission sources, due to its low atmospheric lifetime which results in NH_3 concentration levels in the atmosphere which closely follow the seasonal emission trend.

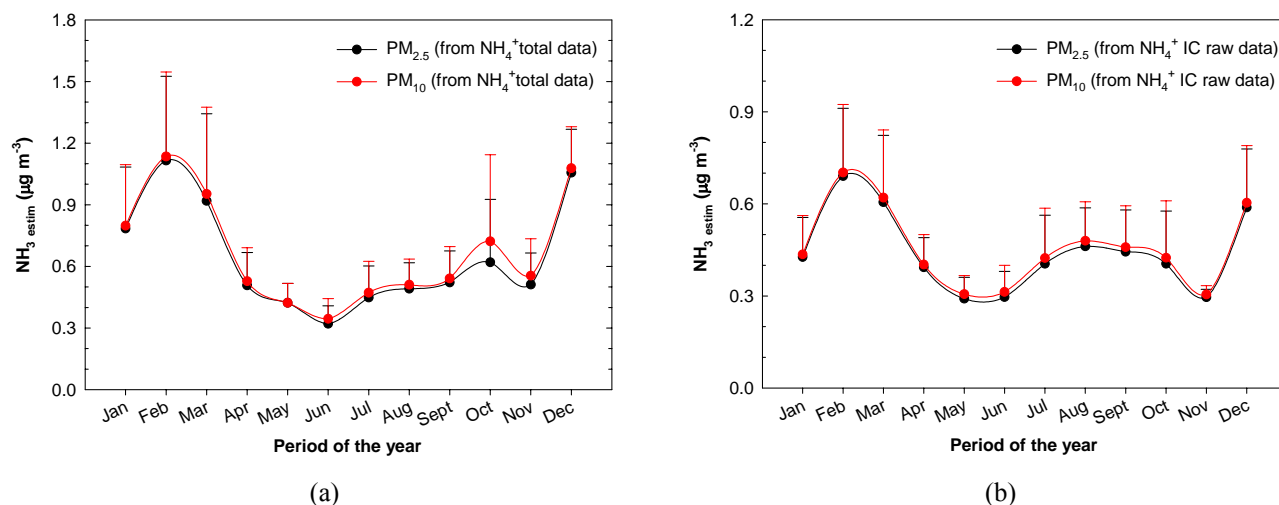


Figure S 1: Time series in NH_3 concentrations derived from ISORROPIA-II runs for the 2016 data-base, both for $\text{PM}_{2.5}$ and PM_{10} scenarios in Iasi, north-eastern Romania.

Moreover, Sutton et al. (2013) claim that together with increased anthropogenic activity, global NH_3 emissions may increase from 65 (48–85) Tg N in 2008 to about 132 (89–179) Tg N by 2100. Most NH_3 emissions are known to result from agricultural productions strongly influenced by climatic interactions. There is, however, recognition about the fact that most of the up to now used approaches failed in recognising that a warm dry-year would tend to give larger NH_3 emissions than a cold-wet year. Estimates in the global NH_3 emission made by Sutton et al., (2013) indicate agricultural soils and crops, including emissions from grazing and land application of animal manure, as a first ammonia ranked source with 28.3 Tg N yr^{-1} contribution. This is immediately followed by excreta from domestic animals (8.7 Tg N yr^{-1}), oceans and volcanoes (8.6 Tg N yr^{-1}), biomass burning (5.5 Tg N yr^{-1}), waste composting and processing (4.4 Tg N yr^{-1}), and by other sources with contributions of < 3.3 Tg N yr^{-1} .

Details presented in FIG. S 1 clearly show that for Iasi, north-eastern Romania, yearly NH_3 distributions as derived from ISORROPIA-II model present clear maxima in February and December in a behaviour suggesting important local sources contributions over the winter season. It might be that this distribution follows actually a trend mainly controlled by the agricultural practices in rural areas surrounding Iasi, mainly related to the timing of manure spreading on agricultural soils. Moreover, in Iasi and in the nearby counties, the contribution brought by open (sheep and goat) barns, operating over the cold season mainly in a “hot-spot” mode, might increase as importance. Manure storage from local and regional closed

barns (pigs and poultry) might also bring important contributions over the winter. Although biomass burning might bring important contribution in terms of global ammonia emissions it is believed that at the interest location this source is overwhelmed by agricultural practices in the area.

Table S 4: Detailed statistics of linear regression analysis for major water soluble ions determined in the PM_{2.5} and PM₁₀ fractions over the total investigated period in Iasi, north-eastern Romania.

	PM fraction	Slope	Pearson coefficient (r)	p-value	Confidence level (%)
Cl ⁻ vs. RH	PM _{2.5} ; PM ₁₀	+	> 0.71	0.010	95.4
Cl ⁻ vs. T	PM ₁₀	-	> 0.59	0.045	95.4
Cl ⁻ vs. PM	PM _{2.5} ; PM ₁₀	+	> 0.70	0.038	95.4
Cl ⁻ vs. MLD	PM _{2.5} ; PM ₁₀	-	> 0.69	0.012	95.4
NO ₃ ⁻ vs. RH	PM _{2.5} ; PM ₁₀	+	> 0.84	< 0.001	99.9
NO ₃ ⁻ vs. T	PM _{2.5} ; PM ₁₀	-	> 0.94	< 0.001	99.9
NO ₃ ⁻ vs. MLD	PM _{2.5} ; PM ₁₀	-	> 0.84	< 0.001	99.9
NO ₃ ⁻ vs. PM	PM _{2.5} ; PM ₁₀	+	> 0.70	0.021	95.4
SO ₄ ²⁻ vs. RH	PM _{2.5} ; PM ₁₀	+	> 0.44	0.177	68
SO ₄ ²⁻ vs. T	PM _{2.5} ; PM ₁₀	-	> 0.41	0.214	68
SO ₄ ²⁻ vs. PM	PM _{2.5} ; PM ₁₀	+	> 0.45	0.162	68
NH ₄ ⁺ (total) vs. RH	PM _{2.5} ; PM ₁₀	+	> 0.80	0.001	95.4
NH ₄ ⁺ (total) vs. T	PM _{2.5} ; PM ₁₀	-	> 0.94	< 0.001	99.9
NH ₄ ⁺ (total) vs. MLD	PM _{2.5} ; PM ₁₀	-	> 0.80	0.001	95.4
NH ₄ ⁺ (total) vs. PM	PM _{2.5} ; PM ₁₀	+	> 0.70	0.023	95.4

Note: RH–relative humidity; T–temperature; MLD–mixing layer depth; PM–particle loading;

Table S 5: Detailed statistics of linear regression analysis for molar concentrations of particulate NH₄⁺ and SO₄²⁻ in PM₁₀ fraction over the cold and warm seasons in Iasi, north-eastern Romania.

	NH ₄ ⁺ from raw IC data			NH ₄ ⁺ (total)		
	Pearson coefficient (r)	p-value	Confidence level (%)	Pearson coefficient (r)	p-value	Confidence level (%)
Cold seasons	0.97	< 0.001	99.9	0.96	< 0.001	99.9
Warm seasons	0.98	< 0.001	99.9	0.97	< 0.001	99.9

Section S 10

The data set from the present work has been investigated through Radar and/or Pie charts in order to identify the potential contributions brought by various sectors long-range transport to the atmospheric PM burden in the area. It should be however emphasized that the PM chemical composition appeared to be mainly driven by the air mass origin and type (e.g., continental, regional), meteorologically-controlled air mass characteristics (buoyancies), geographical context (the Oriental Carpathians chain, with the highest altitude of 1907 m, is facing Iasi ~ 150 km north-westerly distance), etc. As presented in FIG. S 2a, in overall, in terms of sectors contributions the N-NE up to the S (clockwise round) area seems to bring the most important fraction to both the PM_{2.5} and PM₁₀ abundances. Higher loaded events in terms of aerosols mass concentration

were those associated with long-range continental transport, Saharan dust-events, regional transport from more arid areas (S-SE) and buoyancy affected air masses.

Regarding potential local anthropogenic contribution to PM atmospheric burden it should be emphasized that in the immediately nearby area of the sampling point neither important commercial areas nor industrial units are operating and traffic should be the most important contributor. Actually in Iasi, in the post-communist period, the industry has almost completely ceased down and presently the Antibiotic company (7 km from the sampling point, western, W, direction), a small brick plant (8 km, SE) and the heat and power plant (5 km, SE) may account as for the most significant local anthropogenic contributors. However, Iasi is known as an important Romanian university centre (> 42000 students by 2015) with intense activity over university semesters. Traffic in the nearby area and commercial activity in the top hot-spots area of Iasi get more intense over these periods of the year. As for the rural areas surrounding Iasi, or from the nearby counties, farming activities are mainly related to cereal crops, plantation agriculture, open and closed animal barns (cattle, sheep and goat, pigs, poultry).

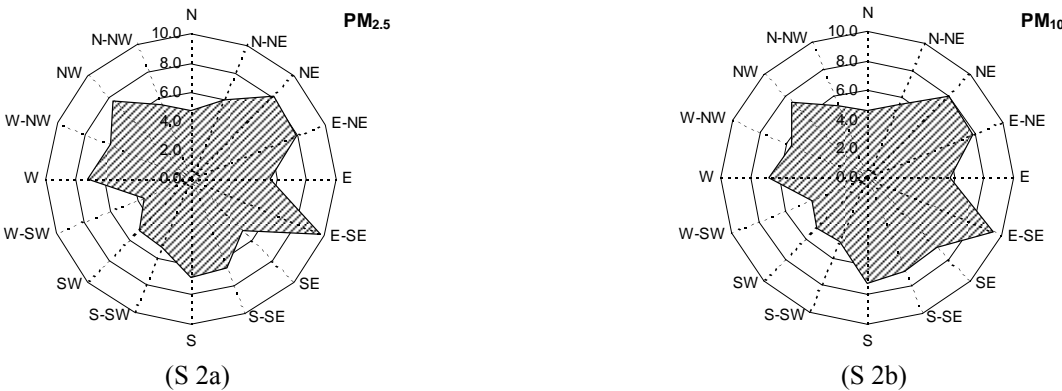
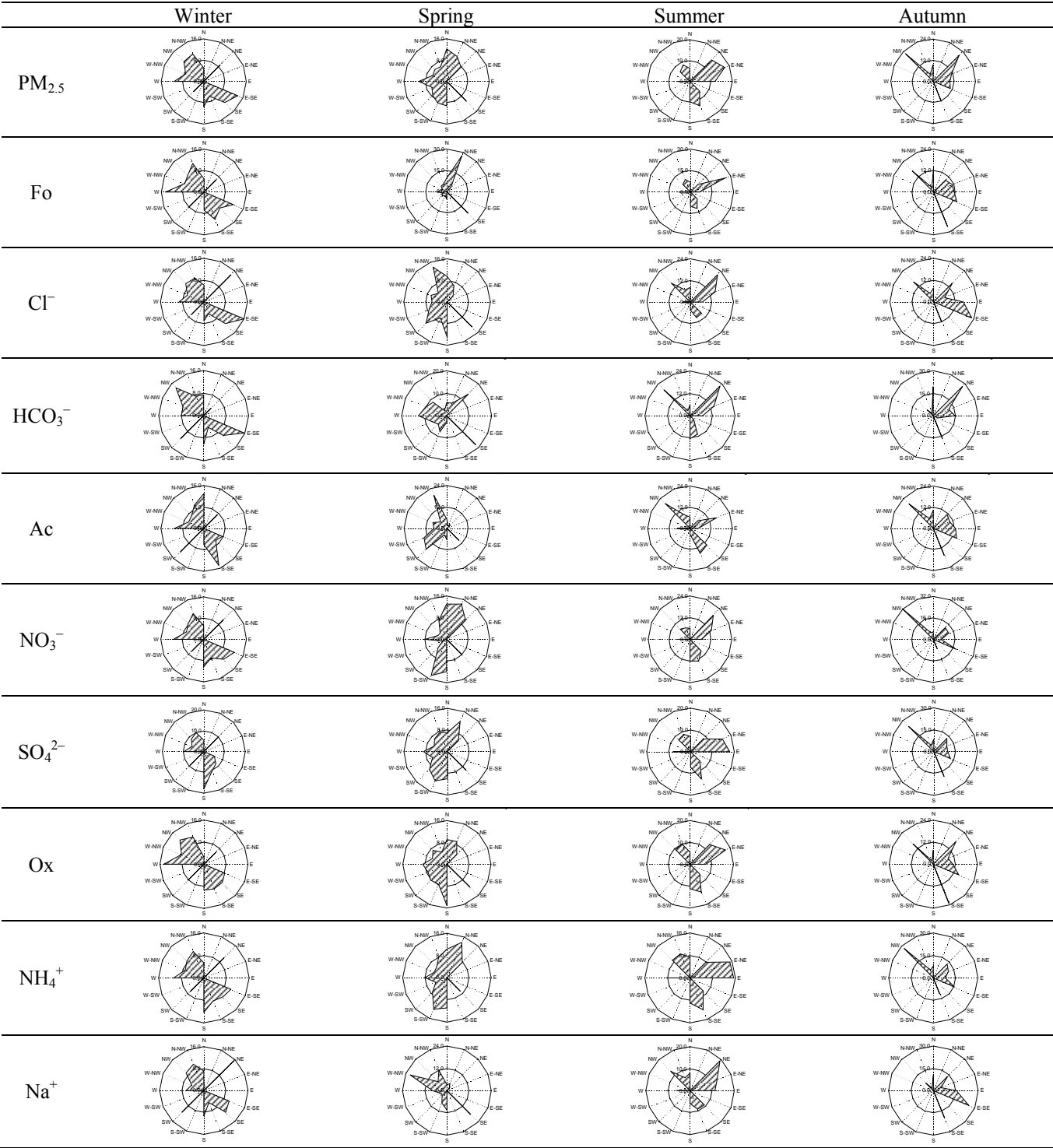


Figure S 2: Averaged annual sectors contributions both in the PM_{2.5} (S 2a) and PM₁₀ (S 2b) fractions.



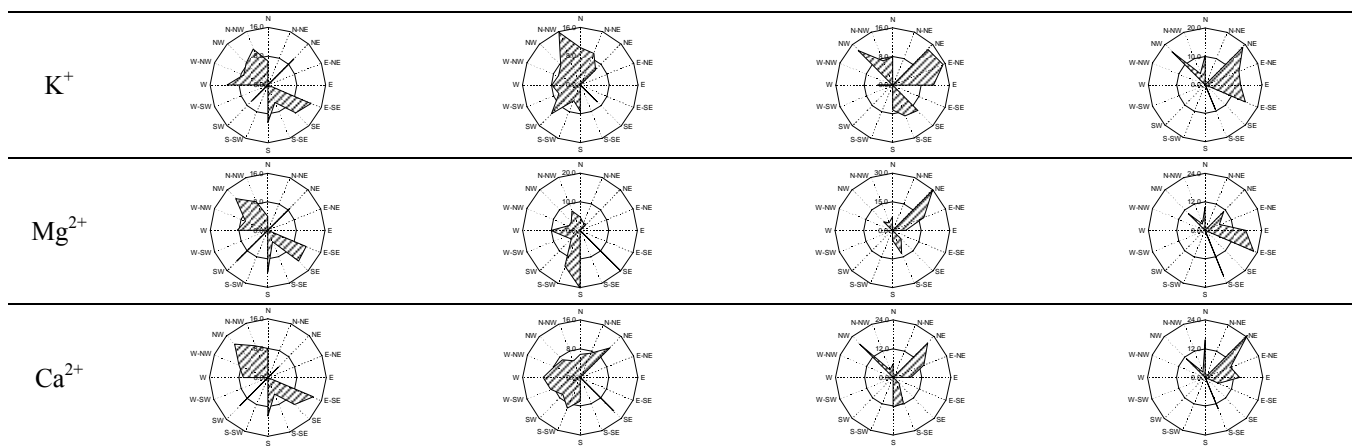
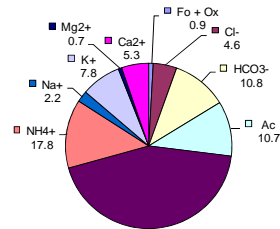
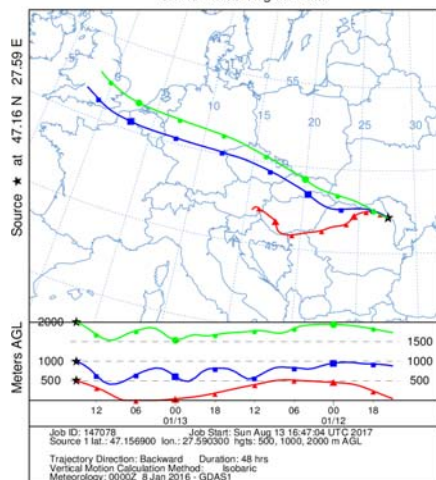
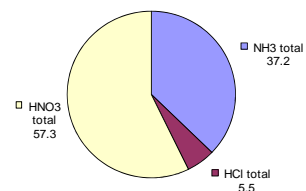


Figure S 3: Particulate inorganic and organic ions seasonal contributions (in the $PM_{2.5}$ fraction) associated with the different identified air mass.

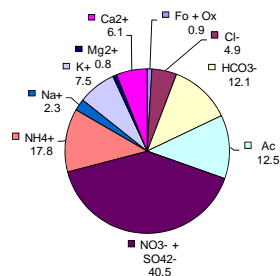
NOAA HYSPLIT MODEL
Backward trajectories ending at 1500 UTC 13 Jan 16
GDAS Meteorological Data



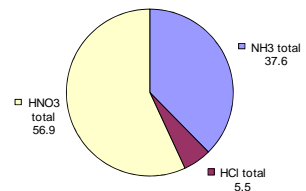
PM_{2.5}



PM_{2.5}

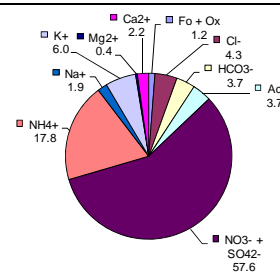
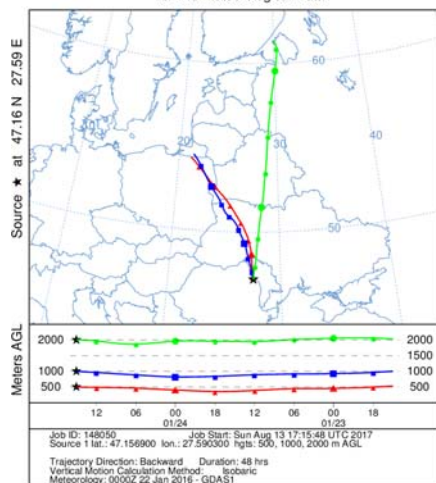


PM₁₀

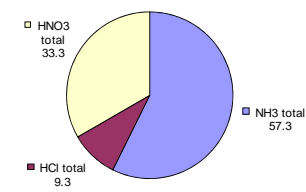


PM₁₀

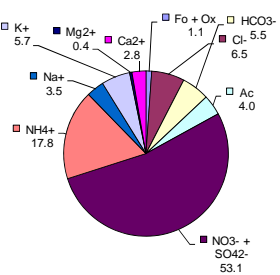
NOAA HYSPLIT MODEL
Backward trajectories ending at 1500 UTC 24 Jan 16
GDAS Meteorological Data



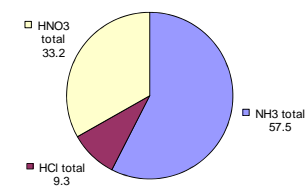
PM_{2.5}



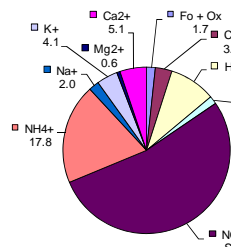
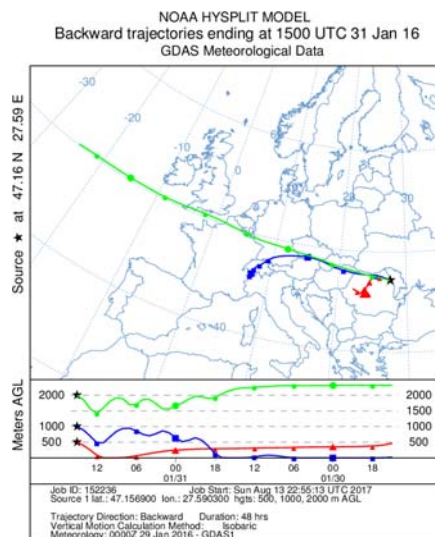
PM_{2.5}



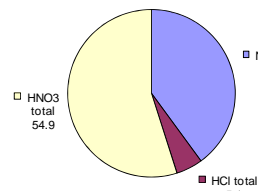
PM₁₀



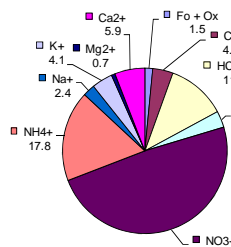
PM₁₀



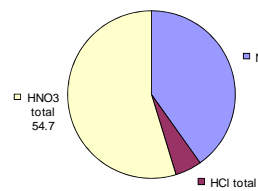
PM_{2.5}



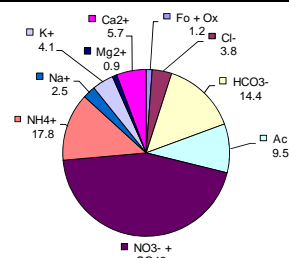
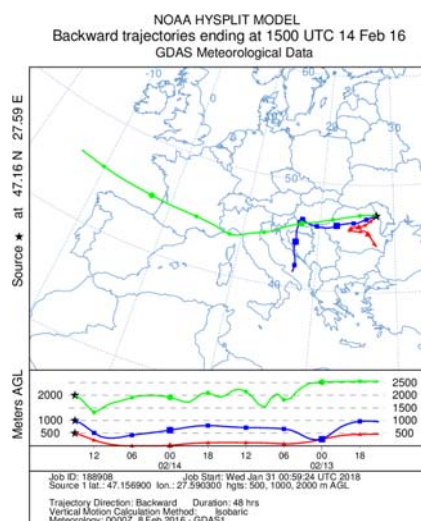
PM_{2.5}



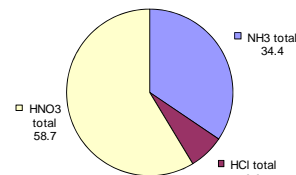
PM₁₀



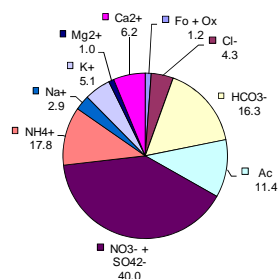
PM₁₀



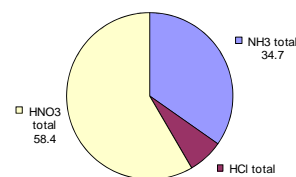
PM_{2.5}



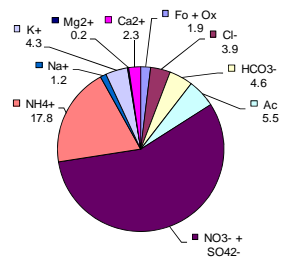
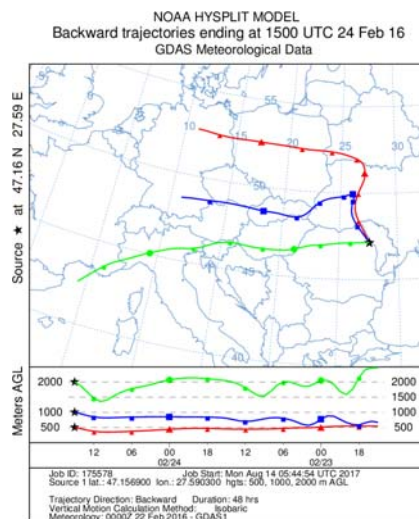
PM_{2.5}



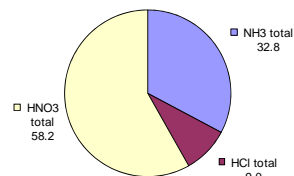
PM₁₀



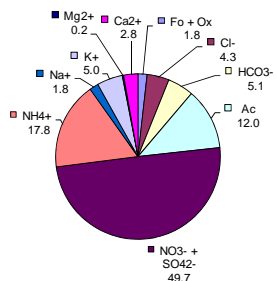
PM₁₀



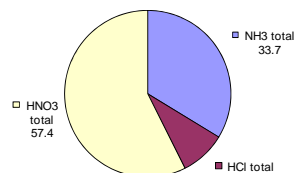
PM_{2.5}



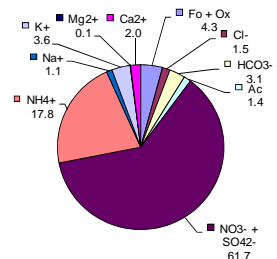
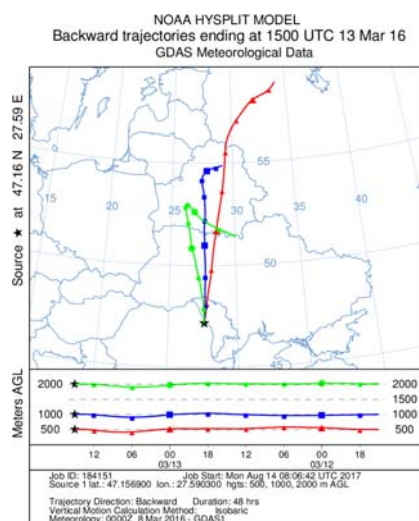
PM_{2.5}



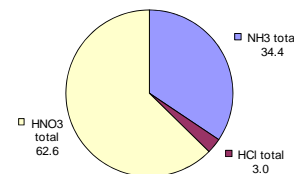
PM₁₀



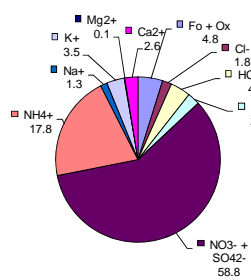
PM₁₀



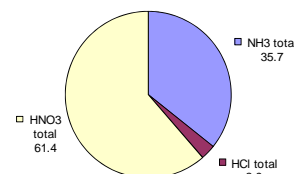
PM_{2.5}



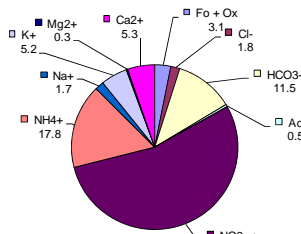
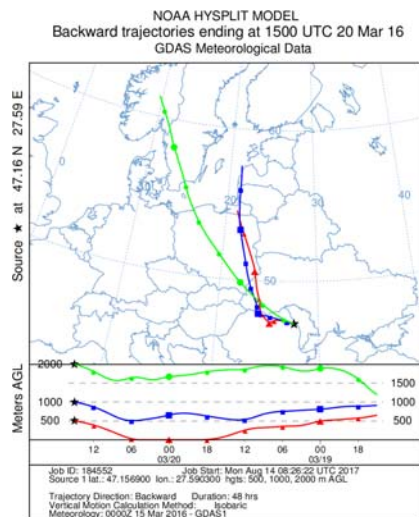
PM_{2.5}



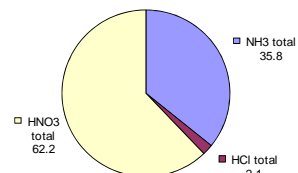
PM₁₀



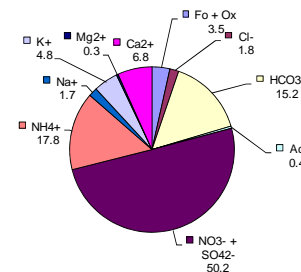
PM₁₀



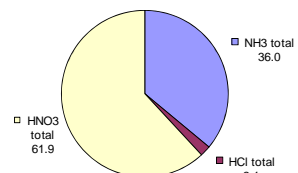
PM_{2.5}



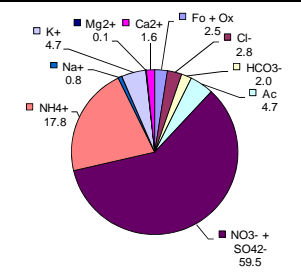
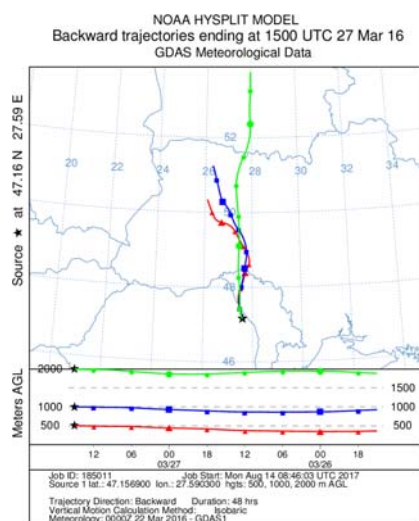
PM_{2.5}



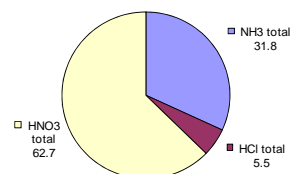
PM₁₀



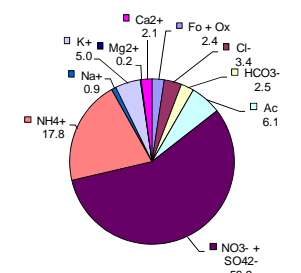
PM₁₀



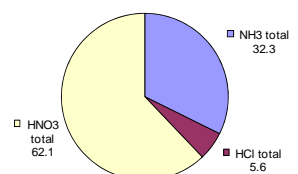
PM_{2.5}



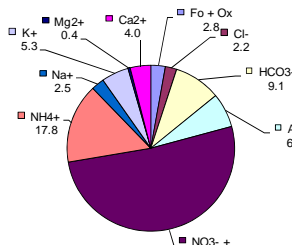
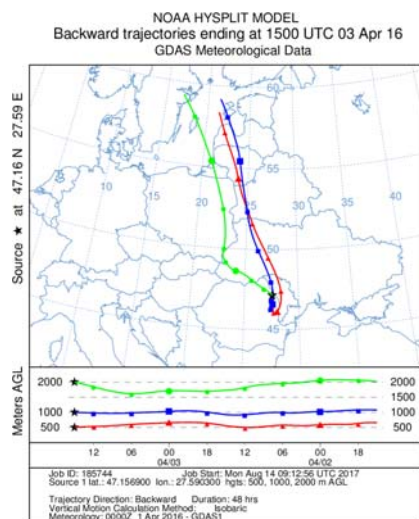
PM_{2.5}



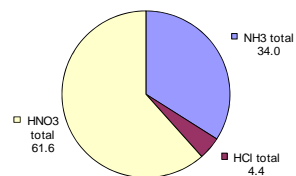
PM₁₀



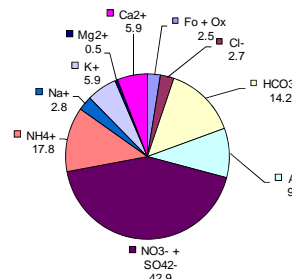
PM₁₀



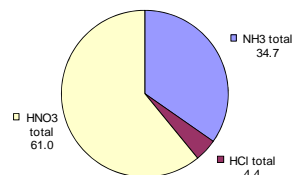
PM_{2.5}



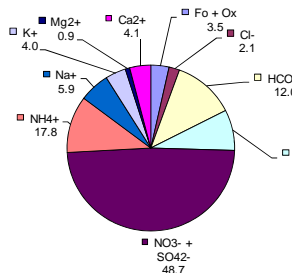
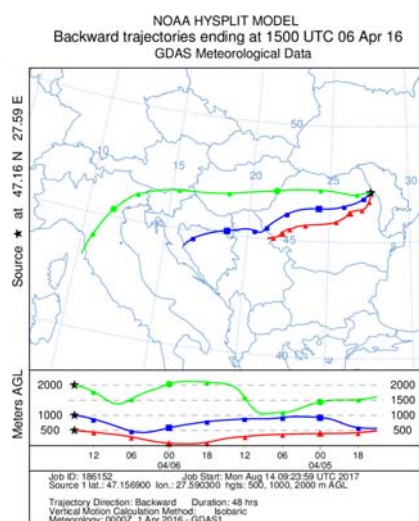
PM_{2.5}



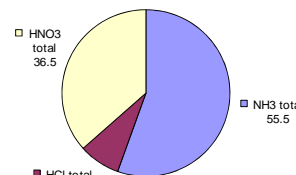
PM₁₀



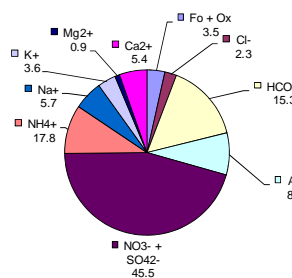
PM₁₀



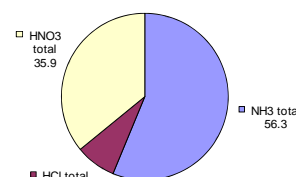
PM_{2.5}



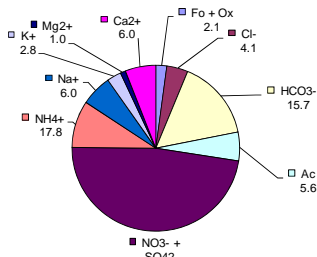
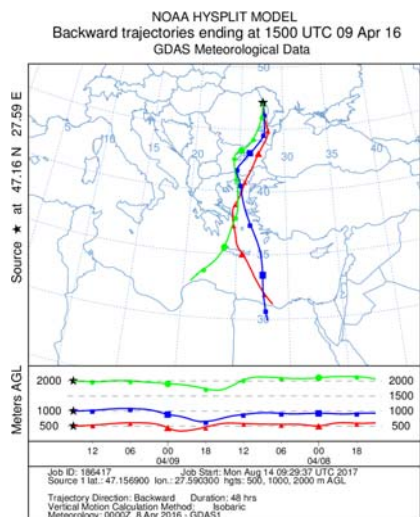
PM_{2.5}



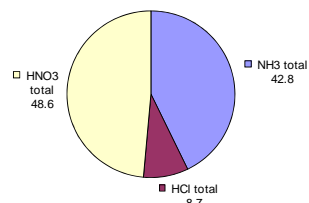
PM₁₀



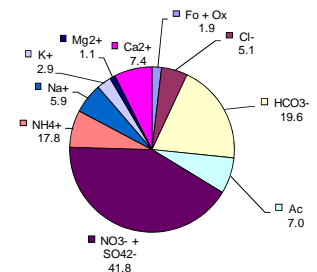
PM₁₀



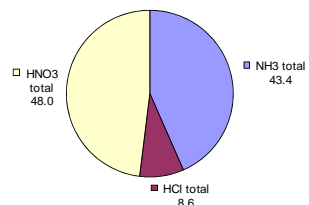
PM_{2.5}



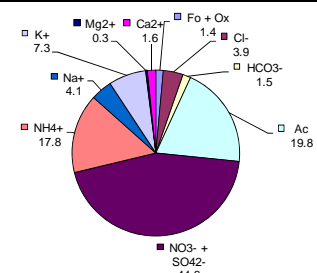
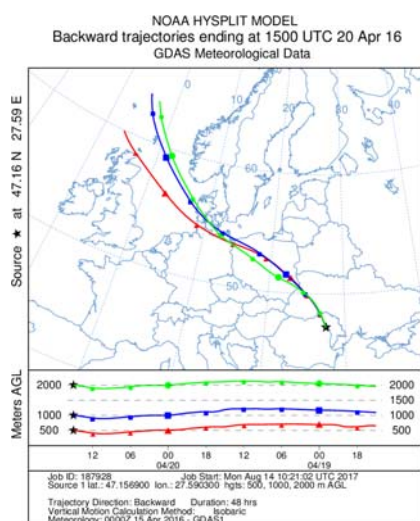
PM_{2.5}



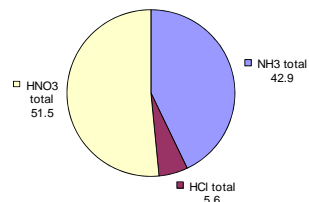
PM₁₀



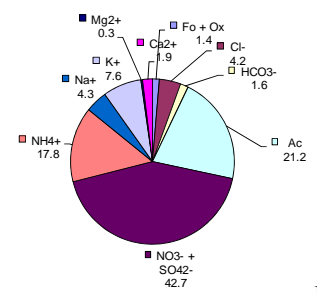
PM₁₀



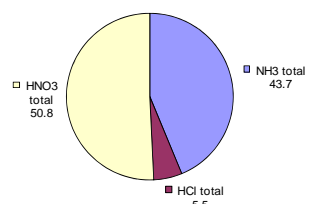
PM_{2.5}



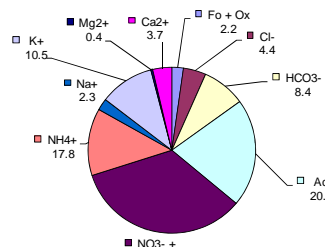
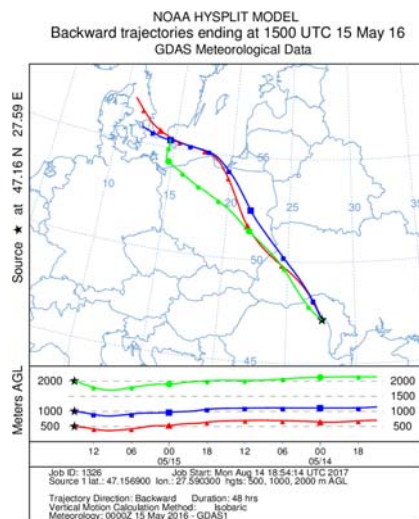
PM_{2.5}



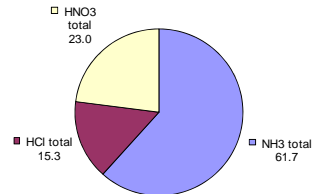
PM₁₀



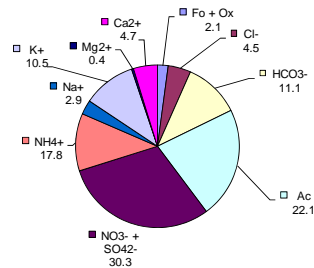
PM₁₀



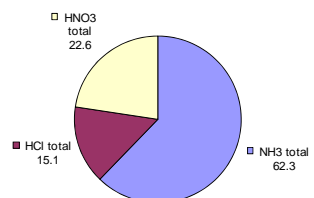
PM_{2.5}



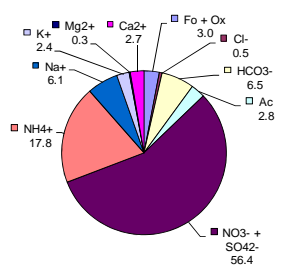
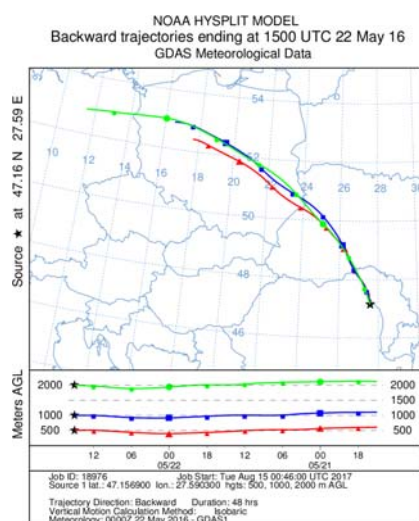
PM_{2.5}



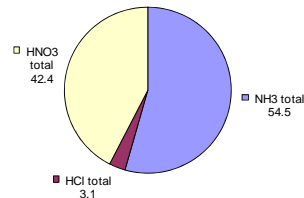
PM₁₀



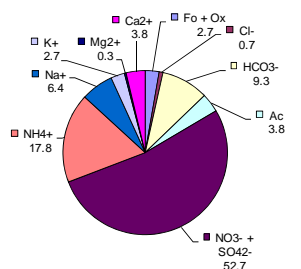
PM₁₀



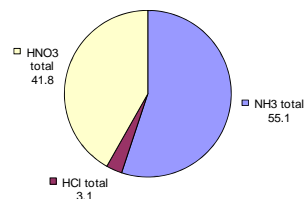
PM_{2.5}



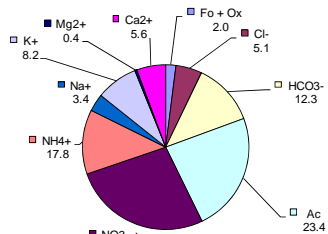
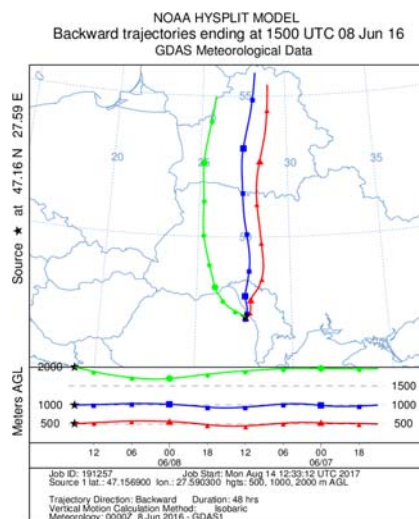
PM_{2.5}



PM₁₀

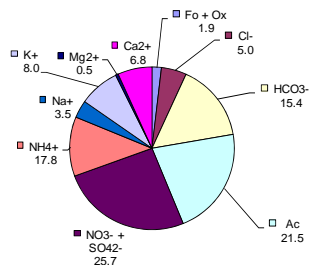


PM₁₀



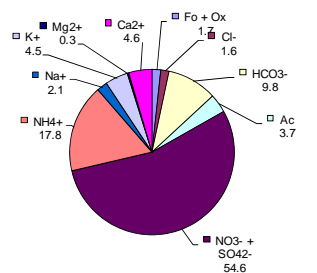
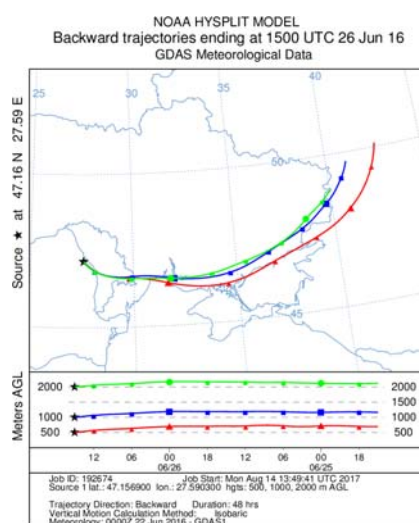
PM_{2.5}

PM_{2.5}



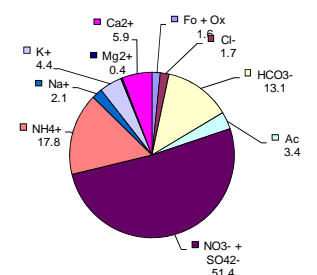
PM₁₀

PM₁₀



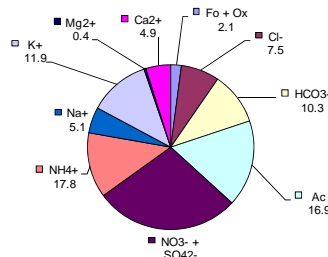
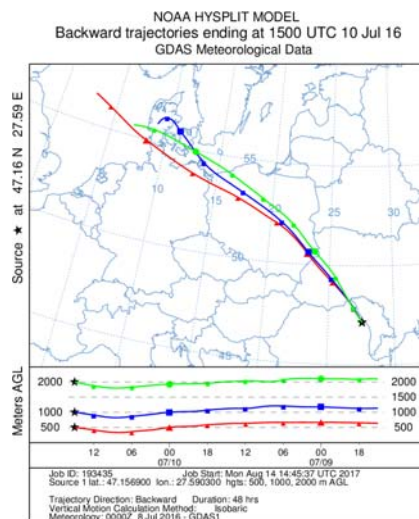
PM_{2.5}

PM_{2.5}

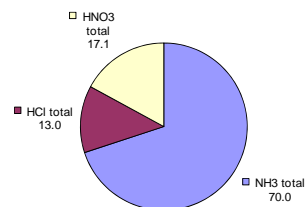


PM₁₀

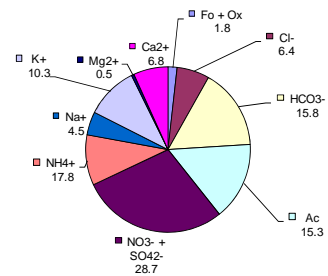
PM₁₀



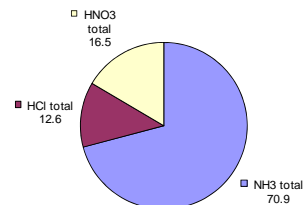
PM_{2.5}



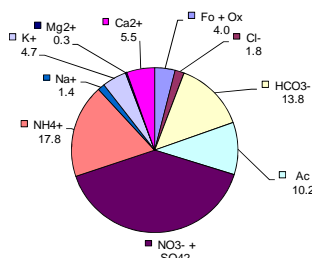
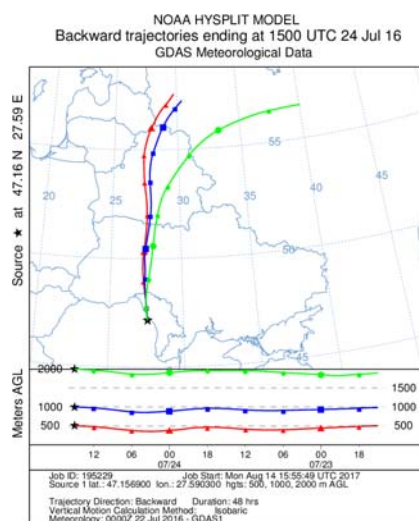
PM_{2.5}



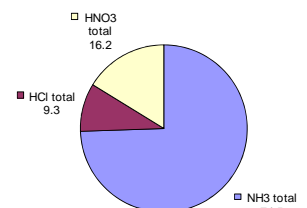
PM₁₀



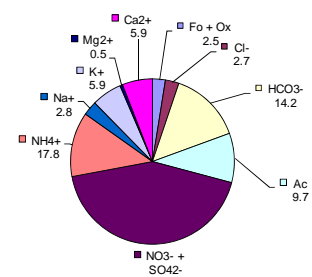
PM₁₀



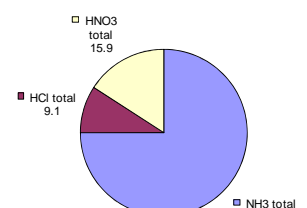
PM_{2.5}



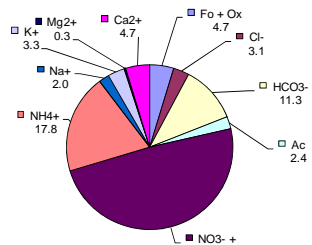
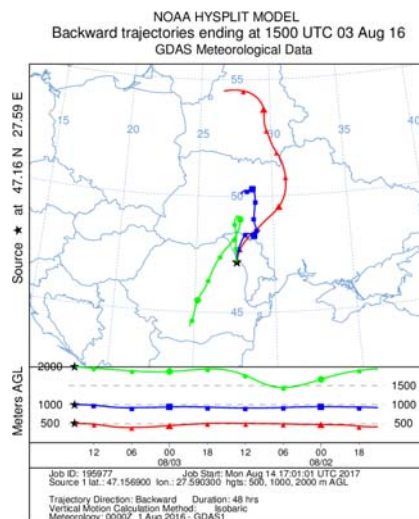
PM_{2.5}



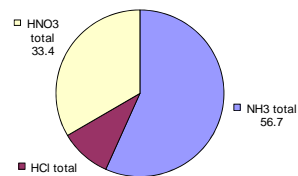
PM₁₀



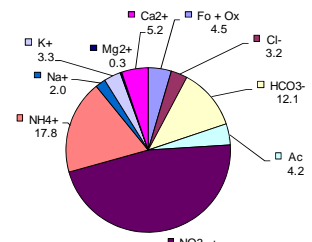
PM₁₀



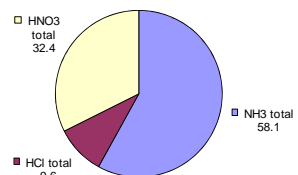
PM_{2.5}



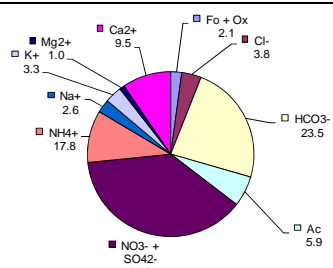
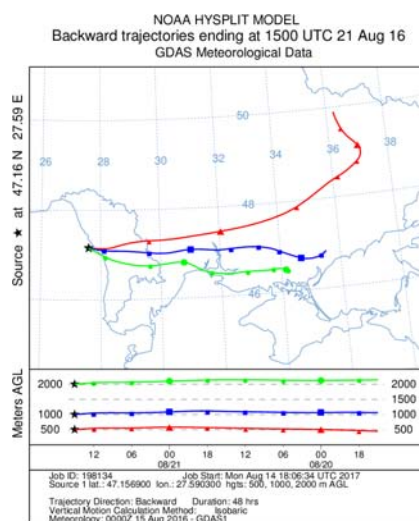
PM_{2.5}



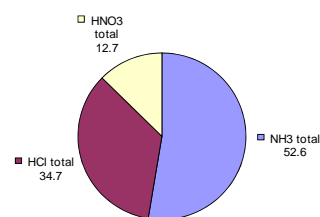
PM₁₀



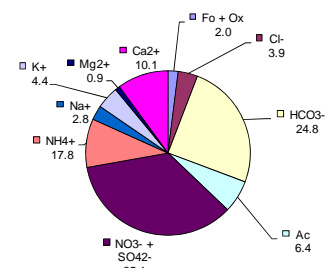
PM₁₀



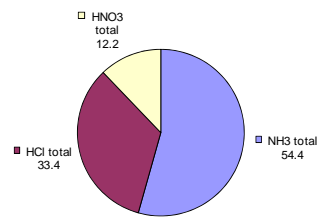
PM_{2.5}



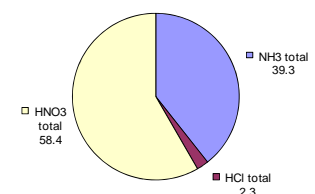
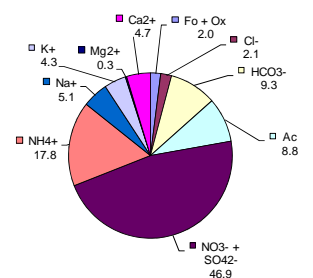
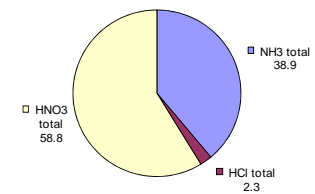
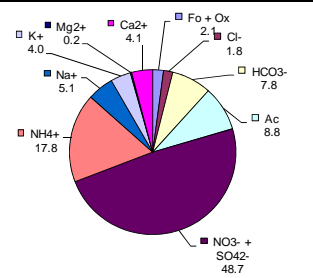
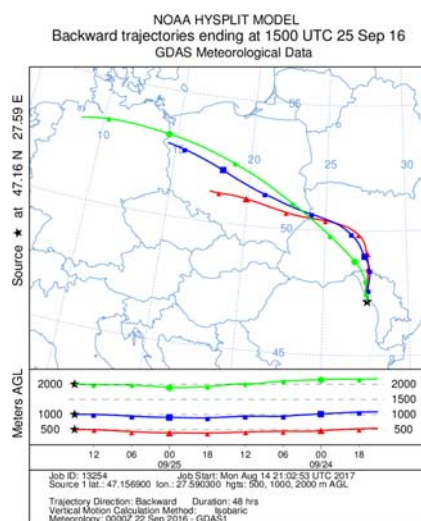
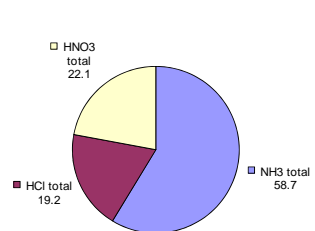
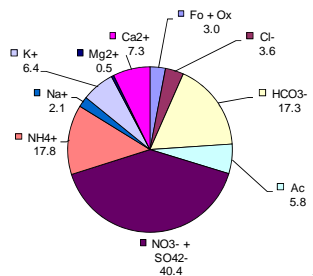
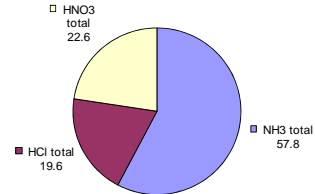
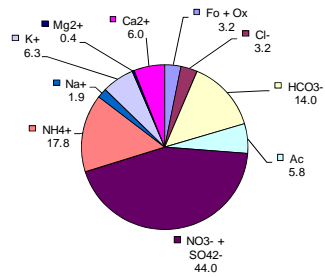
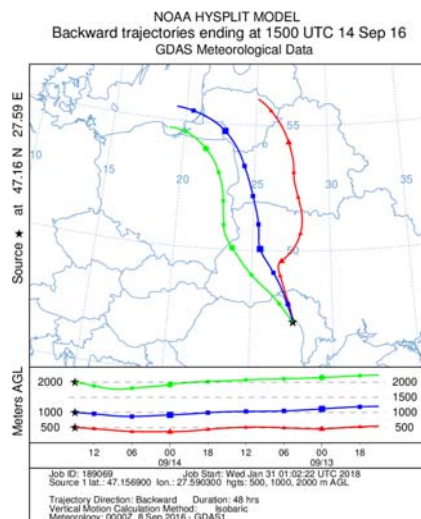
PM_{2.5}



PM₁₀



PM₁₀



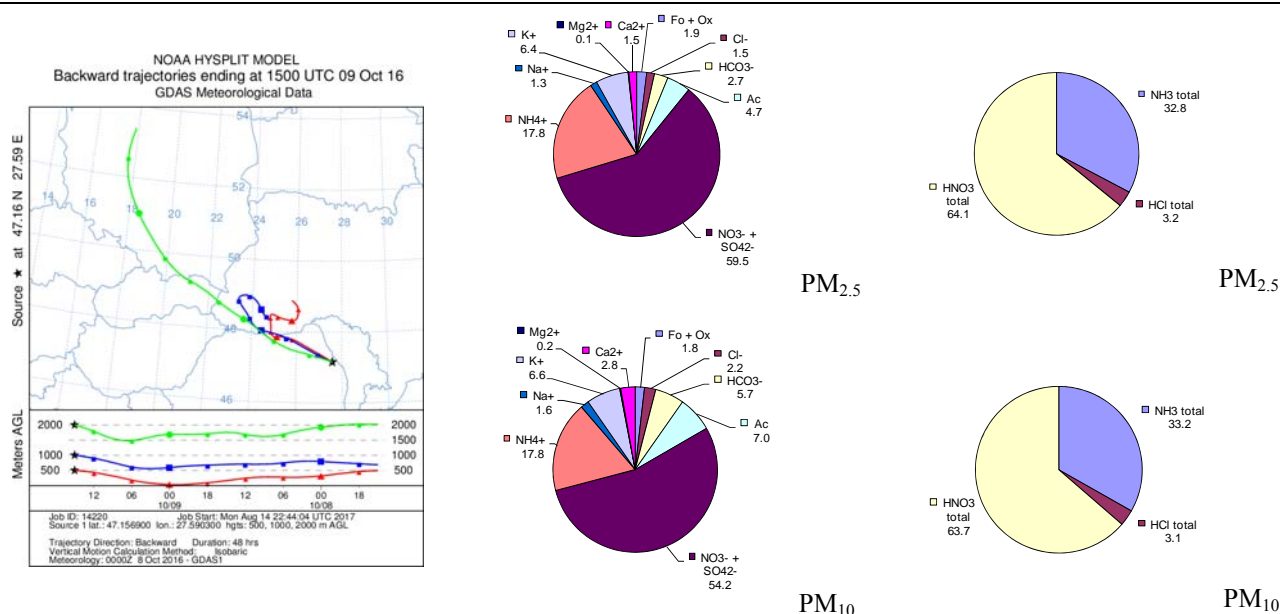


Figure S 4: Trajectory air mass associated percentual contributions for the identified-quantified ions and ISORROPIA-II predicted gaseous NH₃, HNO₃ and HCl both in PM_{2.5} (top) and PM₁₀ (bottom) fractions. Selected investigated events are presented. Note: Fo – formate, Ac – acetate, Ox – oxalate, NH₄⁺ reflects NH₄⁺ total.

It should be also underlined that for ionic species specific for the coarse fraction, i.e. Na⁺ and Ca²⁺, the maxima seems to be mainly induced either by the prevalent direction of the air masses (spring maxima of Na⁺ ion most probably induced by the fact that March and April appeared as months with prevalent southern air masses crossing large continental areas with more salty soil) or by the drought (the summer maxima of Ca²⁺ was mainly influenced by the ionic chemical composition of aerosol samples collected in August 2016, 7 events, a month of the 2016 year without any single raining events). Actually, in August 2016, 1 event was strongly affected by atmospheric driven buoyancy (18.2 % fine particulate Ca²⁺ and 42.1 % fine particulate HCO₃⁻), 1 event was affected by turbulent local air masses (10.7 % fine particulate Ca²⁺ and 24.8 % fine particulate HCO₃⁻) and other 3 events showed contributions brought by air masses crossing larger continental areas (9.8 ± 1.7 % fine particulate Ca²⁺ and 25.3 ± 3.9 % fine particulate HCO₃⁻). Other 2 events sampled at the beginning of August 2016 (of N-NW direction both) in terms of Ca²⁺ and HCO₃⁻ brought contributions as high as (4.3 ± 0.6 % fine particulate Ca²⁺ and 9.7 ± 2.3 % fine particulate HCO₃⁻). High percentual contributions within the identified and quantified species brought by Ca²⁺ and HCO₃⁻ ions were also observed in various events collected all year round which were affected by long-range transport air masses accompanied by atmospheric driven buoyancy or by long-range transport air masses coming from arid areas (e.g. 31 January 2016, 14 February 2016, 20 March 2016, 06 April 2016, 09 April 2016, etc). It has been observed that in average the contributions brought by such events were strongly affecting the distribution of the ionic chemical composition in sampled aerosols.

References

- Alastuey, A., Querol, X., Aas, W., Lucarelli, F., Perez, N., Moreno, T., Cavalli, F., Areskoug, H., Balan, V., Catrambone, M., Ceburnis, D., Cerro, J. C., Conil, S., Gevorgyan, L., Hueglin, C., Imre, K., Jaffrezo, J. L., Leeson, S. R., Mihalopoulos, N., Mitosinkova, M., O'Dowd, C. D., Pey, J., Putaud, J. P., Riffault, V., Ripoll, A., Sciare, J., Sellegri, K., Spindler, G., Yttri, and K. E.: Geochemistry of PM₁₀ over Europe during the EMEP intensive measurement periods in summer 2012 and winter 2013, *Atmos. Chem. Phys.*, 16, 6107–6129, doi:10.5194/acp-16-6107-2016, 2016.
- Arsene, C., Olariu, R. I., and Mihalopoulos, N.: Chemical composition of rainwater in the north-eastern Romania, Iasi region (2003-2006), *Atmos. Environ.*, 41, 9452–9467, doi:10.1016/j.atmosenv.2007.08.046, 2007.
- Arsene, C., Olariu, R. I., Zarmas, P., Kanakidou, M., and Mihalopoulos, N.: Ion composition of coarse and fine particles in Iasi, north-eastern Romania. Implications for aerosols chemistry in the area, *Atmos. Environ.*, 45, 906–916, doi:10.1029/2000JD900066, 2011.
- Backes, A. M., Aulinger, A., Bieser, J., Matthias, V., and Quante, M.: Ammonia emissions in Europe, part I: Development of a dynamical ammonia emission inventory, *Atmos. Environ.*, 131, 55–66, doi: 10.1016/j.atmosenv.2016.01.041, 2016a.
- Backes, A. M., Aulinger, A., Bieser, J., Matthias, V., and Quante, M.: Ammonia emissions in Europe, part II: How ammonia emission abatement strategies affect secondary aerosols, *Atmos. Environ.*, 126, 153–161, doi:10.1016/j.atmosenv.2015.11.039, 2016b.
- Cernat, R.I., Mihaescu, T., Vornicu, M. Vione, D., Olariu, R. I., and Arsene, C.: Serum trace metal and ceruloplasmin variability in individuals treated for pulmonary tuberculosis, *Int. J. Tuberc. Lung Dis.*, 15, 1239–1245, doi: 10.5588/ijtld.10.0445, 2011.
- Dockery, D. W., Cunningham, J., Damokosh, A. I., Neas, L. M., Spengler, J. D., Koutrakis, P., Ware, J. H., Raizenne, M., and Speizer, F. E.: Health effects of acid aerosols on North American children: respiratory symptoms, *Environ. Health Perspect.*, 104 (5), 500–505, 1996.
- Fang, T., Guo, H., Zeng, L., Verma, V., Nenes, A., and Weber, R. J.: Highly acidic ambient particles, soluble metals, and oxidative potential: A link between sulfate and aerosol toxicity, *Environ. Sci. Technol.*, 51, 2611–2620, doi:10.1021/acs.est.6b06151, 2017.
- Guo, H., Xu, L., Bougiatioti, A., Cerully, K. M., Capps, S. L., Hite, J. R., Carlton, A. G., Lee, S. H., Bergin, M. H., Ng, N. L., Nenes, A., and Weber, R. J.: Particle water and pH in the southeastern United States, *Atmos. Chem. Phys.*, 15, 5211–5228, doi: 10.5194/acp-15-5211-2015, 2015.
- Guo, H., Sullivan, A. P., Campuzano-Jost, P., Schroder, J. C., Lopez-Hilfiker, F. D., Dibb, J. E., Jimenez, J. L., Thornton, J. A., Brown, S. S., Nenes, A., and Weber, R. J.: Fine particle pH and the partitioning of nitric acid during winter in the northeastern United States, *J. Geophys. Res.: Atmos.*, 121, 10355–10376, doi: 10.1002/2016JD025311, 2016.
- Gwynn, R. C., Burnett, R. T., and Thurston, G. D.: A time-series analysis of acidic particulate matter and daily mortality and morbidity in the Buffalo, New York, region, *Environ. Health Perspect.* 108 (2), 125–133, 2000.

- Hennigan, C. J., Izumi, J., Sullivan, A. P., Weber, R. J., and Nenes, A.: A critical evaluation of proxy methods used to estimate the acidity of atmospheric particles, *Atmos. Chem. Phys.*, 15, 2775–2790, doi:10.5194/acp-15-2775-2015, 2015. http://ec.europa.eu/research/infocentre/article_en.cfm?artid=31296, 28 October 2013
- Huang, X. F., He, L. Y., Hu, M., Canagaratna, M. R., Sun, Y., Zhang, Q., Zhu, T., Xue, L., Zeng, L. W., Liu, X. G., Zhang, Y. H., Jayne, J. T., Ng, N. L., and Worsnop, D. R.: Highly time-resolved chemical characterization of atmospheric submicron particles during 2008 Beijing Olympic Games using an Aerodyne High-Resolution Aerosol Mass Spectrometer, *Atmos. Chem. Phys.*, 10, 8933–8945, doi:10.5194/acp-10-8933-2010, 2010.
- Ianniello, A., Spataro, F., Esposito, G., Allegrini, I., Hu, M., and Zhu, T.: Chemical characteristics of inorganic ammonium salts in PM_{2.5} in the atmosphere of Beijing (China), *Atmos. Chem. Phys.*, 11, 10803–10822, doi:10.5194/acp-11-10803-2011, 2011.
- Ianniello, A., Spataro, F., Esposito, G., Allegrini, I., Rantica, E., Ancora, M. P., Hu, M., and Zhu, T.: Occurrence of gas phase ammonia in the area of Beijing (China), *Atmos. Chem. Phys.*, 10, 9487–9503, doi:10.5194/acp-10-9487-2010, 2010.
- Lelieveld, J., Evans, J. S., Fnais, M., Giannadaki, D., and Pozzer, A.: The contribution of outdoor air pollution sources to premature mortality on a global scale, *Nature*, 525, 367–371, doi:10.1038/nature15371, 2015.
- Markovic, M. Z., Hayden, K. L., Murphy, J. G., Makar, P. A., Ellis, R. A., Chang, R. Y. W., Slowik, J. G., Mihele, C., and Brook, J.: The effect of meteorological and chemical factors on the agreement between observations and predictions of fine aerosol composition in southwestern Ontario during BAQS-Met, *Atmos. Chem. Phys.*, 11, 3195–3210, doi:10.5194/acp-11-3195-2011, 2011.
- Meskhidze, N., Chameides, W. L., Nenes, A., and Chen, G.: Iron mobilization in mineral dust: Can anthropogenic SO₂ emissions affect ocean productivity?, *Geophys. Res. Lett.*, 30, 2085, doi: 10.1029/2003GL018035, 2003.
- Moya, M., Pandis, S. N., and Jacobson, M. J.: Is the size distribution of urban aerosols determined by thermodynamic equilibrium? An application to Southern California, *Atmos. Environ.*, 36, 2349–2365, doi: 10.1016/S1352-2310(01)00549-0, 2002.
- Oakes, M., Ingall, E. D., Lai, B., Shafer, M. M., Hays, M. D., Liu, Z. G., Russell, A. G., and Weber, R. J.: Iron solubility related to particle sulfur content in source emission and ambient fine particles, *Environ. Sci. Technol.*, 46(12), 6637–6644, doi:10.1021/es300701c, 2012.
- Pathak, R. K. and Chan, C. K.: Inter-particle and gas-particle interactions in sampling artifacts of PM_{2.5} in filter based samplers. *Atmos. Environ.*, 39, 1597–1607, doi:10.1016/j.atmosenv.2004.10.018, 2005.
- Sinclair, D., Countess, R. J., and Hoopes, G. S.: Effect of relative humidity on the size of atmospheric aerosol particles. *Atmos. Environ.*, 8, 1111–1117, doi:10.1016/0004-6981(74)90045-6, 1974.
- Sutton, M. A., Reis, S., Riddick, S. N., Dragosits, U., Nemitz, E., Theobald, M. R., Tang, Y. S., Braban, C. F., Vieno, M., Dore, A. J., Mitchell, R. F., Wanless, S., Daunt, F., Fowler, D., Blackall, T. D., Milford, C., Flechard, C. R., Loubet, B., Massad, R., Cellier, P., Personne, E., Coheur, P. F., Clarisse, L., Van Damme, M., Ngadi, Y., Clerbaux, C., Skjoth, C. A.,

- Geels, C., Hertel, O., Wichink Kruit, R. J., Pinder, R. W., Bash, J. O., Walker, J. T., Simpson, D., Horváth, L., Misselbrook, T. H., Bleeker, A., Dentener, F., and de Vries, W.: Towards a climate-dependent paradigm of ammonia emission and deposition, *Philos. Trans. R. Soc. B. Biol. Sci.*, 368, 20130166, doi:10.1098/rstb.2013.0166, 2013.
- Tsagkogeorgas, G., Roldin, P., Duplissy, J., Rondo, L., Trostl, J., Slowik, J. G., Ehrhart, S., Franchin, A., Kurten, A., Amorim, A., Bianchi, F., Kirkby, J., Petaja, T., Baltensperger, U., Boy, M., Curtius, J., Flagan, R. C., Kulmala, M., Donahue, N. M., and Stratmann, F.: Evaporation of sulphate aerosols at low relative humidity, *Atmos. Chem. Phys.*, 17, 8923–8938, doi:10.5194/acp-17-8923-2017, 2017.
- Zhang, D., Shi, G. Y., Iwasaka, Y., and Hu, M.: Mixture of sulfate and nitrate in coastal atmospheric aerosols: individual particle studies in Qingdao (36°04'N, 120°21'E), China, *Atmos. Environ.*, 34, 2669–2679, 2000.
- Zhao, M., Wang, S., Tan, J., Hua, Y., Wu, D., and Hao, J.: Variation of urban atmospheric ammonia pollution and its relation with PM_{2.5} chemical property in winter of Beijing, China, *Aerosol Air Qual. Res.*, 16, 1378–1389, doi:10.4209/aaqr.2015.12.0699, 2016.